A Doctoral Dissertation

Effect of bimatoprost on the regulation of hair growth

Jung-Il Kang

Department of Medicine

Graduate School

Jeju National University

August, 2011

Bimatoprost의 모발성장 효과

지도교수 강 희 경

강 정 일

이 논문을 의학 박사학위 논문으로 제출함

2011년 8월

강정일의 의학 박사학위 논문을 인준함

심사위원장 유 은 숙 印

위 원 박 덕 배 印

위 원 이 창 흠 印

위 원 현 진 원 印

위 원 강 희 경 印

제주대학교 대학원

2011년 8월

Effect of bimatoprost on the regulation of hair growth

Jung-Il Kang

(Supervised by Professor **Hee-Kyoung Kang**)

A thesis submitted in partial fulfillment of the requirement for degree of doctor of philosophy in Medicine

Date Approved:

June 28, 2011

Eunsook Yoo

DeokBAE PARK

Lee Chang Hoon

Hyun Jin Won

Heekyung Kang

Department of Medicine

Graduate School, Jeju National University

August, 2011

CONTENTS

LIST OF TABLES

LIST OF FIGURES

PART Ⅰ

Hair growth promoting effect and action mechanisms of bimatoprost, $PGF_{2\alpha}$ analogue

1. Abstract

Prostaglandin analogues have various biological activities such as pro-inflammation, carcinogenesis, and hair growth. However, the precise mechanisms underlying the role of prostaglandin analogues in the regulation of hair growth have not been fully elucidated. This study was conducted to evaluate the effects of prostaglandin analogues on the growth of hair. When immortalized rat vibrissa dermal papilla cells (DPC) were treated with prostaglandin analogues such as latanoprost, bimatoprost, unoprostone isopropyl ester and travoprost, treatment with bimatoprost led to DPC proliferation compared to control. The effect of bimatoprost on the growth of vibrissa follicles was also examined. Bimatoprost treatment significantly increased the length of vibrissa follicles hair fibers. We therefore examined the effects of bimatoprost on the DPC cell cycle. Treatment of DPCs with bimatoprost resulted in a decreased sub-G1 population, which was accompanied by increased cyclin E and CDK2 levels. To elucidate the mechanism of bimatoprost-induced cell cycle progression, we examined the expression of β-catenin which plays an important role in hair growth. Bimatoprost increased nuclear β-catenin levels and also up-regulated the expression of Cox-2, a downstream target of the Wnt/β-catenin signaling pathway. We also examined the proliferative effects of prostaglandin analogues in NIH3T3 fibroblasts. Minoxidil, a potent

hair-growth agent, can induce proliferation in these cells by opening K_{ATP} channels. Bimatoprost significantly increased the proliferation of NIH3T3 fibroblasts. This reagent induced cell cycle progression, but decreased the expression of $p27^{kip1}$ in NIH3T3 fibroblasts. Treatment of NIH3T3 fibroblasts with bimatoprost resulted in down-regulation of Bax expression and up-regulation of Bcl-2. These observations indicate that bimatoprost exerts an anti-apoptotic effect. Up-regulation of β-catenin and Cox-2, a Wnt/β-catenin target gene, by bimatoprost was observed in NIH3T3 fibroblasts. We also investigated whether the effects of bimatoprost on proliferation were related to opening of the K_{ATP} channels. Glibenclamide, a K_{ATP} channel blocker, inhibited bimatoprost-induced proliferation as well as cell cycle progression in NIH3T3 fibroblasts. Bimatoprost and minoxidil induced the phosphorylation of Akt, whereas glibenclamide attenuated bimatoprost-induced phosphorylation of Akt. Pre-treatment of NIH3T3 fibroblasts with glibenclamide attenuated the up-regulation of Bcl-2, β-catenin, and Cox-2 by bimatoprost. Taken together, these results indicate that bimatoprost increased the hair growth by promoting cell cycle progression of DPCs through up-regulation of β-catenin and Cox-2. In addition, bimatoprost increased the proliferation of NIH3T3 fibroblasts by activating anti-apoptotic pathways through the up-regulation of β-catenin and activation of K_{ATP} channels. The current study demonstrated that bimatoprost might serve as a potential therapeutic agent for treating hair loss.

2. Introduction

Hair is produced by hair follicles which have a complex structure. The hair follicle is composed of a hair shaft (HS), inner root sheath (IRS), outer root sheath (ORS), matrix, and underlying dermal papilla cells. Throughout the life time of mammals, hair follicles undergo hair cycle changes such as growth (anagen), involution (catagen), and resting (telogen) phases. Changes of morphological structure occur during the hair cycle as follows. The epithelium of hair follicles and dermal papilla undergo regression during catagen. During telogen, permanent regions of hair follicles remain to prepare for anagen (Paus *et al.,* 1999). The volume of the dermal papilla is maximal during the anagen phase, whereas volume of dermal papilla cells decreases during the catagen to telogen transition (Ibrahim *et al.,* 1982). A previous study found that the volume of the dermal papilla determines the size of hair follicles through the proliferation and migration of matrix cells (Elliott *et al.,* 1999).

Dermal papilla cells are mesenchymally-derived cells which play a pivotal role in the morphogenesis, regeneration, and growth of hair (Stenn *et al.,* 2001). Paracrine and autocrine factors are produced by dermal papilla cells, and regulation of hair growth depends on interaction between the dermal papilla and matrix cells (Hamada *et al.,* 2006). Previous studies indicated that growth and regeneration of hair follicles are mediated by multiple

signaling pathways. Vascular endothelial growth factor (VEGF; (Lachgar *et al.,* 1996), keratinocyte growth factor (KGF; (Danilenko *et al.,* 1995) and fibroblast growth factor-7 (FGF-7; (Iino *et al.,* 2007) were reported to promote hair growth, whereas transforming growth factor-β1 (TGF-β1; (Foitzik *et al.,* 2000a), TGF-β2 (Soma *et al.,* 1998), Dickkopf-related protein-1 (DKK-1; (Kwack *et al.,* 2008) and interferon-γ (IFN-γ; (Ito *et al.,* 2005) were not. A previous study is being conducted to examine ways to treat hair loss (Cotsarelis *et al.,* 2001). Nevertheless, the incidence of hair loss is increasing all over the world. Only two Food and Drug Administration (FDA)-approved drugs (finasteride and minoxidil) are currently used to treat hair loss. Hair loss is partly caused by dihydrotestosterone (DHT) that induce the miniaturization of dermal papilla and hair follicles (Jahoda, 1998, Kwack *et al.,* 2008). DHT production is increased by 5α-reductase activity that induces the conversion of testosterone to DHT (Steers, 2001); DHT is then transported to epithelial cells (Ekman, 2000). It is well-known that the progression of hair loss is reduced by finasteride through inhibition of 5α-reductase activity (Kaufman, 1996). On the other hand, the actions of minoxidil, another treatment for hair loss, are not fully understood but some underlying mechanisms have been revealed. Minoxidil was shown to have anti-apoptotic effects on dermal papilla cells (Han *et al.,* 2004). Minoxidil also exerts mitogenic effects on NIH3T3 fibroblasts via the opening of K^+ channels (Sanders *et al.,* 1996). Hair growth is promoted by

some reagents that open K^+ channels including minoxidil (Clissold *et al.,* 1987), diazoxide (Koblenzer *et al.,* 1968), and pinacidil (Harmon *et al.,* 1993). K^+ channels are ubiquitous membrane proteins which play a crucial role in a number of physiologic activities such as cell proliferation, immune function, and insulin secretion (Shieh *et al.,* 2000, Trauner *et al.,* 2004). In particular, cell proliferation can be blocked by K^+ channel blockers in T lymphocytes (Lewis *et al.,* 1988) and melanoma cells (Nilius *et al.,* 1992). In many type of cancer cells, K^+ channels blockers also inhibit the transition from G1 to S phase (Villalonga *et al.,* 2007).

ATP-sensitive K^+ channels (K_{ATP} channels) are heteromeric complexes composed of four inwardly-rectifying K^+ channel (Kir6.X) subunits and four sulfonylurea receptor (SUR) subunits (Babenko *et al.,* 1998). Recently, the expression of K_{ATP} channels subunits was identified in human hair follicles, and SUR2B in dermal papilla showed responses to minoxidil (Shorter *et al.,* 2008). The signaling pathway responsible for proliferation via K_{ATP} channels is complex, but general regulators such as ERK and Akt are known to control these actions (Goni-Allo *et al.,* 2008, Huang *et al.,* 2009). Minoxidil can prevent neurotoxicity in striatum through activation of Akt (Goni-Allo *et al.,* 2008). The phosphatidylinositol 3-kinase/Akt (PI3K/Akt) pathway is important for cell proliferation, apoptosis (Pene *et al.,* 2002), and cell cycle regulation (Fatrai *et al.,* 2006). In particular, Akt is an important

regulator of apoptosis, and influences balance between repression of pro-apoptotic factors and activation of anti-apoptotic factors (Woo *et al.,* 2004).

The Wnt/β-catenin pathway plays a pivotal role in hair follicle development and differentiation (DasGupta *et al.,* 1999). Wnt, a large family of secreted cysteine-rich glycoproteins, has been implicated in multiple processes such as cell proliferation, cell adhesion, and stem cell regulation (Moon *et al.,* 1997, Suda *et al.,* 2008). β-catenin is a main component of the Wnt pathway, and the level of β-catenin is regulated by degradation complexes such as adenomatous polyposis coli (APC), glycogen synthase kinase-3β (GSK-3β), axin, and casein kinase Ⅰ. Wnt binds to Frizzled (FZ) receptor as well as low-density lipoprotein (LDL) receptor-related protein 5/6 (LRP 5/6), which activates disheveled (DSH). This results in the stabilization of β-catenin in the cytoplasm. Stable β-catenin enters the nucleus and forms a complex with lymphoid enhancer-binding factor (LEF)/T-cell factor (TCF) transcription factors (Behrens *et al.,* 1996, Omer *et al.,* 1999). Nuclear β-catenin may then activate target genes such as cyclin D1 (Tetsu *et al.,* 1999), c-Myc (He *et al.,* 1998), and cyclooxygenase-2 (Howe *et al.,* 1999).

Cell cycle progression is a key process for cell proliferation (Igata *et al.,* 2005). In mammals, the cell cycle is tightly regulated by the modulation of cyclin/cyclin-dependent kinases (CDKs) and CDK inhibitors. In the quiescent state, expression of $p27^{kip1}$, a CDK

inhibitor, is maintained at higher levels. After stimulation with mitogen, the expression of cyclin D, a sensor of growth factors, is upregulated whereas the expression of $p27^{kip1}$ is downregulated (Sherr, 1996). During the cell cycle, cyclin D/CDK4 and cyclin E/CDK2 complexes promote cell cycle progression (Radzio-Andzelm *et al.,* 1995).

Prostaglandins (PGs) are a family of eicosanoids that regulate several biological functions such as inflammation (Seibert *et al.,* 1994) and gastrointestinal cytoprotection (Miller *et al.,* 1979). The PG family includes prostacyclin (PGI_2), thromboxane (TXA_2), prostaglandin E_2 (PGE_2), ad prostaglandin F_2 (PGF_2), and is produced by arachidonic acid (AA) oxidation. The roles of cyclooxygenases (Cox-1 and Cox-2) in PG synthesis have been identified in previous studies (Lee *et al.,* 2003). The expression of Cox-2 is induced by stimuli such as cytokines (Arias-Negrete *et al.,* 1995). Cancer cell proliferation is increased by PGE through the Wnt/β-catenin pathway (Castellone *et al.,* 2005).

Metabolism of PG in human hair follicles has been observed (Colombe *et al.,* 2007). In human hair follicles, several PG receptors such as ones for prostaglandin E_2 (EP_1, EP_2, EP_3 and EP_4), prostaglandin D_2 (DP_1 and DP_2), prostaglandin I_2 (IP), thromboxane A_2 (TP) and prostaglandin $F_{2\alpha}$ (FP; (Colombe *et al.,* 2008) are expressed. In a previous study, latanoprost, a $PGF_{2\alpha}$ analogue, was reported to increase hair growth and (Johnstone *et al.,* 2002). Topical and systemic application of 16,16-dimethyl PGE_2 prevents radiation-induced hair loss (Hanson *et al.,* 1992). $PGF_{2\alpha}$ and its analogues stimulate the transition from telogen to anagen (Sasaki *et al.,* 2005a)(Sasaki *et al.,* 2005b)

. Bimatoprost, the trade name of 17-phenyl-trinor $PGF_{2\alpha}$ ethyl amide, has been used for treating ocular hypertension (Woodward *et al.,* 2001), and may exert its effects through FP

receptors (Woodward *et al.,* 2008). Although several reports have noted the growth of eyelashes induced by bimatoprost (Cohen, 2010, Tauchi *et al.,* 2010), studies examining the effect of bimatoprost on hair growth have been limited to eyelashes. In this study, we examined the more general effect of bimatoprost on hair growth. We also determined whether bimatoprost could increase hair growth by opening K_{ATP} channels. We found that bimatoprost may increase hair growth through the up-regulation of β-catenin and Cox-2, and activation of K_{ATP} channels. The study suggests that bimatoprost could be a useful agent for treating hair loss.

3. Materials and Methods

3.1. Reagents

9α,11α,15*R*-trihydroxy-17-phenyl-18,19,20-trinorprost-5*Z*-en-1-oic acid, isopropyl ester (latanoprost), 17-phenyl-trinor prostaglandin $F_{2\alpha}$ ethyl amide (bimatoprost), 13,14-dihydro-15-keto-20-ethyl $PGF_{2\alpha}$ isopropyl ester (unoprostone isopropyl ester), and 16-m-trifluoromethylphenoxy tetranor $PGF_{2\alpha}$ isopropyl ester (travoprost) were kindly provided by Samil Pharmaceutical (Seoul, South Korea). 3-(4,5-dimethylthiazol-2-yl)-2,5-diphenyltetrazoliumbromide (MTT), propidium iodide (PI), minoxidil, minoxidil sulfate, Earle's balanced salt solution (EBSS), phosphate buffered saline (PBS), insulin and hydrocortisone were from Sigma (St. Louis, MO, USA). Fetal bovine serum (FBS) and bovine calf serum (BCS) were purchased from Invitrogen (Carlsbad, CA, USA). Williams' medium with E- and L-glutamine was from Gibco (Grand Island, NY, USA). NADPH was obtained from Calbiochem (San Diego, CA, USA). Glibenclamide was purchased from Tocris (Bristol, UK). Antibodies against Akt, phospho-Akt, and Bcl-2 were from Cell Signaling Technology (Beverly, MA, USA). Antibodies against β-catenin, Cox-2, CDK2, cyclin E, caspase-3, Bax, SUR2B, Kir6.1, and tubulin-α were purchased from Santa Cruz Biotechnology (Santa Cruz, CA, USA). Antibody against β-actin was from Sigma. HRP-

conjugated goat anti-rabbit IgG, goat anti-mouse IgG, and mouse anti-goat IgG were from Santa Cruz Biotechnology. Goat anti-rabbit antibody conjugated to Alexa Fluor 594 was from Invitrogen. Aprotinin and leupeptin were from Calbiochem. Nonidet P-40 (NP-40) was from Roche (Basel, Switzerland); West-zol-enhanced chemilumin, a Western blotting detection reagent, was from iNtRON Biotechnology (Sungnam, South Korea).

3.2. Cell culture

The rat vibrissa immortalized dermal papilla cell line (Filsell *et al.,* 1994) was kindly provided by the Skin Research Institute, Amore Pacific Corporation R&D Center, South Korea. Immortalized dermal papilla cells (DPCs) were cultured in Dulbecco's Modified Eagle's Medium (DMEM; Hyclone Inc., Logan, UT, USA) supplemented with 10% FBS and penicillin/streptomycin (100 units/mL and 100 μg/mL, respectively) at 37°C in a humidified atmosphere containing less than 5% CO_2. NIH3T3 mouse embryonic fibroblasts was purchased from the American Type Culture Collection (ATCC; Manassas, VA, USA) and cultured in ATCC-formulated DMEM supplemented with 10% (v/v) heat-inactivated BCS at 37°C in a humidified atmosphere containing less than 5% CO_2.

3.3. Cell viability assay

The effect of bimatoprost on the proliferation of immortalized DPC was evaluated by measuring metabolic activity using an MTT assay. Immortalized DPCs (1.0×10^4 cells/mL) were seeded in a 96-well plate. The cells were cultured for 24 h to allow attachment and then cultured in serum-free DMEM for another 24 h. The cells were treated with for 4 d with minoxidil (75 μM) or latanoprost, bimatoprost, unoprostone isopropyl ester, and travoprost (0.024, 0.24, or 2.4 μM); vehicle (DMSO diluted 1:1000 in serum-free DMEM) was added as a control. NIH3T3 fibroblasts (1.0×10^4 cells/mL) were seeded in 96-well plates. The cells were pre-incubated for 24 h in DMEM supplemented with 10% BCS to aid attachment, then washed twice with PBS and incubated for another 24 h in DMEM containing 1.5% BCS.The cells were then treated for 4 d with minoxidil (75 μM) or latanoprost, bimatoprost, unoprostone isopropyl ester, and travoprost (0.024, 0.24, or 2.4 μM); vehicle (DMSO diluted 1:1000 in serum-free DMEM) was added as a control. In some case, 50 μM glibenclamide was added to inhibit the opening of K_{ATP} channels. Next, the cells were treated with 50 μL (2 mg/mL) of MTT dye and incubated at 37°C for 4 h. The plates were centrifuged at 1000 rpm for 5 min at room temperature, and the media was carefully removed. Dimethyl sulfoxide (200 μL/well) was added to dissolve the formazan crystals. Cell viability was determined by measuring the absorbance at 540 nm using a microplate reader (BioTek Instruments, Inc., Winooski, VT, USA). All experiments were performed at least three times.

3.4. Isolation and culturing of rat vibrissa follicles

Male Wistar rats (3 wk of age) were supplied by Orient Bio (Seongnam, Gyeonggi, Korea). All animals were cared for using protocols (20070002) approved by the Institutional Animal Care and Use Committee (IACUC) of Jeju National University (South Korea). The rat vibrissa follicles were isolated from 23-day-old male Wistar rats as previously described (Philpott *et al.,* 2000). Both the left and right mystacial pads were removed from the rats and placed in a 1:1 (v:v) solution of EBSS and PBS that contained 100 unit/mL of penicillin and 100 μg/mL of streptomycin. Anagen vibrissa follicles were carefully dissected under a stereomicroscope (Olympus, Tokyo, Japan). Using this method, we were able to routinely isolate more than 40 follicles from each animal. The isolated follicles were then placed in 24-well plates that contained 500 μL of Williams's medium E supplemented with 2 mM L-glutamine, 10 μg/mL insulin, 50 nM hydrocortisone, 100 unit/mL penicillin, and 100 μg/mL of streptomycin. The follicles were incubated at 37°C in a humidified atmosphere containing less than 5% CO_2. The isolated follicles were treated with bimatoprost (0.024, 0.12, 0.24, or 1.2 μM) and vehicle (DMSO diluted 1:1000 in Williams' medium E) as a control. Minoxidil sulfate (MS) was used as a positive control for the culture systems (Buhl *et al.,* 1990). The culture medium was changed every 3 d and photographs of the cultured rat vibrissa follicles

were taken using an Olympus stereomicroscope for 3 wk. The length of the hair follicles was measured using a DP controller (Olympus, Tokyo, Japan).

3.5. Rat prostatic 5α-reductase assay

Male Spargue-Dawley (SD) rats (8 wk old) were purchased from Dae-Han Biolink (Eumsung, South Korea), and given a standard laboratory diet with water *ad libitum*. All animals were cared for by using protocols (20070002) approved by the IACUC of Jeju National University. Male SD rats (8 wk old) were sacrificed with CO_2. The rat prostates were removed from their capsules, washed with saline, and stored at -80°C. Frozen tissues were thawed on ice and procedures were carried out at 4°C. The tissues were homogenized with a Polytron homogenizer (Brinkman Instruments, Westbury, NY, USA) in 5-6 tissue volumes of medium A (0.32 M sucrose, 1 mM dithiothreitol (DTT), 0.2 mM phenylmethylsulfonylfluoride (PMSF); and 20 mM potassium phosphate buffer, pH 6.6). The homogenates were centrifuged at 1500 g for 20 min. The pellets were recovered, washed with three tissue volumes of medium A, and centrifuged two additional times at 400 g for 10 min. The washed pellets were suspended in medium A and stored at -80°C until use. The suspension (2.5 mg protein/mL as determined by the Bradford assay using Bio-Rad reagents) was used as source of 5α-reductase. 5α-reductase activities were analyzed as

previously described (Hirosumi *et al.,* 1995). The reaction mixture had a final volume of 500 µL and contained 1mM DTT, 40 mM potassium phosphate buffers, 2 mM NADPH, and 120 nCi [1,2,6,7-^{3}H] testosterone. Triplicate reactions were initiated when the reaction mixture was added to the rat prostatic enzyme fraction (250 µg of protein) containing 0.2% DMSO (as a control), or bimatoprost (0.024, 0.24, or 2.4 µM). 2nM Finasteride (Merck-Sharpe-Dohme, Whitehouse Station, NJ, USA) was used as a positive control. The mixture was incubated at 37°C for 60 min, and then stopped by adding 1 mL of ethyl acetate and mixing for 1 min. After centrifugation at 1000 g for 5 mim, the organic phase was removed, dried under a heating plate, dissolved in 50 µL of ethyl acetate containing 500 µg/mL of testosterone and 500 µg/mL DHT, and applied to a silica gel 60 F254 TLC plate (Merck). The plate was developed in a solvent system consisting of an ethyl acetate:cyclohexane (1:1) solution, and the plate was air dried. Testosterone was visualized under UV light (254 nm) and DHT was detected using a 10% H_2SO_4 solution and posteriorly heating the plate. Under these conditions, DHT develops a classical dark yellow color. Areas containing androgen were cut off and the strips were soaked in 5 mL of ULTIMA GOLD^{TM} Cocktail (PerkinElmer, Waltham, MA, USA) and radioactivity was measured by a liquid scintillation counter (Packard Bioscience, Meriden, CT, USA). The activity of 5α-reductase was expressed as a ratio calculated by the equation [DHT/(T+DHT)] x 100.

3.6. Cell cycle analysis

The effect of bimatoprost on cell cycle progression was analyzed by flow cytometry after staining the cells with PI (Fried *et al.,* 1976). The immortalized DPCs (1.0×10^5 cells/mL in 100 mm dishes) were incubated with bimatoprost (0.12, 0.24, 1.2, or 2.4 μM) for 24 h. NIH3T3 fibroblasts (1.0×10^5 cells/mL in 100 mm dishes) were treated with minoxidil (75 μM) or bimatoprost (0.12, 0.24, 1.2, or 2.4 μM) for 48 h. In some cases, NIH3T3 fibroblasts were pre-treated with glibenclamide (50 μM) with or without bimatoprost (0.12, 0.24, 1.2, or 2.4 μM) for 48 h. Cells were trypsinized and washed twice with PBS. The cells were fixed overnight with 70% ethanol at -20°C. Next, the cells were washed with PBS, and incubated with 50 μg/mL RNase A at 37°C for 30 min. The cells were stained with a 50 μg/mL PI solution in the dark for 15 min. Flow cytometry analysis was performed using a FACScan flow cytometer (Becton-Dickinson, San Jose, CA, USA). Histograms were analyzed with Cell Quest software (Becton-Dickinson).

3.7. Western blot analysis

Immortalized DPC (1.0×10^5 cells/mL in 100 mm dishes) were pre-incubated in serum-free DMEM for 24 h, and then treated with bimatoprost (0.12, 0.24, 1.2, or 2.4 μM) for 24 h.

Additionally, NIH3T3 fibroblasts were seeded in 100 mm dishes at a density of 1.0×10^6 cells/dish. After incubating for 24 h, the cells were cultured in DMEM medium supplemented with 1.5% BCS for 24 h. The cells were then treated with bimatoprost (0.12, 0.24, 1.2, or 2.4 μM) or minoxidil (75 μM) for 48 h. Some cells were treated with bimatoprost (2.4 μM) for 0, 24, and 48 h. Other cells were pre-incubated with glibenclamide (50 μM) for 30 min, and then treated with bimatoprost (0.12, 0.24, 1.2, or 2.4 μM) or minoxidil (75 μM) for 48 h. The cells were trypsinized and washed twice with cold PBS. The cells were lysed in a lysis buffer (50 mM Tris–HCl (pH 7.5), 150 mM NaCl, 2 mM EDTA, 1 mM EGTA, 1 mM $NaVO_3$, 10 mM NaF, 1 mM DTT, 1 mM PMSF, 25 μg/mL aprotinin, 25 μg/mL leupeptin, and 1% NP-40) to obtain whole cell proteins and kept on ice for 30 min. The cell lysates were centrifuged at 15,000 rpm at 4°C for 15 min. Supernatants were stored at -20°C until analysis. Protein concentrations were determined by the Bradford method (Bradford, 1976). Equal amounts of protein were separated by sodium dodecyl sulfate polyacrylamide gel electrophoresis (SDS-PAGE) on 8~12% gels. The proteins were then transferred onto a polyvinylidene fluoride (PVDF) membrane (Bio-Rad, Hercules, CA, USA) in a glycine transfer buffer (192 mM glycine, 25 mM Tris-HCl (pH 8.8), 20% (v/v) MeOH) at 100 V for 2 h. After blocking with 5% nonfat dried milk in Tween-20-TBS (T-TBS) containing (50 mM Tris (pH 7.6), 150 mM NaCl, 0.1% Tween-20), the membrane was incubated with specific primary antibodies. Table 1 shows the primary antibodies

used for Western blotting. The membrane was incubated with secondary HRP-conjugated antibodies (1:5000 dilution) at room temperature for 1 h. The membrane was treated with West-zol reagent (INtRON), and then exposed to X-ray films (AGFA, Mortsel, Belgium) to detect protein bands. Band intensities were quantified with NIH Image software (http://rsb.info.nih.gov/ij/).

3.8. Immunofluorescence microscopy

Immortalized DPCs were seeded in chamber slides and pre-incubated in serum-free DMEM for 24 h. The cells were treated with bimatoprost (2.4 μM) for 0, 12, 18, and 24 h. Additionally, NIH3T3 fibroblasts were seeded in chamber slides and cells were cultured in DMEM supplemented with 1.5% BCS for 24 h. The cells were then treated with bimatoprost (2.4 μM) for 0, 1, 3, and 6 h. For immunofluorescence studies, the cells were fixed in 4% paraformaldehyde (PFA) for 15 min, washed in PBS, and permeabilized with 0.1% Triton X-100. After washing, the cells were then blocking with 1% bovine serum albumin (BSA) in T-TBS for 1 h at room temperature. The cells were incubated overnight with a rabbit polyclonal β-catenin antibody at 4°C. After being washed twice with PBS, the cells were incubated with a anti-rabbit secondary antibody coupled to Alexa Fluor 594 at room temperature for 1 h. Next, the cells were washed twice with PBS and mounted in VECTASHIELD with 4, 6-diamido-2-phenylindole (DAPI; Vector Laboratories, Burlingame, CA, USA). The cells

were examined by fluorescence microscopy (BX51, Olympus).

3.9. Statistical analysis

All results are expressed as the mean ± standard deviation (SD) or standard error (SE) of at least three independent experiments. Student's *t*-test was used to determine statistical significance (*P*-value <0.05) of the differences between the various experimental and control group results.

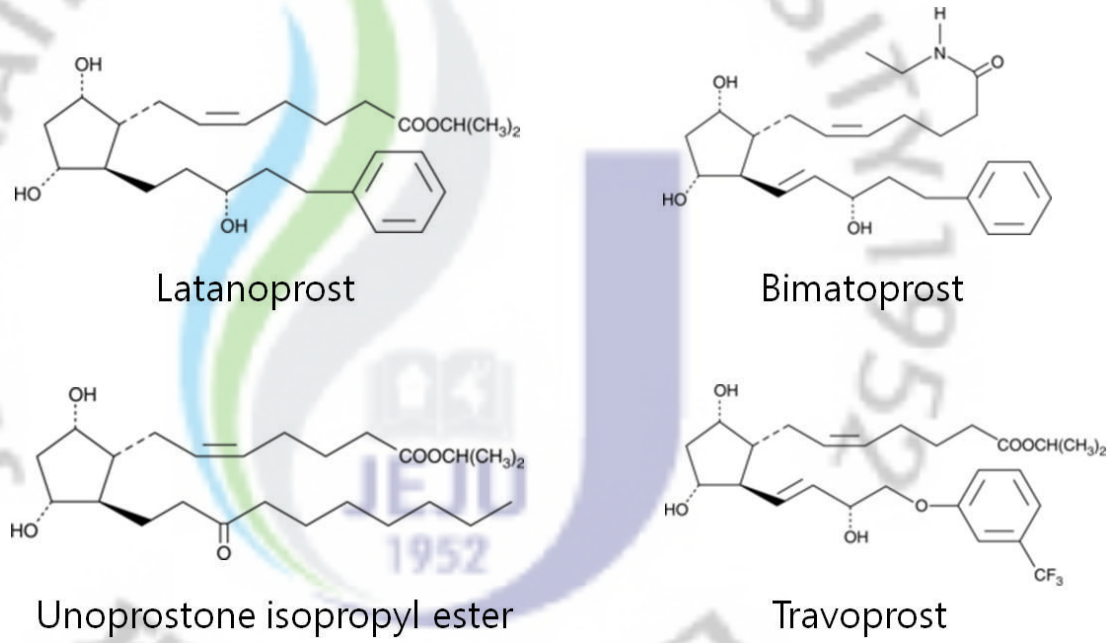

Figure 1. The structure of prostaglandin analogues.

Table 1. Antibodies used in Western blot analysis on immortalized DPC and NIH3T3 fibroblasts.

Antibody	Origin	Company
CDK2	Rabbit polyclonal	Santa Cruz Biotechnology
Cyclin E	Rabbit polyclonal	Santa Cruz Biotechnology
$p27^{kip1}$	Rabbit polyclonal	Santa Cruz Biotechnology
Procaspase-3	Rabbit polyclonal	Santa Cruz Biotechnology
Bax	Rabbit polyclonal	Santa Cruz Biotechnology
Tubulin-α	Mouse monoclonal	Santa Cruz Biotechnology
β-catenin	Rabbit polyclonal	Santa Cruz Biotechnology
Cox-2	Goat polyclonal	Santa Cruz Biotechnology
SUR2B	Goat polyclonal	Santa Cruz Biotechnology
Kir6.1	Goat polyclonal	Santa Cruz Biotechnology
Bcl-2	Rabbit monoclonal	Cell signaling Technology
phospho-Akt	Rabbit polyclonal	Cell signaling Technology
Akt	Rabbit polyclonal	Cell signaling Technology
β-actin	Mouse monoclonal	Sigma

4. Results

4.1. Bimatoprost increases the proliferation of immortalized DPC and elongation of rat vibrissa follicles, but not 5α-reductase inhibition

To evaluate the effects of PG analogues on cell proliferation in hair follicles, the proliferation of immortalized DPCs was examined. When immortalized DPCs were treated with the different PG analogues (0.024, 0.24, or 2.4 μM) for 96 h, bimatoprost increased the proliferation of immortalized DPCs compared to control (Table 2). To determine whether bimatoprost increased hair growth, we examined the effect of bimatoprost using a vibrissa follicle organ culture. Rat vibrissa follicles were treated with bimatoprost (0.024, 0.12, 0.24, or 1.2 μM), and the effect on hair fiber growth in the vibrissa follicles was observed for 3 wk. As shown in Fig. 2A, treatment with bimatoprost increased in the length of the vibrissa follicles (0.024 μM, 126.8 ± 11.3%; 0.12 μM, 175.6 ± 34.2%; 0.24 μM, 146.3 ± 15.9%; 1.2 μM, 82.9 ± 12.4%). These data suggest that bimatoprost stimulates hair growth.

Furthermore, inhibition of 5α-reductase activity is known to be important for preventing hair loss (Kaufman, 1996). When we examine the effect of bimatoprost on 5α-reductase, we found that bimatoprost slightly inhibited 5α-reductase activity (Fig. 2B). These results suggest that the effect of bimatoprost on the hair growth involves the proliferation of immortalized DPCs rather than inhibition of 5α-reductase.

Table 2. Effects of prostaglandin analogues on the proliferation of immortalized DPC.

Concentration (μM)	Proliferation (% of Control)		
	0.024	0.24	2.4
Latanoprost	95.6 ± 0.9	102.2 ± 2.1	92.6 ± 2.1
Bimatoprost	104.9 ± 1.9	106.3 ± 5.3 *	101.8 ± 6.6
Unoprostone isopropyl ester	92.1 ± 6.1	96.1 ± 4.7	18.1 ± 6.8
Travoprost	104.8 ± 0.3	103.2 ± 10.3	44.5 ± 3.7

(A)

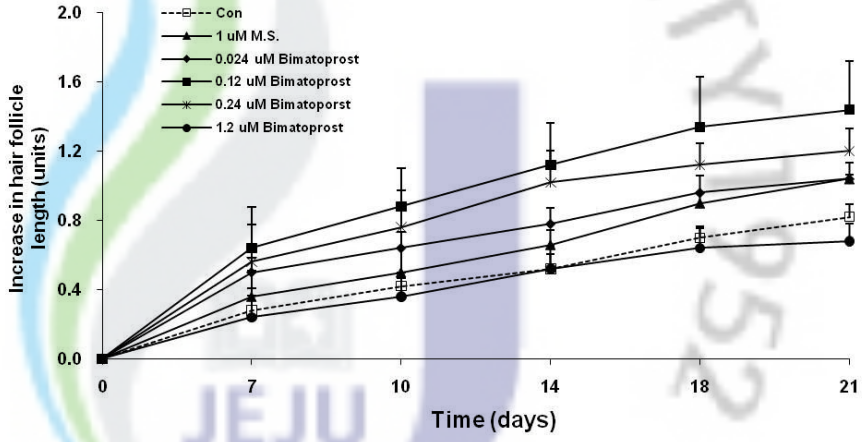

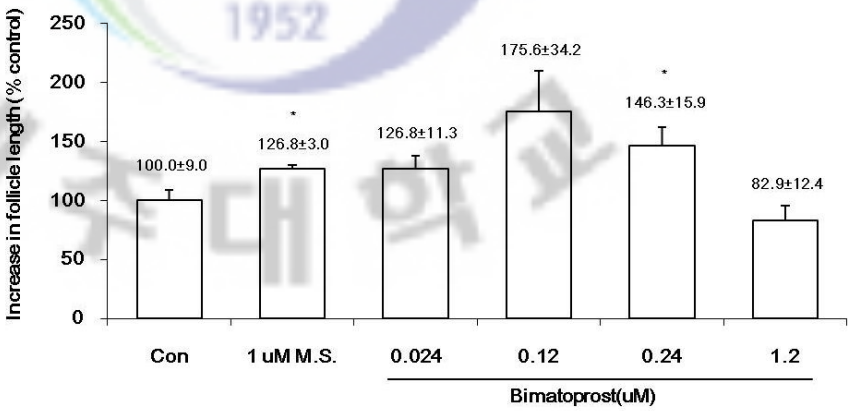

(B)

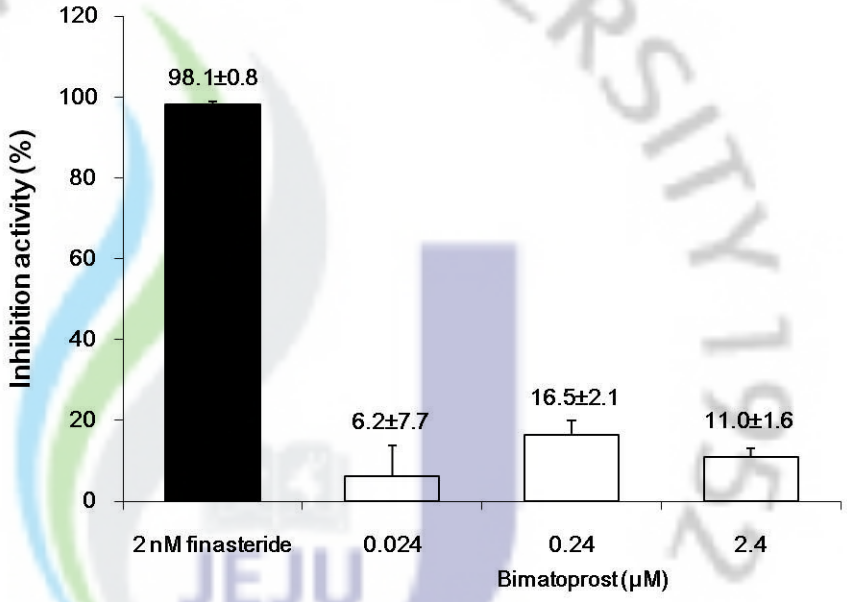

Figure 2. Bimatoprost increases rat vibrissa follicle elongation but not does not inhibit 5α-reductase. (A) Cultures of rat vibrissa follicles were established as described in "Materials and Methods". Minoxidil sulfate (MS) served as a positive control. The difference in the length of vibrissa follicles of the control group on day 21 was considered to be 100%. Data are expressed as the mean ± SE of three independent experiments. (B) 5α-reductase inhibition was measured as described in "Materials and Methods". The inhibition ratio representing the conversion of testosterone to DHT was calculated and expressed as a percentage of the control. Finasteride was used as a positive control. Data are expressed as the mean ± SD of three independent experiments. *$p < 0.05$ compared to the control.

4.2. Bimatoprost increases the proliferation of immortalized DPC through the regulation of the cell cycle, Wnt/β-catenin, and Cox-2

To further explore the effect of bimatoprost on immortalized DPC proliferation, cell cycle progression was analyzed by flow cytometry for 24 h. Fig. 3A shows that bimatoprost reduced the population of sub-G1 phase cells (1.2 μM, 12.11%; 2.4 μM, 8.59%) compared to the percentage of control cells in the sub-G1 phase (16.01%). Moreover, the population of cells in the S phase slightly increased from 3.89% to 5.33% following treatment with bimatoprost (2.4 μM), and the percentage of cells in the G2/M phase increased from 15.86% to 17.94%. These results suggest that bimatoprost stimulates the proliferation of immortalized DPCs by altering the cell cycle.

To determine whether bimatoprost-induced cell cycle progression is related to the expression of cell cycle-associated proteins, immortalized DPCs were treated with various concentrations of bimatoprost for 24 h. The resulting cell extracts were analyzed by immunoblotting for cyclin E and CDK2, which are required for the G1-to-S phase transition in mammalian cells (Radzio-Andzelm *et al.,* 1995). Consistent with the flow cytometry result, bimatoprost increased the expression of cyclin E and CDK2 (Fig. 3B). We also determined whether bimatoprost-induced cell cycle progression is related to $p27^{kip1}$ expression using immunoblot analysis. Bimatoprost did not affect the protein level of $p27^{kip1}$

in immortalized DPCs (Fig. 3B). These results indicate that bimatoprost increased the expression of cyclin E and CDK2, and led to changes in the cell cycle of immortalized DPC.

In the presence of Wnt signaling, β-catenin migrates to the nucleus and activates the transcription of cyclin D1 (Tetsu *et al.,* 1999). To investigate the contribution of β-catenin to cell cycle progression, Western blot analysis was performed. When immortalized DPCs were treated with various concentrations of bimatoprost for 24 h, bimatoprost increased the total level of β-catenin (Fig. 3C). To evaluate whether bimatoprost also induced nuclear tanslocation of β-catenin, immortalized DPCs were treated with bimatoprost (2.4 μM) for 0, 12, 18, and 24 h. At all time points, increased nuclear β-catenin levels were confirmed using immunofluorescence microscopy (Fig. 3D). Cox-2 expression is increased by various stimului such as cytokines and growth factors. Rofecoxib, a selective Cox-2 inhibitor, reduces tumor growth by decreasing cyclin D1 levels and increasing $p21^{waf1}$ expression (Tseng *et al.,* 2002). The expression patterns of cyclin D1 and cyclin E in neurons are similar to those of Cox-2 (Hoozemans *et al.,* 2002). In particular, induction of Wnt was reported to cause transcriptional activation of Cox-2 (Howe *et al.,* 1999). We thus investigated the effect of bimatoprost on Cox-2 expression. Treatment of immortalized DPCs with various concentrations of bimatoprost caused up-regulation of Cox-2 expression (Fig. 3E). These results suggest that bimatoprost can induce cell cycle progression at least in part via up-

regulation of β-catenin and Cox-2.

(A)

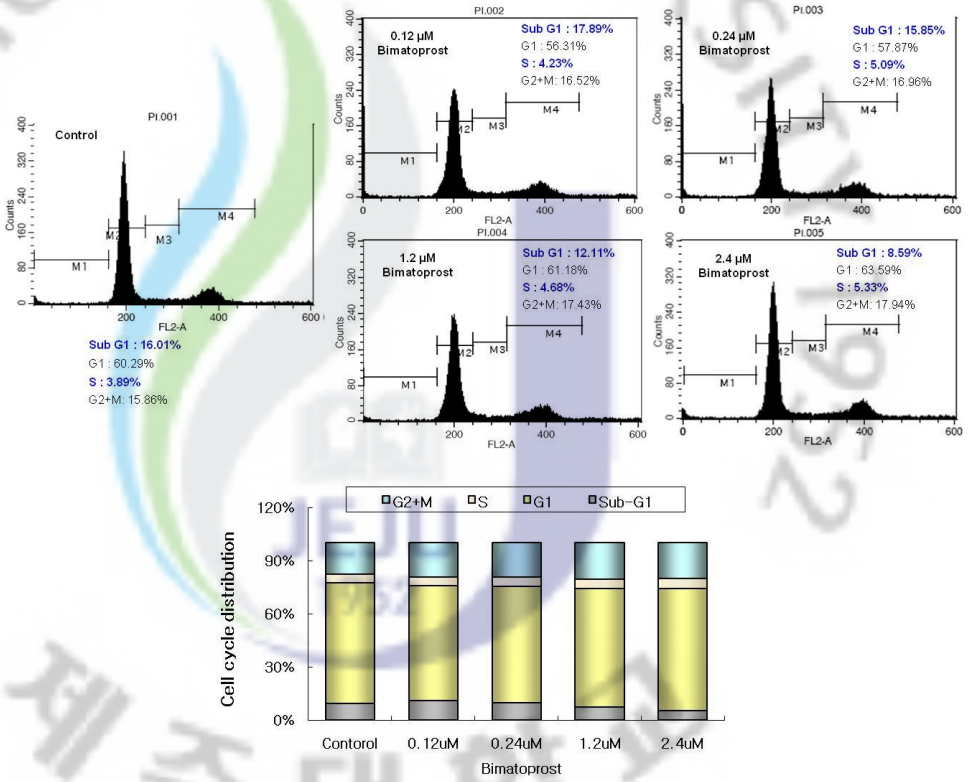

(B)

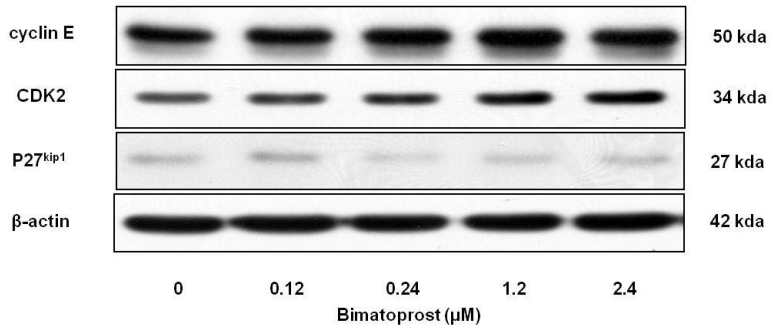

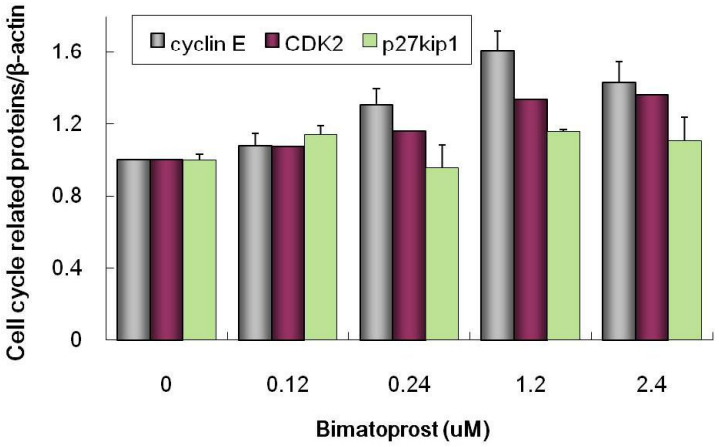

(C)

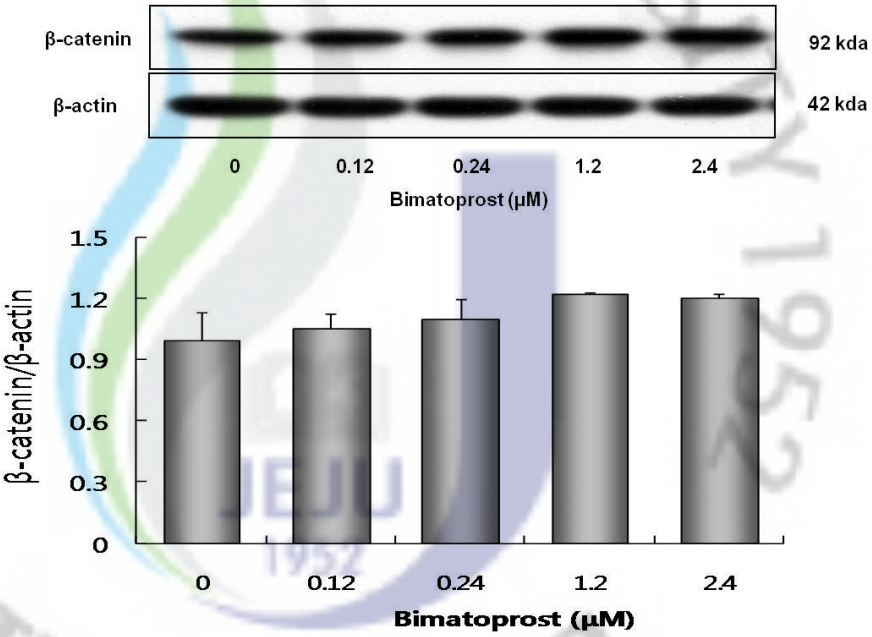

(D)

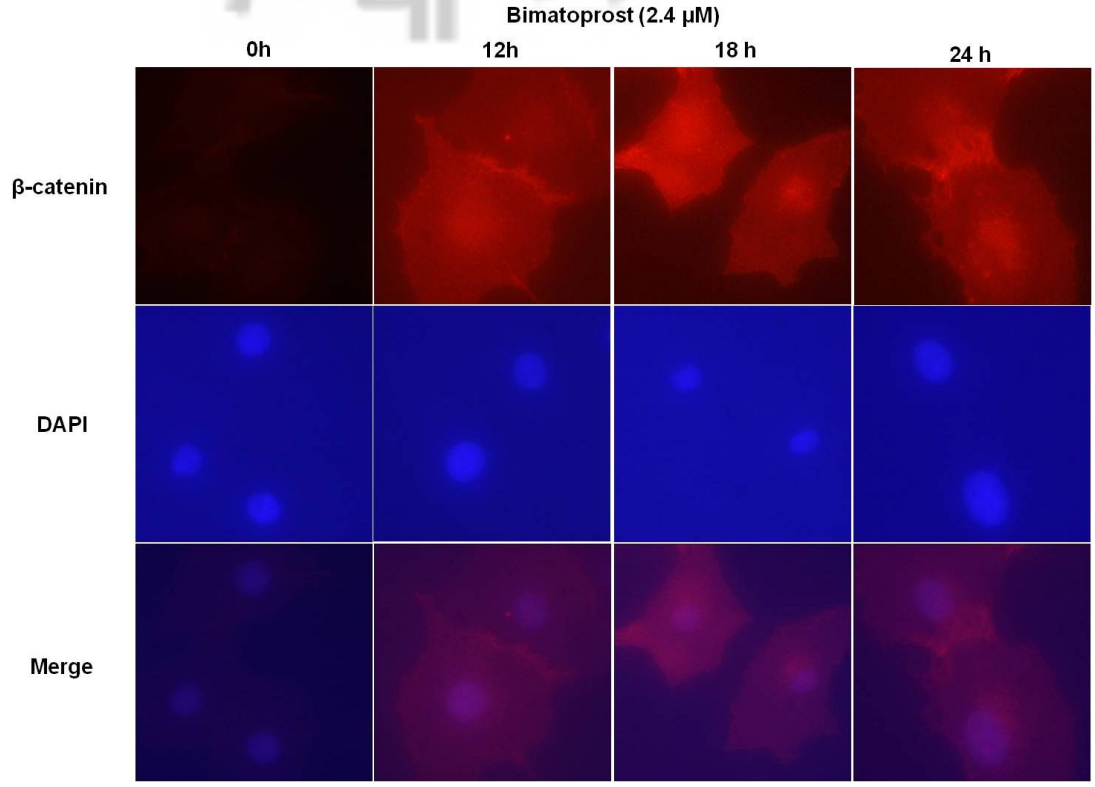

(E)

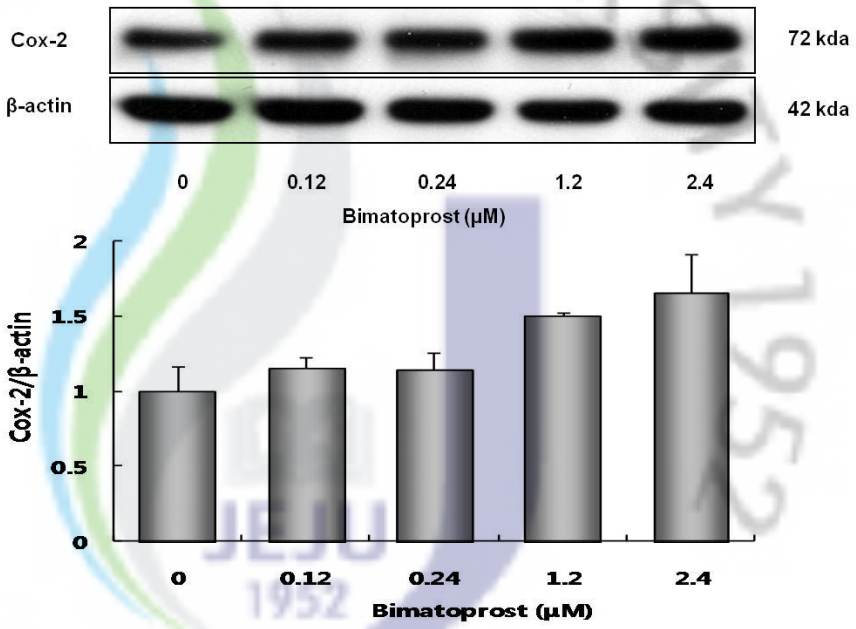

Figure 3. Bimatoprost increases the proliferation of immortalized DPCs through the regulation of the cell cycle, Wnt/β-catenin, and Cox-2. (A) Immortalized DPCs were treated with various concentrations of bimatoprost for 24 h. Cells were collected and fixed with 70% ethanol. The fixed cells were stained with PI and analyzed by flow cytometry. (B) The immortalized DPCs were treated with various concentrations of bimatoprost for 24 h. Lysates were prepared from the immortalized DPCs, and the effects of bimatoprost on the expression of cyclin E, CDK2, and $p27^{kip1}$ were analyzed by Western blotting using specific antibodies. (C) Immortalized DPCs were treated with or without bimatoprost for 24 h. The expression of β-catenin was measured in whole cell lysates from immortalized DPCs by Western blotting. The lower panel presents the mean ± SE of three independent experiments.

(D) Immortalized DPCs were treated with bimatoprost (2.4 μM) for 0, 12, 18, and 24 h. For immunostaining, the cells were prepared as described in “Materials and Methods”. Nuclei were stained with DAPI (blue). Subcellular localization of β-catenin (red) was analyzed using fluorescence microscopy. (E) Immortalized DPCs were treated with or without bimatoprost for 24 h. The expression of Cox-2 was measured in whole cell lysates from immortalized DPCs by Western blotting. The lower panel displays the mean ± SE of three independent experiments.

4.3. Bimatoprost increases NIH3T3 fibroblast proliferation through the regulation of cell cycle and apoptosis

In the absence of streptomycin, reagents that open K_{ATP} channel such as minoxidil have a mitotic effect on NIH3T3 fibroblasts (Sanders *et al.,* 1996). Using an MTT assay, we therefore examined whether PG analogues increase the proliferation of NIH3T3 cells. As shown in Table 3, NIH3T3 fibroblast proliferation was significantly increased by treatment with PG analogues. Among these compounds, we chose bimatoprost for further studies because this reagent increased the proliferation of both immortalized DPC and NIH3T3 fibroblasts.

To determine whether the proliferative effects of bimatoprost on NIH3T3 fibroblasts is mediated through cell cycle progression, cell cycle distribution was analyzed by flow cytometry for 48 h. Among the control cells, 21.35 ± 7.96% were in the sub-G1 phase. When NIH3T3 fibroblasts were treated with bimatoprost (0.12, 0.24, 1.2, or 2.4 μM), the percentage of cells in the sub-G1 phase decreased by 8.68 ± 4.36%, 5.20 ± 1.48%, 3.85 ± 0.82%, and 4.95 ± 0.93%, respectively (Fig. 4A). After treatment with minoxidil (75 μM), the percentage of cells in the sub-G1 phase also decreased by 13.81 ± 5.13%.

To determine whether bimatoprost-induced cell cycle progression is related to the expression of $p27^{kip1}$, NIH3T3 fibroblasts were treated with bimatoprost (2.4 μM) for 0, 24,

and 48 h. Bimatoprost decreased the expression $p27^{kip1}$ (Fig. 4B). To examine whether bimatoprost could block apoptosis induced by incubation with low serum media, NIH3T3 fibroblasts were incubated for 24h in DMEM medium supplemented with 1.5% BCS. The cells were then treated with bimatoprost (2.4 μM) for 0, 24 and 48 h. Bimatoprost treatment resulted in the inhibition of apoptosis through decreased Bax levels along with increased Bcl-2 levels (Fig. 4C). These results suggest that bimatoprost might have potent mitogenic activity in NIH3T3 fibroblasts by down-regulation of $p27^{kip1}$, and Bax, and up-regulation of Bcl-2.

Table 3. Effects of prostaglandin analogues on the proliferation of NIH3T3 fibroblasts.

Concentration (μM)	Proliferation (% of Control)			
	0.024	0.12	0.24	1.2
Latanoprost	143.5 ± 3.3 *	146.1 ± 11.3 *	145.0 ± 18.2 *	158.3 ± 14.6
Bimatoprost	123.1 ± 11.3 **	136.6 ± 10.6 **	135.3 ± 13.6 **	149.8 ± 14.4 **
Unoprostone isopropyl ester	100.4 ± 7.1	105.5 ± 6.6	107.0 ± 8.6	110.8 ± 10.3
Travoprost	142.2 ± 13.8 *	150.4 ± 12.1 *	141.3 ± 12.5 *	142.7 ± 10.5 *
Minoxidil (75 uM)	121.9 ± 11*			

(A)

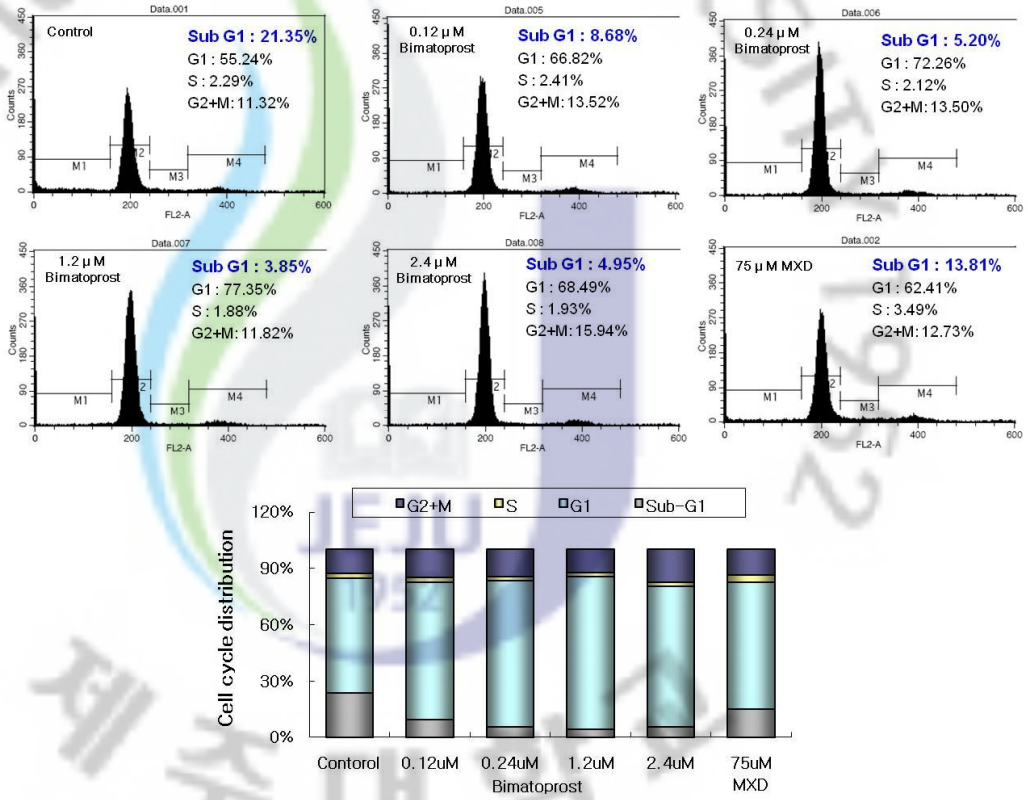

(B)

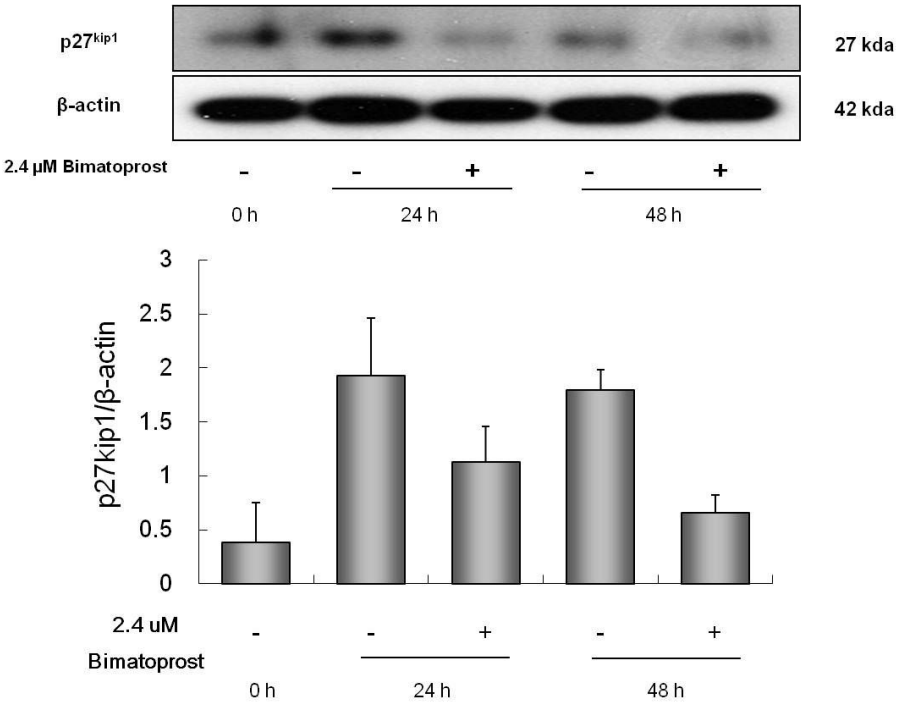

(C)

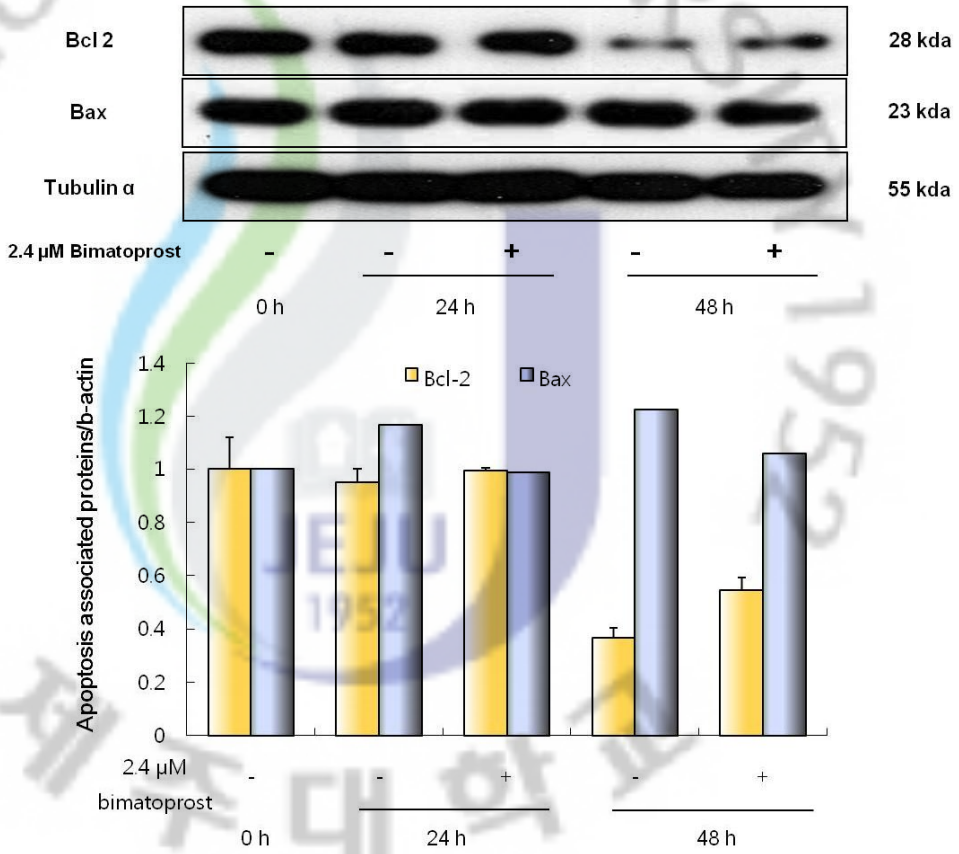

Figure 4. Bimatoprost increases the proliferation of NIH3T3 fibroblasts through cell cycle regulation and inhibition of apoptosis. (A) NIH3T3 fibroblasts were treated with various concentrations of bimatoprost and minoxidil (MXD) for 48 h. The fixed cells were stained with PI and analyzed by flow cytometry. (B and C) NIH3T3 fibroblasts were treated with bimatoprost (2.4 μM) for 0, 24, and 48 h. Lysates were prepared from NIH3T3 fibroblasts and the effects of bimatoprost on the expression $p27^{kip1}$, Bcl-2, and Bax were analyzed by Western blotting with specific antibodies. The lower panel displays the mean ± SE of three independent experiments.

4.4. Bimatoprost regulates the expression of β-catenin and Cox-2 in NIH3T3 fibroblasts

Up-regulation of β-catenin expression is a crucial event during cell proliferation (Masckauchan *et al.,* 2005). To determine whether bimatoprost increased the expression of β-catenin in NIH3T3 fibroblasts, the cell were treated with bimatoprost (0.12, 0.24, 1.2, or 2.4 μM) or minoxidil (75 μM) for 48 h. The cell extracts were analyzed by Western blotting. Bimatoprost treatment increased the level of β-catenin compared to control cells treated with vehicle (Fig. 5A). After treatment with bimatoprost (2.4 μM) for 0, 1, 3, and 6 h, the localization of β-catenin was analyzed by immunofluorescence microscopy. Consistent with the total protein levels, treatment with bimatoprost increased the nuclear translocation of β-catenin (Fig. 5B).

Etopic expression of β-catenin increases the level of Cox-2 in chondrocytes (Kim *et al.,* 2002). By immunoblotting, we examined whether bimatoprost could increase the expression of Cox-2. When NIH3T3 fibroblasts were incubated with bimatoprost (0.12, 0.24, 1.2, or 2.4 μM) or minoxidil (75 μM) for 48 h, both reagents up-regulated the expression of Cox-2 compared to control cells treated with vehicle (Fig. 5C). These results indicate that bimatoprost increased the expression β-catenin and Cox-2 in NIH3T3 fibroblasts.

(A)

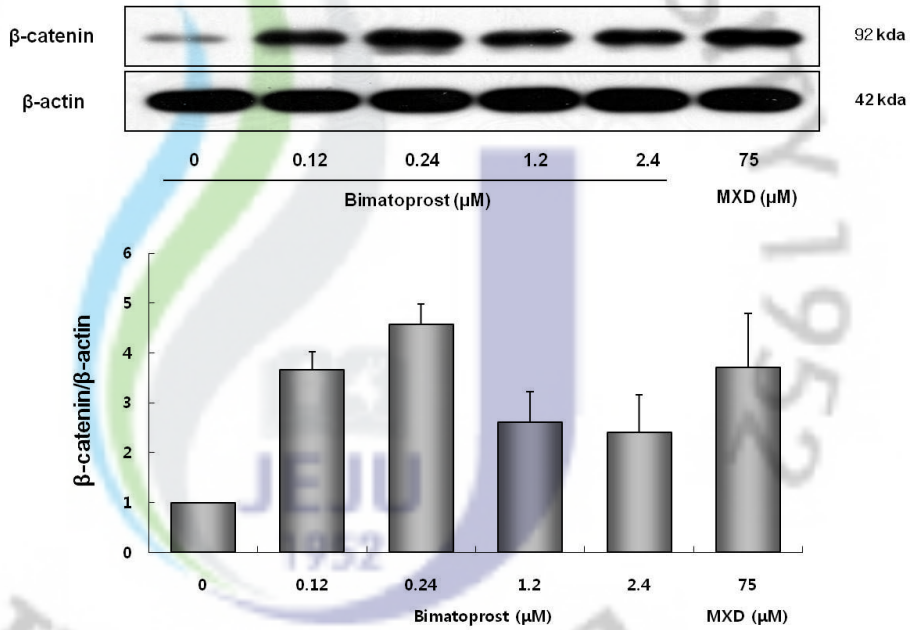

(B)

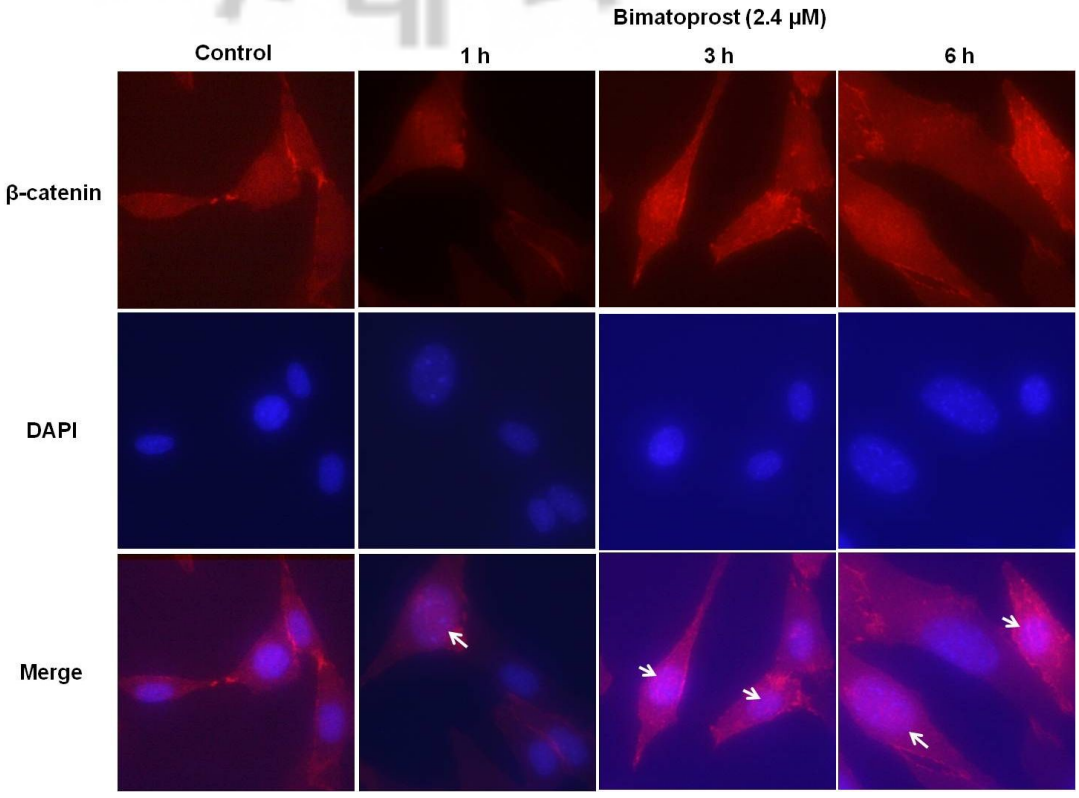

(C)

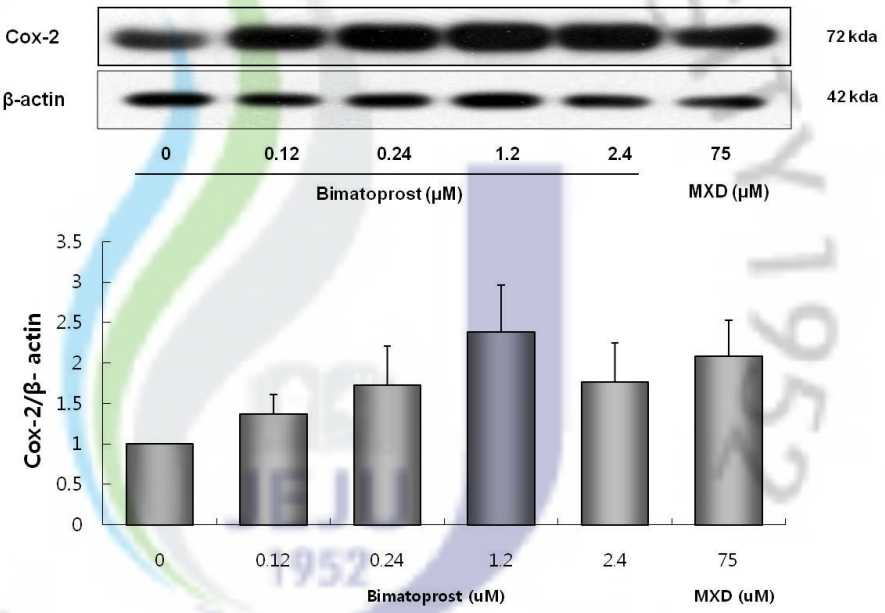

Figure 5. Bimatoprost regulates the expression of β-catenin and Cox-2 in NIH3T3 fibroblasts. (A) NIH3T3 fibroblasts were treated with various concentrations of bimatoprost and MXD for 48 h. Whole cell lysates from NIH3T3 fibroblasts were analyzed for the expression of β-catenin by Western blotting. The lower panel shows the mean ± SE of three independent experiments. (B) NIH3T3 fibroblasts were treated with bimatoprost (2.4 μM) for 0, 1, 3, and 6h. For immunostaining, cells were prepared as described in "Materials and Methods". Nuclei were stained with DAPI (blue). Cellular localization of β-catenin (red) was analyzed using fluorescence microscopy. (C) NIH3T3 fibroblasts were treated with various concentrations of bimatoprost and MXD for 48 h. The expression of Cox-2 was measured in whole cell lysates from NIH3T3 fibroblasts were by Western blotting. The lower panel displays the mean ± SE of three independent experiments.

4.5. Bimatoprost increases the proliferation of NIH3T3 fibroblasts through K_{ATP} channels

We examined the expression of K_{ATP} channels in immortalized DPCs and NIH3T3 fibroblasts. Whole cell lysates were analyzed by immunoblotting, and we found that SUR2B and Kir6.1, two K_{ATP} channel subunits, were expressed in immortalized DPCs and NIH3T3 fibroblasts (Fig. 6A). In particular, bimatoprost significantly increased the proliferation of NIH3T3 fibroblasts (Table 3). To examine whether proliferation of NIH3T3 is regulated by K_{ATP} channels, NIH3T3 fibroblasts were pre-treated with glibenclamide (50 μM), a K_{ATP} channel blocker, for 30 min prior to incubation with bimatoprost for 48 h. As shown in Fig. 6B, glibenclamide inhibited bimatoprost-induced proliferation. Stimulation of NIH3T3 fibroblasts with glibenclamide (50 μM) for 2 d did not alter cell proliferation compared to control cells treated with vehicle (Fig. 6B). These results imply that bimatoprost increased the proliferation of NIH3T3 fibroblasts via K_{ATP} channels.

To further examine the effect of bimatoprost on cell cycle regulation, NIH3T3 fibroblasts were pre-treated with glibenclamide (50 μM) for 30 min. The cells were subsequently treated with bimatoprost (0.12, 0.24, 1.2, or 2.4 μM) or minoxidil (75 μM) for 48 h. Change of cell cycle distribution was analyzed by flow cytometry. As shown in Fig. 6C, glibenclamide increased the population of cell in the sub-G1 phase by 30.64% whereas population of

control cells in the sub-G1 phase was 14.98%. The increased number of cells in the sub-G1 phase induced by glibenclamide was attenuated by bimatoprost (0.12 μM, 22.69%; 0.24 μM, 19.79%; 1.2 μM, 18.31%; and 2.4 μM, 14.88%). Minoxidil also decreased the sub-G1 cell population compared to the control cells; this effect was also attenuated by glibenclamide. These results suggest that bimatoprost reduced the accumulation of cells in the sub-G1 phase via activation of K_{ATP} channels.

(A)

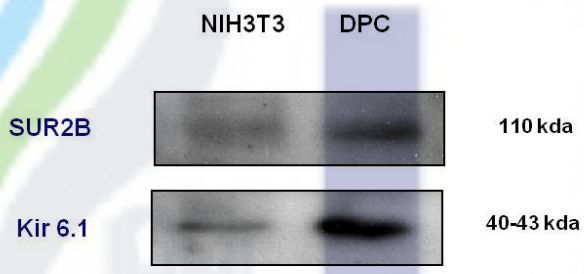

(B)

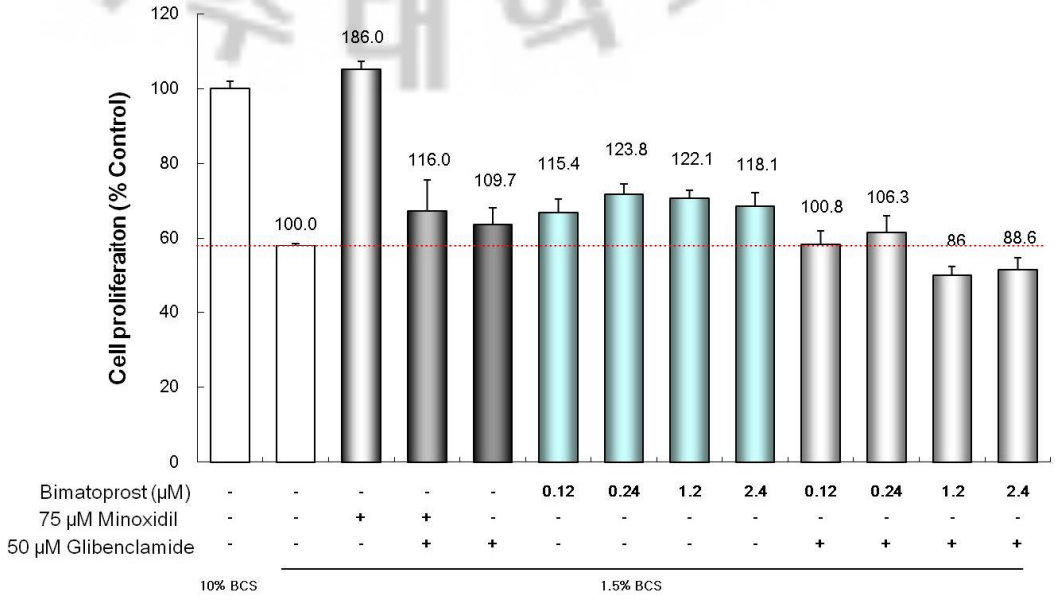

(C)

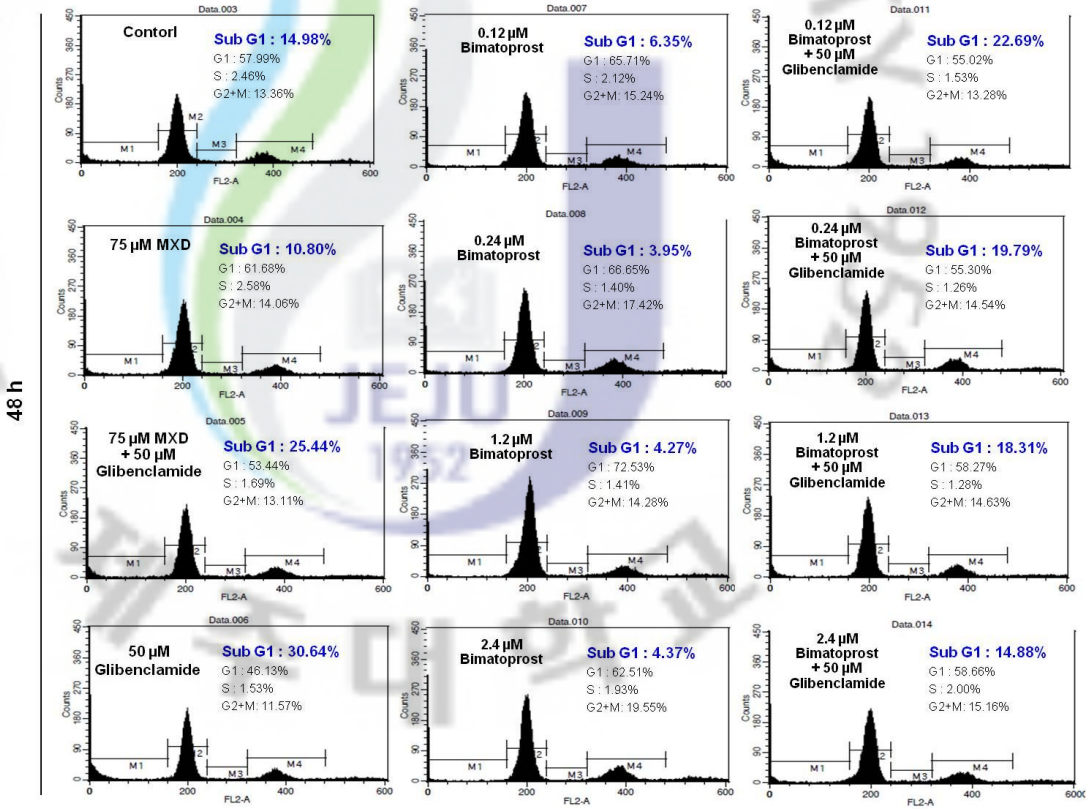

Figure 6. Bimatoprost increases the proliferation of NIH3T3 fibroblasts by opening K_{ATP} channels. (A) The expression of SUR2B and Kir6.1 was measured in whole cell lysates by Western blotting. (B) NIH3T3 fibroblasts were pre-incubated with glibenclamide (50 μM) for 30 min and then treated with bimatoprost (0.12, 0.24, 1.2, or 2.4 μM) or MXD (75 μM) for 48 h. After 2 d, cell viability was measured using an MTT assay. NIH3T3 fibroblast viability is expressed as a percentage of control cell growth in 1.5% BCS for 48 h. Data are presented as the mean ± SE of three independent experiments. (C) NIH3T3 fibroblasts were

pre-incubated with glibenclamide (50 μM) for 30 min and then treated with bimatoprost (0.12, 0.24, 1.2, or 2.4 μM) or MXD (75 μM) for 48 h. Cells were collected and fixed with 70% ethanol. The fixed cells were stained with PI and analyzed by flow cytometry.

4.6. Bimatoprost regulates the expression of apoptosis factors, β-catenin, and Cox-2 via the PI3K/Akt pathway

The PI3K/Akt signaling pathway is crucial for cell survival and proliferation (Datta *et al.,* 1999). To evaluate whether PI3K/Akt signaling is required for NIH3T3 proliferation, the cells were treated with bimatoprost (0.12, 0.24, 1.2, or 2.4 μM) or minoxidil (75 μM) for 15 min. Total proteins were obtained and then analyzed by immunoblotting. As shown in Fig. 7A, phosphorylation of Akt was increased after treatment with bimatoprost. Minoxidil treatment also resulted in a dramatic increase of Akt phosphorylation (Fig. 7A). These observations indicate that bimatoprost increased cell proliferation through activation of the PI3K/Akt pathway.

To further elucidate whether Akt phosphorylation is regulated by K_{ATP} channels, the effects of glibenclamide, a K_{ATP} channel blocker, were evaluated. NIH3T3 fibroblasts were pre-treated with glibenclamide (50 μM) for 30 min prior incubation with bimatoprost (2.4 μM) or minoxidil (75 μM) for 48 h. As shown in Fig. 7B, glibenclamide attenuated bimatoprost-induced phosphorylation of Akt. These data suggest that the effects of bimatoprost on Akt phosphorylation are mediated through K_{ATP} channels.

The Akt pathway plays an important role in the regulation of apoptosis (Datta *et al.,* 1999, Yamaguchi *et al.,* 2001). Bcl-2 is also involved in apoptosis regulation (Vander Heiden *et al.,*

1999, Yang *et al.,* 1997). In this study, the effects of bimatoprost and glibenclamide on the expression of Bcl-2 were examined in NIH3T3 fibroblasts. As shown in Fig. 7C, bimatoprost treatment increased the level of Bcl-2. Glibenclamide reversed bimatoprost-induced changes in Bcl-2 expression. These results suggest that bimatoprost decreased apoptosis through the activation of K_{ATP} channels.

To investigate whether K_{ATP} channels could control the up-regulation of β-catenin and Cox-2 through bimatoprost, NIH3T3 fibroblasts were pre-treated with glibenclamide (50 μM) for 30 min. After subsequent treatment with bimatoprost (2.4 μM) or minoxidil (75 μM) for 48 h, glibenclamide was found to effectively inhibit the up-regulation of β-catenin and Cox-2 expression by induced bimatoprost as well as the up-regulation of β-catenin and Cox-2 levels induced by minoxidil (Fig. 7D). These results indicate that bimatoprost could increase the expression of β-catenin and Cox-2 through activation of K_{ATP} channels, which led to the proliferation of NIH3T3 fibroblasts.

(A)

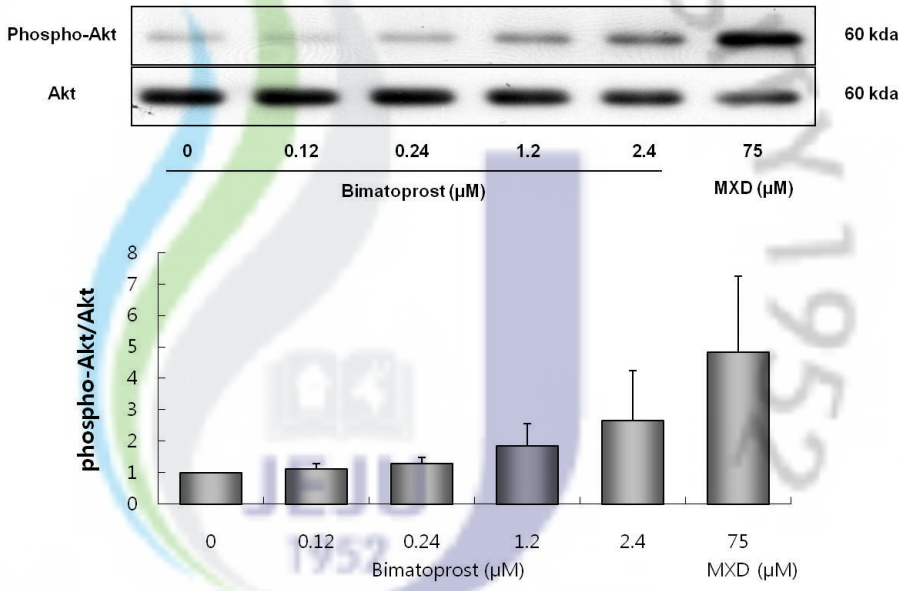

(B)

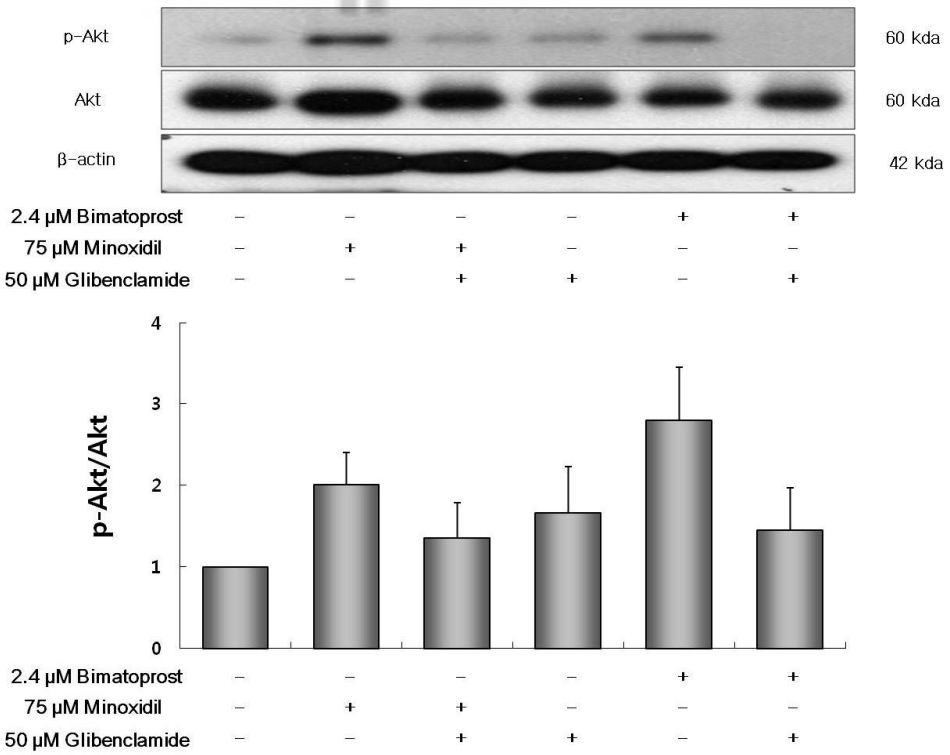

(C)

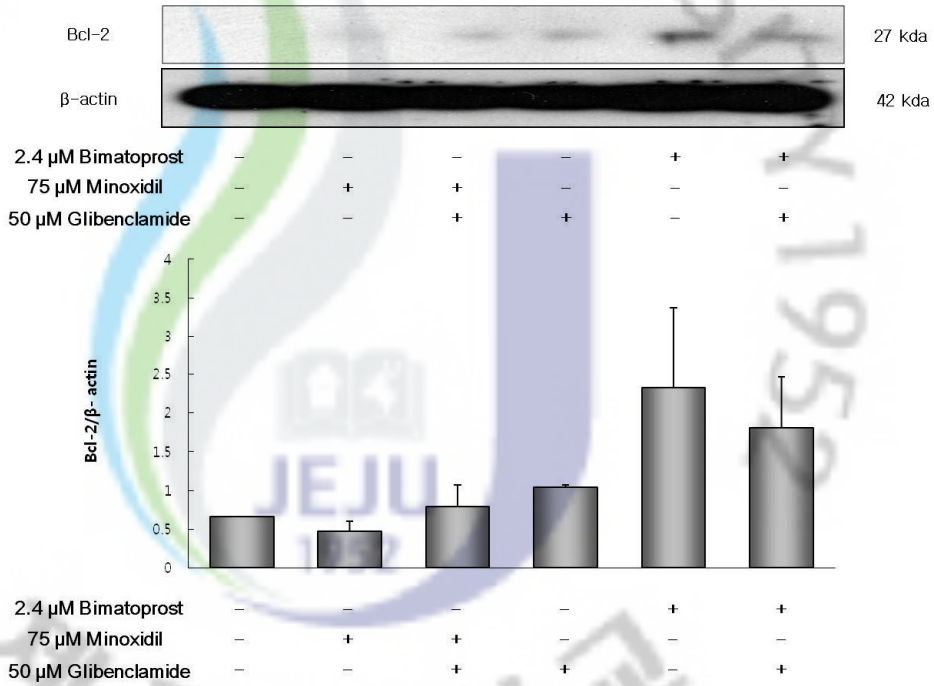

(D)

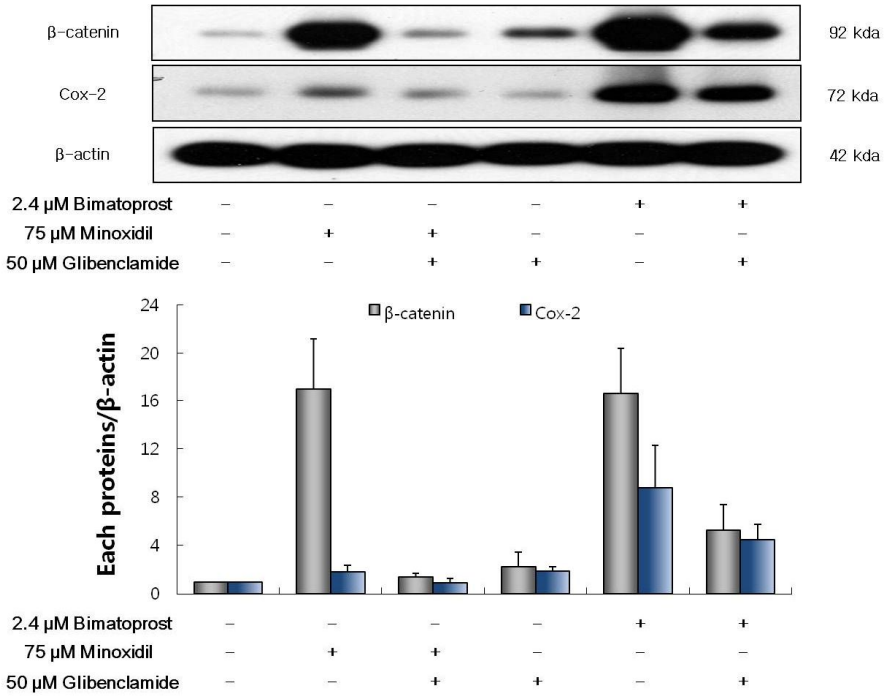

Figure 7. Bimatoprost regulates the expression of apoptosis factors β-catenin and Cox-2 via PI3K/Akt pathway regulation. (A) NIH3T3 fibroblasts were treated with bimatoprost or MXD for 15 min. The expression of phospho-Akt and Akt was measured in whole cell lysates by Western blotting. The lower panel displays the mean ± SE of three independent experiments. (B, C and D) NIH3T3 fibroblasts were pre-incubated with glibenclamide (50 μM) for 30 min and then treated with bimatoprost (2.4 μM) or MXD (75 μM) for 48 h. The expression of phospho-Akt, Akt, Bcl-2, β-catenin, and Cox-2 was measured in whole cell lysates by Western blotting. The lower panel shows the mean ± SE of three independent experiments.

5. Discussion

Alopecia is a common issue in today's society. Identifying agents that are effective against alopecia would improve the quality of life for individuals with this condition. PGE_2 and $PGF_{2\alpha}$ analogues are known to promote hair growth (Johnstone *et al.,* 2002, Sasaki *et al.,* 2005a), but the mechanisms of their actions are not fully understood. PGE_2 can increase cell proliferation via the Wnt/β-catenin pathway (Castellone *et al.,* 2005) while the production of PGE_2 is increased by minoxidil, a compound that opens K_{ATP} channels (Michelet *et al.,* 1997). These findings indicate that K_{ATP} channels may regulate Wnt/β-catenin and PG pathways. Conversely, we hypothesized that PGs could act as activators of K_{ATP} channels and lead to increased cell proliferation. In this study, we investigated the effects of PG analogues on cell proliferation, and demonstrated that bimatoprost, a PGF2a analogue, promote proliferation through the Wnt/β-catenin pathway, Cox-2 expression, and K_{ATP} channels.

Hair follicles are complex mini-organs which contain several epithelial cells (HS, IRS, and ORS) and specialized dermal cells (DPCs). DPCs play important roles in the regulation of hair growth cycle (Stenn *et al.,* 2001). K_{ATP} channel subunits, including Kir 6.1 and SUR2B, expressed in DPCs are responsible for minoxidil action (Shorter *et al.,* 2008). DNA synthesis

in hair follicles enhanced by minoxidil sulfate in a time-dependent manner (Imai *et al.,* 1993) while minoxidil may promote hair growth by stimulating cell proliferation and PG synthesis (Messenger *et al.,* 2004). Minoxidil also has a mitogenic effect on NIH3T3 fibroblasts through K_{ATP} channels (Sanders *et al.,* 1996).

Among the PG analogues we tested, bimatoprost showed promoted the proliferation of immortalized DPCs and NIH3T3 fibroblasts (Table 2 and 3) and increased hair-fiber length in vibrissa follicles (Fig. 2A). We further investigated the effect of bimatoprost on cell cycle regulation in immortalized DPCs and NIH3T3 fibroblasts. The mammalian cell cycle is a tightly regulated process. The transition from G1 to S phase is driven by activation of cyclins/CDKs. (Prall *et al.,* 1997). Previous reports showed that regulators of cell cycle components (include cyclins/CDKs and CDK inhibitos) have pivotal roles in cell proliferation (Johnson *et al.,* 1999). Treatment with bimatoprost induced cell cycle progression in immortalized DPCs and NIH3T3 fibroblasts (Fig. 3A and 4A). Moreover, bimatoprost increased the expression of cyclin E and CDK2 in immortalized DPCs (Fig. 3B). Bimatoprost treatment resulted in decreased sub-G1 populations and $p27^{kip1}$ expression in NIH3T3 fibroblasts (Fig. 4A and B). However, stimulation of immortalized DPCs with bimatoprost did not affect the level of $p27^{kip1}$ (Fig. 3B).

It is well known that a characteristic of apoptosis is accumulation of cell in the sub-G1

phase (Bunz *et al.,* 1999). Control of apoptosis depends upon the balance between anti- and pro-apoptotic factors (Zhang *et al.,* 2000). Activation of apoptotic factors results in cytochrome-c release and caspase activation (Yang *et al.,* 1997). In the present study, we examined whether bimtoprost can control apoptosis-related factors such as Bax, and Bcl-2 in NIH3T3 fibroblasts. As shown in Fig. 4C, bimatoprost decreased Bax level, and increased the level of Bcl-2. These results indicate that bimatoprost induces proliferation through the down-regulation of $p27^{kip1}$, and Bax, and the up-regulation of Bcl-2, cyclin E, and CDK2. PGE_2 inhibits apoptosis via up-regulation of Bcl-2 (Sheng *et al.,* 1998). $PGF_{2\alpha}$ increases cell survival *in vitro* and *in vivo* by up-regulating BRUCE, inhibitor of apoptosis protein (Jansen *et al.,* 2008). Taken together, these results suggest that PGs can promote cell survival by blocking apoptotic events.

PI3K/Akt is a major regulator of cell survival and apoptosis. Akt phosphorylation appears to promote cell survival (Datta *et al.,* 1999). Activation of Akt is known to effectively suppress cell death through the down-regulation of several apoptosis-related factors (Yamaguchi *et al.,* 2001). Previous studies revealed that the Akt signaling pathway is also involved in opening K_{ATP} channels. Diazoxide, a reagent that causes K_{ATP} channels to open, helps to protect apoptosis via the Akt pathway (Wang *et al.,* 2004). In human DPCs, minoxidil increases cell proliferation through activation of Akt (Han *et al.,* 2004). These

studies indicate that the K_{ATP} channels may be involved in the regulation of cell proliferation through the Akt pathway. In this study, expression of SUR2B and Kir6.1 was observed in immortalized DPCs and NIH3T3 fibroblasts (Fig. 6A). Glibenclamide, a compound that blocks K_{ATP} channels, inhibited cell proliferation and cell cycle progression promoted by bimatoprost in NIH3T3 fibroblasts (Fig. 6B and C). Bimatoprost induced the phosphorylation of Akt in NIH3T3 fibroblasts (Fig. 7A); this was attenuated by treatment with glibenclamide (Fig. 7B). On the other hand, we also found that glibenclamide attenuated the effects of bimatoprost on the expression of Bcl-2, anti-apoptotic factor (Fig. 7C). These results indicate that bimatoprost-induced proliferation of NIH3T3 fibroblasts might be mediated through the regulation of K_{ATP} channels.

Cell cycle regulators such as cyclin D1 are also known to be Wnt targets (). Wnt/β-catenin is an important regulator of cell proliferation (Logan *et al.,* 2004, Rulifson *et al.,* 2007). Wnt/β-catenin also plays an important role in hair growth and regeneration (Ito *et al.,* 2007, Ouji *et al.,* 2006, Ouji *et al.,* 2008). Repression of GSK3β can cause β-catenin stabilization and translocation into the nucleus. Accumulation of nuclear β-catenin results in the activation of target genes such as *Cox-2* (Howe *et al.,* 1999). In the present study, bimatoprost increased the expression of total and nuclear β-catenin in immortalized DPCs (Fig. 3C and D) and NIH3T3 fibroblasts (Fig. 5A and B). Expression of Cox-2 is increased by the

induction of Wnt (Howe *et al.,* 1999) as well as the activation of β-catenin (Kim *et al.,* 2002). Bimatoprost may have increased the expression of Cox-2 through up-regulation of β-catenin (Fig. 3E and 5C). On the other hand, glibenclamide attenuated the increases of β-catenin and Cox-2 levels by bimatoprost (Fig. 7D). These results indicate that bimatoprost could have mitogenic effects via the up-regulation of β-catenin and opening of KATP channels.

In summary, bimatoprost increased the growth of hair-fibers through the proliferation of immortalized DPCs. Bimatoprost induced cell cycle progression of immortalized DPCs through the up-regulation of cyclin E and CDK2. Additionally, bimatoprost increased β-catenin and Cox-2 expression in these cells. In NIH3T3 fibroblasts, bimatoprost decreased the sub-G1 population through the down-regulation of $p27^{Kip1}$, and Bax along with the upregulation of Bcl-2. Bimatoprost also increased the expression of β-catenin and Cox-2 in NIH3T3 fibroblasts by opening the K_{ATP} channels. Taken together, these results demonstrate that bimatoprost might have therapeutic potential as a treatment for hair loss.

PART Ⅱ

Effect of dihydrotestosterone in immortalized dermal papilla cells

1. Abstract

The action of dihydrotestosterone (DHT) in dermal papilla cells of hair follicles is believed to be involved in androgenetic alopecia. However, the action mechanisms of DHT are not fully understood. The effects of DHT on dermal papilla cells, regulator of hair cycle and hair follicle growth, were examined in immortalized dermal papilla cells (DPC). DHT did not affect the proliferation of immortalized DPC. Flow cytometry analysis revealed that DHT could increase cell cycle arrest, which was accompanied by an increase in the $p27^{kip1}$ level and decreases in the cyclin E, cyclin D1 and CDK2 levels. Although the expression of $p27^{kip1}$ was also increased by treatment with U0126, an inhibitor of MEK/ERK1/2, U0126 did not influence the increase of $p27^{kip1}$ by DHT. The transforming growth factor-β (TGF-β) pathway is associated with catagen transition of hair follicles. We found that DHT did not affect the expression TGF-β2. However, treatment of DPC with DHT resulted in phosphorylation and nuclear translocation of Smad2/3, a mediator of the TGF-β pathway. On the other hand, DHT induced HSP27 phosphorylation via p38 MAPK pathway and nuclear translocation of HSP27 in DPC. Treatment of DPC with DHT decreased the expression of total and nuclear β-catenin, which is an important regulator in hair growth and proliferation. DHT-induced down-regulation of β-catenin was attenuated by LiCl, a glycogen synthase

kinase-3β (GSK-3β) inhibitor. DHT decreased the expression of Cox-2, wnt target gene, and Nuclear factor-κB p65 (NF-κB p65). U1026 also decreased the expression of Cox-2, whereas SB203580, a p38 MAPK inhibitor, increased the expression of Cox-2. However, U0126 and SB203580 were not associated with a decrease in the Cox-2 level by DHT. These results suggest that DHT-induced cell cycle arrest is mediated through activation of TGF-β/Smad and HSP27 and inhibition of β-catenin.

2. Introduction

Alopecia, loss of hair, is roughly divided into three types: androgenetic alopecia (AGA), telogen effluvium (TE) and alopecia areata (AA) (Paus *et al.,* 1999). AGA is the most common type of alopecia. AGA is characterized by miniaturization of the hair follicle and shortening of anagen phase (Whiting, 1998). A previous study suggested that AGA may be modulated by 5α-reductase inhibition (Kaufman, 1996). Conversion of testosterone to dihydrotestosterone (DHT) is regulated by 5α-reductase, and finasteride is known to repress the progression of AGA through inhibition of 5α-reductase (Kaufman, 1996). However, repression of 5α-reductase in human results in harmful effects including gynaecomastia and reduced libido (Libecco *et al.,* 2004). Androgens play important roles during development (Gray *et al.,* 2001), and DHT, a potent androgen, is synthesized in the prostate, testes and hair follicles (Carson *et al.,* 2003). Androgen receptor (AR) is expressed in various tissues including prostate and hair follicles (Gelmann, 2002). DHT has higher affinity than testosterone for AR. AR expression is higher in AGA patients than in normal subjects (Hibberts *et al.,* 1998). Previous studies suggest that AGA may be caused by DHT in different ways: The miniaturization of dermal papilla and hair follicles is induced by DHT, which leads to transition from anagen to catagen (Sinclair, 1998). DHT increases the levels

of transforming growth factor-β1 (TGF-β1) and TGF-β2 in dermal papilla cells (DPC), which leads to decreased proliferation of epithelial cells (Hibino *et al.,* 2004, Inui *et al.,* 2002). Up-regulation of dickkopf related protein-1 (DKK-1) by DHT can cause repression of the growth of epithelial cells in hair follicles (Kwack *et al.,* 2008).

DPC, mesenchymal-derived cells, are located at the base of the hair follicle. DPC is known to be an important regulator of hair growth and hair follicle regeneration (Stenn *et al.,* 2001). Several para- and autocrine factors are produced by DPC and then transferred to epithelial cells, which causes apoptosis of epithelial cells in the hair follicles (Kwack *et al.,* 2008). The hair cycle and hair growth involve the cell number and volume of DPC (Elliott *et al.,* 1999, Ibrahim *et al.,* 1982). AR is expressed in DPC, which are the target organ of androgens such as testosterone and DHT (Itami *et al.,* 1991). Furthermore, DPC of AGA patients express AR at higher level than non-AGA subjects (Hibberts *et al.,* 1998). These studies indicate that DHT may regulate the function of DPC and repress hair growth. Nevertheless, the mechanisms of actions of DHT in DPC are still poorly understood.

TGF-β is a major regulator in hair follicle morphogenesis and hair loss (Foitzik *et al.,* 2000a)(Foitzik *et al.,* 2000b, Paus *et al.,* 1997, Soma *et al.,* 2002). TGF-β evokes a signaling pathway through TGF-β receptor subtypes (R I, II and III). TGF-β binding to TGF-β R II forms a complex with TGF-β R I, which leads to activation of TGF-β R I (Derynck *et al.,*

1997). Signaling transduction of TGF-β pathway is mediated by Smads (Smad 2, 3, 4 and 7). Among these, phosphorylation of Smad2/3 by TGF-β induces the nuclear translocation of Smad2/3. Nuclear Samd2/3 then activates target genes through the interaction with DNA binding protein (Tsukazaki *et al.,* 1998). Previous reports suggest that TGF-β R I and TGF-β R II are expressed in epithelial cell of hair follicles (Paus *et al.,* 1997). Hair follicles are regressed by TGF-β1 (Foitzik *et al.,* 2000b) and TGF-β2 (Soma *et al.,* 2002).

Heat shock protein (HSP) is a molecular chaperone that is involved in folding, trafficking and transcriptional activity of steroid receptor (Edwards *et al.,* 2005). HSP27 is a ubiquitously expressed member of small HSP family, and it plays a role in actin polymerization (Lavoie *et al.,* 1993) and apoptosis (Takayama *et al.,* 2003). HSP27 is activated by androgens, and its relationship with AR has been identified in prostate cancer (Zoubeidi *et al.,* 2007). HSP27 binds to AR or AR coactivator such as hydrogen peroxide-inducible clone-5/androgen receptor coactivator, 55kDa (hic-5/ARA55), which has been reported to interact with HSP27 (Jia *et al.,* 2001). HSP27 binding to AR induces the nuclear translocation of HSP27/AR complexes in prostate cancer (Zoubeidi *et al.,* 2007). HSP27 can be phosphorylated on three serine residues (Ser^{15}, Ser^{78} and Ser^{82}) and then exerts its functions (Huot *et al.,* 1995). Previous studies have shown that HSP27 is phosphorylated through activation of p38 (Rane *et al.,* 2001) and Akt (Rane *et al.,* 2003). HSP27 is

expressed in the granular layer of keratinocytes (Gandour-Edwards *et al.,* 1994) and human hair follicles (Adly *et al.,* 2006). Recently, one study showed that expression of HSP27 increased in balding DPC compared to non-balding DPC (Bahta *et al.,* 2008).

β-Catenin is a key molecule in the wnt/β-catenin pathway, which is involved in hair follicle development, differentiation (Huelsken *et al.,* 2001) and hair-growth (Ouji *et al.,* 2007). Phosphorylation and degradation of β-catenin is mediated by an inhibitory complex that includes adenomatous polyposis coli (APC), glycogen synthase kinase-3β (GSK-3β), axin and casein kinase I. In particular, phosphorylation of GSK-3β is required for stabilization of β-catenin. After wnts binding to Frizzled (FZ)/low-density lipoprotein (LDL) receptor-related protein 5/6 (LRP 5/6) receptor, wnts can cause phosphorylation of GSK-3β. This leads to the stabilization and nuclear translocation of β-catenin (Behrens *et al.,* 1996, Omer *et al.,* 1999). Nuclear β-catenin binding to lymphoid Enhancer-binding Factor (LEF)/T-cell factor (TCF) can activate transcription of a target gene (Vlad *et al.,* 2008). (2'Z,3'E)-6-bromoindirubin-3'-oxime (BIO), a GSK-3β inhibitor, increases the nuclear translocation of β-catenin and hair-shaft growth (Yamauchi *et al.,* 2009). These studies indicate that β-catenin can act as an important mediator in the regulation of hair growth.

Previous studies have shown that prostaglandins (PGs) have an important role in the regulation of eyelash growth (Johnstone *et al.,* 2002) and hair growth (Sasaki *et al.,* 2005a).

PGs are a family of eicosanoids, which are derived from arachidonic acid. They are divided into prostacyclin (PGI_2), prostaglandin E_2 (PGE_2), prostaglandin F_2 (PGF_2) and so on. PGE increases the cell proliferation through wnt/β-catenin pathway (Castellone *et al.,* 2005). On the other hand, the enzymes implicated in the metabolism of PGs are expressed in human hair follicles (Colombe *et al.,* 2007). PG receptors are also expressed in human hair follicle (Colombe *et al.,* 2008). 16,16-Dimethyl PGE_2 protects against radiation-induced alopecia (Hanson *et al.,* 1992). $PGF_{2\alpha}$ has been reported to promote the growth of eyelashes and hair (Sasaki *et al.,* 2005a, Tosti *et al.,* 2004). Latanoprost and bimatoprost, $PGF_{2\alpha}$ analogues, stimulate eyelash growth and pigmentation (Cohen, 2010, Johnstone *et al.,* 2002, Tauchi *et al.,* 2010). The role of cyclooxygenases (Cox) in the PG pathway has also been identified (Lee *et al.,* 2003). Cox exists as two isoforms, Cox-1 and Cox-2. Cox-1 is constitutively expressed in most cells, whereas Cox-2 is induced by stimuli such as cytokines (Arias-Negrete *et al.,* 1995). Minoxidil, a hair-growing agent, can increase the expression of Cox-1 and the production of PGE_2 (Michelet *et al.,* 1997), which indicates that Cox may play a crucial role in hair growth. Expression of wnt-1 stabilizes β-catenin and induces expression of Cox-2 (Howe *et al.,* 1999). Forced β-catenin expression also induces the expression of Cox-2 (Kim *et al.,* 2002). Cox-2 expression is mediated through binding of NF-κB in the promoter region of Cox-2 (Schmedtje *et al.,* 1997). Nuclear factor-κB (NF-κB), an inducible

transcription factor, has a pivotal role in the inflammation process (Sha, 1998). Expression of Cox-2 is correlated with NF-κB p65, a member of the NF-κB family, but not with NF-κB p50 (Charalambous *et al.,* 2009).

Control of cell proliferation is mediated by the regulation of apoptosis, survival and cell cycle (Evan *et al.,* 2001). These processes are regulated by multiple signaling pathways such as mitogen activated protein kinase (MAPK) and Akt. The MAPK pathway regulates various physiological changes such as differentiation, transformation (Cowley *et al.,* 1994) and proliferation (Zhang *et al.,* 2002). Stimulation with growth factors activates the p42/44 MAPK (ERK1/2) pathway and leads to transition to S phase (Zhang *et al.,* 2002). ERK1/2 is also reported to be an important mediator in mitogenesis. ERK inhibitor induces G1 arrest, which indicates that the ERK pathway is involved in cell cycle regulation (Koyama *et al.,* 2007). On the other hand, p38 MAPK has crucial roles in survival, apoptosis and inflammation. For example, stresses including UV irradiation, heat shock and cytokines activate p38 MAPK (Herlaar *et al.,* 1999, Zhang *et al.,* 2002). Many earlier studies indicate that Akt is also important in cell survival (Datta *et al.,* 1999). Activation of Akt reduces the cell death and cell cycle arrest (Chang *et al.,* 2003, Yamaguchi *et al.,* 2001), whereas inhibition of Akt increases apoptosis (Zhou *et al.,* 1998). Progression and arrest of cell cycle are mediated by cyclins, which bind to CDKs (CDK1, CDK2, CDK4 and CDK6). The

cyclins comprise two groups: G1/S cyclins (cyclin A, D and E) and G2/M cyclins (cyclin B) (Johnson *et al.,* 1999, Sherr, 1996). Withdrawal of growth factors can induce the expression of CDKs inhibitor such as $p27^{kip1}$ and prevent cell cycle progression (Sherr, 1996). Growth factor enhances the level of cyclin D1 transcription (Watts *et al.,* 1994). Antiestrogen-induced growth arrest is attenuated by induction of cyclin D1 (Wilcken *et al.,* 1997).

Although many studies on the relationship between AGA and DHT have been reported, it is not clear how alopecia is caused by DHT. The action mechanisms of DHT on DPC have not been fully elucidated, although DHT binding to AR in DPC of hair follicle leads to hair cycle regulation. In the present study, we investigated the action mechanisms of DHT on the regulation of TGF-β/Smad, HSP27 and β-catenin in DPC.

3. Materials and Methods

1. Reagents

The following reagents were obtained commercially: DHT was from TCI (Tokyo, Japan); 3-(4,5-dimethylthiazol-2-yl)-2,5-diphenyltetrazoliumbromide (MTT), propidium iodide (PI), and the GSK3β inhibitor, lithium chloride (LiCl), were from Sigma (St. Louis, MO, USA); p38 MAPK inhibitor, SB203580, and MEK inhibitor, U0126, were from Biosource (Camarillo, CA, USA); antibodies against ERK1/2, phospho-ERK1/2, p38, phospho-p38 and phospho-HSP27 were from Cell Signaling Technology (Beverly, MA, USA); antibodies against β-catenin, Cox-2, CDK2, CDK4, Cyclin E, $p27^{kip1}$, NFκB p65, Smad2/3, HSP27, PCNA, SUR2B, Kir6.1 and Tubulin-α were from Santa Cruz Biotechnology (Santa Cruz, CA, USA); antibody against β-actin was from Sigma; antibody against Cyclin D1 was from BD Biosciences (San Diego, CA, USA); antibody against Lamin B1 was from Abcam (Cambridge, UK); HRP-conjugated goat anti-rabbit, goat anti-mouse and mouse anti-goat IgGs were from Santa Cruz Biotechnology; goat anti-rabbit Alexa Fluor 594 and chicken anti-goat Alexa Fluor 488 were from Invitrogen (Carlsbad, CA); aprotinin and leupeptin were from Calbiochem (San Diego, CA, USA); Nonidet P-40 (NP-40) was from Roche (Indianapolis, IN, USA); Western blotting detection reagent, West-zol enhanced chemilumin, was from Intron Biotechnology (Sungnam, Korea).

3.2. Cell culture

Rat vibrissa immortalized dermal papilla cell line (Filsell *et al.,* 1994) was kindly provided by the Skin Research Institute, Amore Pacific Corporation R&D Center, South Korea. The dermal papilla cells (DPC) were cultured in DMEM (Hyclone Inc., UT, USA) supplemented with 10% FBS and penicillin/streptomycin (100 unit/mL and 100 μg/mL, respectively) at 37°C in a humidified atmosphere under 5% CO_2.

3.3. Cell viability assay

The effect of DHT on the proliferation of immortalized DPC was evaluated by measuring the metabolic activity in the MTT assay (Scudiero *et al.,* 1988). The immortalized DPC (1.0×10^4 cells/mL) were seeded into 96-well plates. After 24 h to allow attachment, cells were cultured for 24 h in serum-free DMEM, and then treated with 10, 100 or 1000 nM DHT and vehicle (ethanol diluted 1:1000 in serum-free DMEM) as a control for 4 days. Cells were then treated with 50 μL of (2 mg/mL) MTT dye and incubated at 37°C for 4 h. The plates were centrifuged at 1000 rpm for 5 min at room temperature and the media was then carefully aspirated. Then 200 μL/well of dimethyl sulfoxide was added to dissolve the formazan crystals. Cell viability was determined by measuring the absorbance at 540 nm

using a microplate reader (BioTek Instrument, Inc., VT, USA). All experiments were performed at least three times.

3.4. Cell cycle analysis

The effect of DHT on cell cycle progression was analyzed by flow cytometry after staining the cells with PI (Fried *et al.,* 1976). The immortalized DPC (1.0×10^5 cells/mL in 100mm dishes) were incubated with 10, 100 or 1000 nM DHT for 24. In some cases, the cells were treated with 100 nM DHT for 0, 24 and 48 h. Cells were collected and washed twice with PBS. The cells were fixed with 70% ethanol overnight at -20 ℃. Cells were washed with PBS and incubated with 50 µg/mL RNase A at 37 ℃ for 30min. The cells were stained with 50 µg/mL PI solution for 15 min in the dark. Flow cytometry analysis was performed using a FACScan Flow Cytometer (Becton-Dickinson, San Jose, CA, USA). Histograms were analyzed with the software program Cell Quest (Becton-Dickinson, San Jose, CA, USA) (Krishan A, 1975).

3.5. Western blot analysis

The immortalized DPC (1.0×10^5 cells/mL in 100mm dishes) were pre-incubated for 24 h under serum-free conditions, and the cells were treated with DHT at indicated concentrations

for 24 h. In some cases, the cells were pre-incubated with 20 μM U0126 or 20 μM SB203580 for 1 h, and then treated with 100 nM DHT for 24 h. In other cases, immortalized DPC were treated with 100 nM DHT for 0, 5, 15, 30 and 60min. The cells were washed twice with ice-cold PBS. The cells were lysed in lysis buffer [50 mM Tris–HCl (pH 7.5), 150 mM NaCl, 2 mM EDTA, 1 mM EGTA, 1 mM $NaVO_3$, 10 mM NaF, 1 mM dithiothreitol (DTT), 1 mM Phenylmethylsulfonylfluoride (PMSF), 25 μg/ml aprotinin, 25 μg/ml leupeptin and 1% NP-40] to obtain whole cell protein and kept on ice for 30 min. The cell lysates were centrifuged at 15,000 rpm at 4 ℃ for 15 min. Supernatants were stored at -20 ℃ until analysis. To obtain nuclear and cytoplasmic fractions, cultured cells were treated with DHT with or without LiCl for 24 h. Other cells were treated with 100 nM DHT for 0, 1, 2 or 4 h. The cells were washed two times with cold PBS. Cells were lysed with 1 mL of lysis buffer (1 mM Tris-HCl, pH7.9, 10 mM NaCl, 3 mM $MgCl_2$ and 1% NP-40) at 4 ℃ for 10 min. After centrifugation at 3000 x g, the supernatants were harvested as cytoplasmic fractions. The pellets were suspended in extraction buffer (20 mM HEPES, pH 7.9, 20% glycerol, 1.5 mM $MgCl_2$, 0.2 mM EDTA, 1mM DTT and 1mM PMSF), and kept on ice for 1 h. The lysates were centrifuged at 14,000 x g for 15 min, and the supernatants were harvested as nuclear fractions and stored at -70 ℃. Protein concentration was determined by the Bradford method (Bradford, 1976). Equal amounts of protein were separated on 8~12% Sodium dodecyl sulfate polyacrylamide gel electrophoresis (SDS-PAGE) gels. And then proteins

were transferred onto polyvinylidene fluoride (PVDF) membranes (Bio-Rad, Hercules, CA, USA) with a glycine transfer buffer [192 mM glycine, 25 mM Tris-HCl (pH 8.8), 20% MeOH (v/v)] at 100 V for 2h. After blocking with 5% nonfat dried milk in Tween-20-TBS (T-TBS) (50 mM Tris, pH 7.6, 150 mM NaCl, 0.1% Tween-20), each membrane was incubated with specific primary antibodies at 4 °C overnight. Table 4 shows the antibodies used for western blotting. The membrane was incubated with a secondary HRP antibody (1:5000) at room temperature for 1 h. The membrane was exposed on X-ray film (AGFA, Belgium), and protein bands were detected using West-zol (Intron, Korea). Band intensities were quantified with the NIH Image software (http://rsb.info.nih.gov/ij/).

3.7. Immunofluorescence microscopy

The immortalized DPC were seeded in chamber slides and pre-incubated in serum-free DMEM for 24h. The cells were treated with DHT for 24 h. In some experiments, cultured cells were treated with DHT with or without LiCl for 24 h. For immunofluorescence, cells were fixed in 4% paraformaldehyde (PFA) for 15 min, washed in PBS, and permeabilized with 0.1% Triton X-100. After washing, the cells were blocked with 1% BSA at room temperature for 1 h. The cells were incubated with primary antibody at 4 °C overnight. The primary antibodies included anti-β-catenin, -Smad 2/3 and –HSP27. After two washes with

PBS, the cells were incubated with secondary antibody coupled to Alexa Fluor 594 or Alexa Fluor 488 at room temperature for 1 h. Next, the cells were washed in PBS and mounted in Vectastain (Vector Laboratories) containing 4, 6-diamido-2-phenylindole (DAPI). Images were visualized by fluorescence microscopy (BX51, Olympus).

3.8. Statistical analysis

All results were expressed as means ± standard deviation (SD) or standard error (SE) of at least three independent experiments. The Student's t-test was used to determine the statistical significance (P-value<0.05) of the differences between the values for the various experimental and control groups.

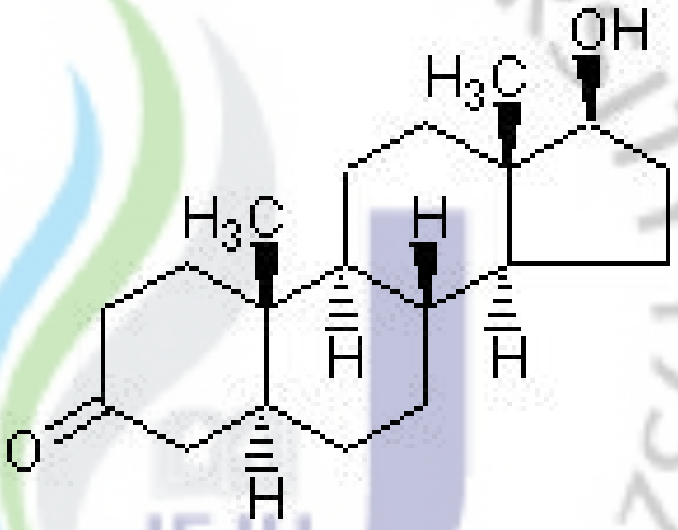

Figure 8. The structure of dihydrotestosterone (DHT).

Table 4. Antibodies used in Western blot analysis on immortalized DPC.

Antibody	Origin	Company
CDK2	Rabbit polyclonal	Santa Cruz Biotechnology
Cyclin E	Rabbit polyclonal	Santa Cruz Biotechnology
$p27^{kip1}$	Rabbit polyclonal	Santa Cruz Biotechnology
TGF-β2	Rabbit polyclonal	Santa Cruz Biotechnology
Smad2/3	Goat polyclonal	Santa Cruz Biotechnology
Tubulin-α	Mouse monoclonal	Santa Cruz Biotechnology
β-catenin	Rabbit polyclonal	Santa Cruz Biotechnology
Cox-2	Goat polyclonal	Santa Cruz Biotechnology
HSP27	Goat polyclonal	Santa Cruz Biotechnology
PARP	Rabbit polyclonal	Santa Cruz Biotechnology
NF-κB p65	Rabbit polyclonal	Santa Cruz Biotechnology
PCNA	Rabbit polyclonal	Santa Cruz Biotechnology
Cyclin D1	Mouse monoclonal	BD Biosciences
Lamin B1	Rabbit polyclonal	Abcam
Phospho-ERK1/2	Rabbit polyclonal	Cell signaling Technology
ERK1/2	Rabbit polyclonal	Cell signaling Technology
phospho-HSP27	Goat polyclonal	Cell signaling Technology
phospho-p38	Rabbit polyclonal	Cell signaling Technology
p38	Rabbit polyclonal	Cell signaling Technology
β-actin	Mouse monoclonal	Sigma

4. Results

4.1. DHT attenuates the cell cycle progression without changing the proliferation of immortalized DPC

DHT is known to repress hair growth (Naito *et al.,* 2008), but the mechanisms of action of DHT in DPC are poorly understood. Using the MTT assay, we examined whether DHT affects the viability of immortalized DPC. DHT did not affect the proliferation of immortalized DPC (Fig. 9A). To further elucidate the effect of DHT in immortalized DPC, cell cycle distribution was analyzed by flow cytometry. As shown in Fig. 9B, when immortalized DPC were treated with 10, 100 or 1000 nM for 24h, DHT inhibited cell cycle progression compared to control cells treated with vehicle. DHT increased the cell population of G1 phase to 53.83% at 10 nM, 52.93% at 100 nM and 50.7% at 1000 nM, whereas the population of G1 phase cells in control cells was 49%. After treatment with 100 nM DHT for 0, 24 and 48 h, G1 arrest was significantly increased (0 h, 53.10%; 24 h, 55.83%; 48 h, 64.33%), whereas the population of S phase cells was decreased (0 h, 9.83%; 24 h, 9.84%; 48 h 6.06%). These data indicate that DHT induced cell cycle arrest at G1 phase without reducing cell proliferation.

To elucidate the mechanisms of DHT-induced cell cycle arrest, the expressions of cell

cycle-associated proteins were examined. $P27^{Kip1}$, a CDK inhibitor, antagonizes the activation of cyclins/CDKs and inhibits transition of S phase (Sherr *et al.,* 1999). The immortalized DPC were treated with 10, 100 or 1000 nM DHT for 24 h. Total cell extracts were analyzed by immunoblotting for $p27^{Kip1}$, cyclin D1 and cyclin E. DHT treatment resulted in increased $p27^{Kip1}$ expression, whereas the expressions of cyclin D1 and cyclin E were decreased (Fig. 9C). After treatment with 100 nM DHT for 0, 6, 12, 24 and 48 h, the expression of $p27^{Kip1}$ was increased, whereas the expression of CDK2 was inhibited by DHT in a time-dependent manner (Fig. 9C). These results suggest that DHT altered the expression of $p27^{Kip1}$, CDK2, cyclin D1 and cyclin E and caused cell cycle arrest in immortalized DPC. Activation of the ERK pathway increases the expression of cyclin D1 (Lavoie *et al.,* 1996), whereas repression of ERK attenuates cell proliferation (Whelchel *et al.,* 1997). DHT did not inhibit the activation of ERK1/2 in immortalized DPC (Fig. 9D). U0126 induces $p27^{kip1}$ expression and cell cycle arrest (Gysin *et al.,* 2005). We thus investigated the effect of U0126 on the expression of cell cycle-related proteins. U0126 increased the expression of $p27^{kip1}$ and decreased the expression of CDK2 in immortalized DPC. However, DHT-induced up-regulation of $p27^{kip1}$ was not altered by U0126 in immortalized DPC (Fig. 9E). On the other hand, inhibition of p38 MAPK increased the expression of cyclin D1 (Lavoie *et al.,* 1993). We thus examined whether p38 MAPK plays a role in the expression of $p27^{kip1}$ in

immortalized DPC. As shown in Fig. 9E, the expression of $p27^{kip1}$ was reduced in immortalized DPC that were treated with SB203580, a p38 MAPK inhibitor. Nevertheless, SB203580 was not associated with a decrease of $p27^{kip1}$ by DHT in immortalized DPC. These results indicate that DHT can inhibit cell cycle progression through a MAPK-independent pathway.

(A)

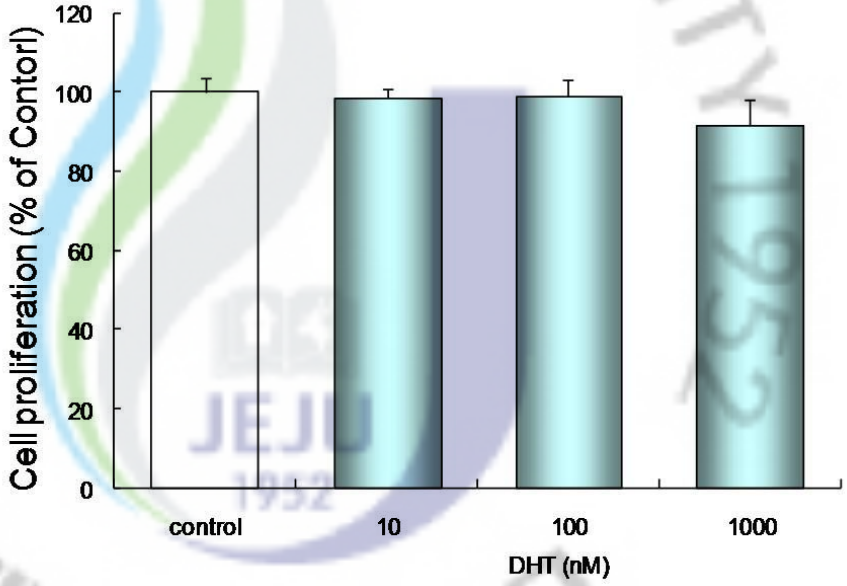

(B)

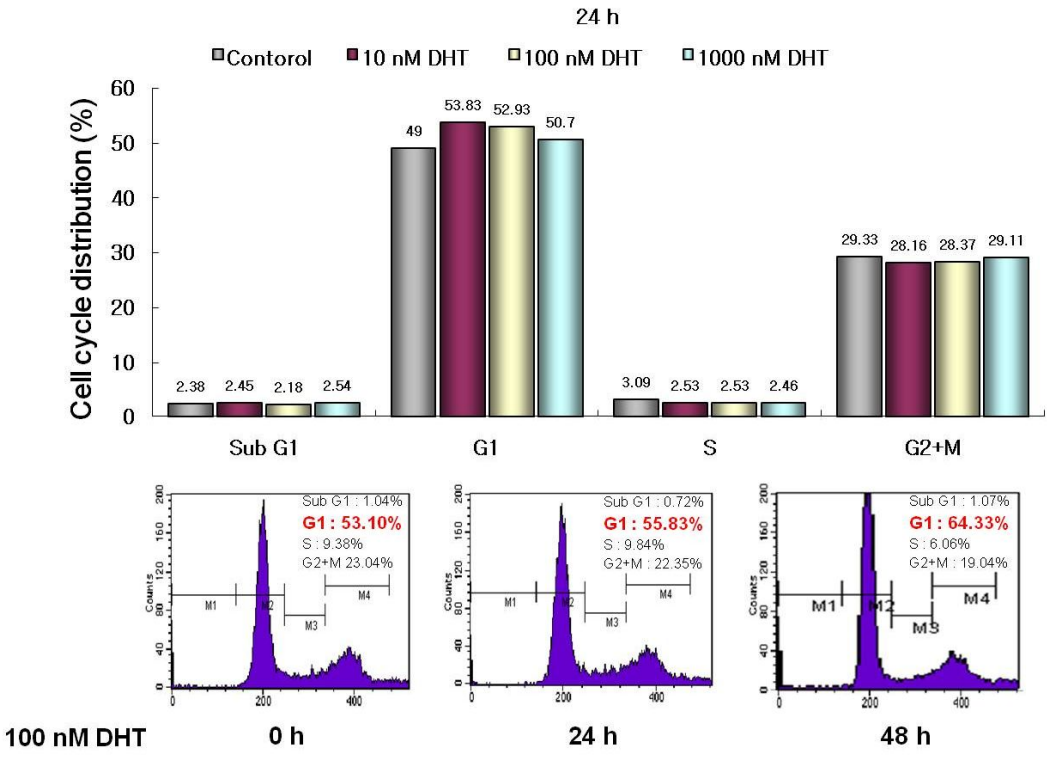

(C)

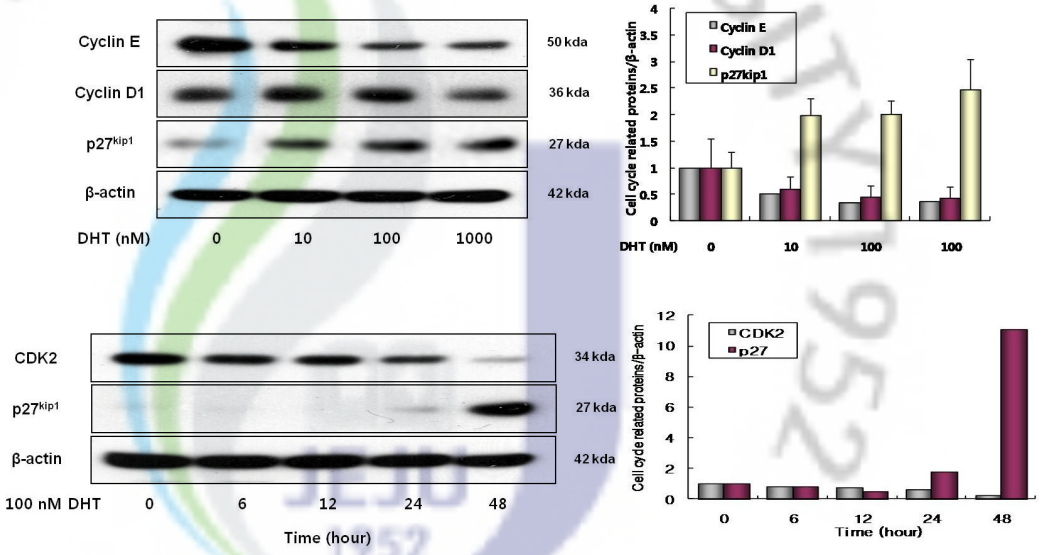

(D)

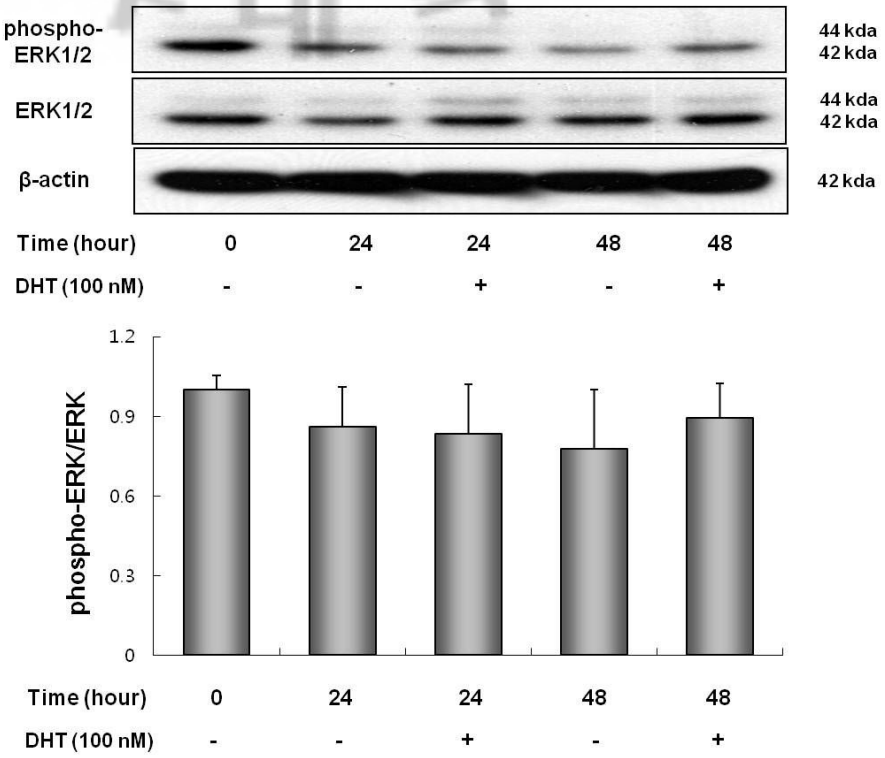

(E)

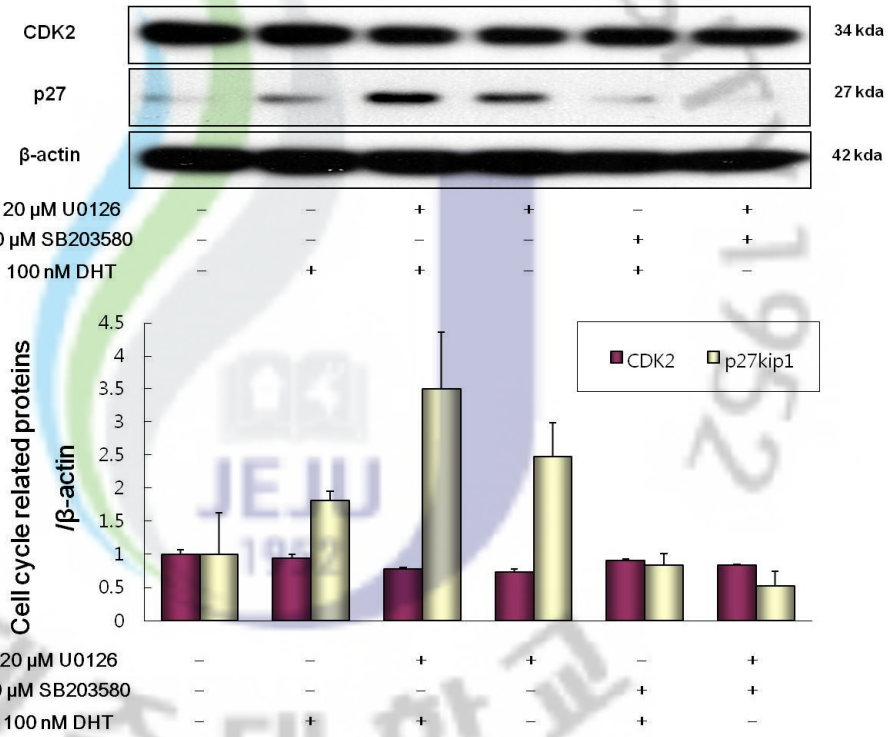

Figure 9. DHT attenuates the cell cycle progression without changing the proliferation of immortalized DPC. (A) The immortalized DPC were stimulated with 10, 100 and 1000 nM DHT for 96 h. Cell viability was measured using the MTT assay. Proliferation of immortalized DPC was evaluated compared to control. Data are presented as mean ± SD from three independent experiments. (B) The immortalized DPC were treated with 10, 100 and 1000 nM DHT for 24 h. In some cases, the cells were treated with 100 nM DHT for 0, 24 and 48 h. Cells were collected and then fixed with 70% ethanol. Fixed cells were stained with PI and analyzed by flow cytometry. (C) The immortalized DPC were treated with

various concentrations of DHT for 24 h or with 100 nM DHT for 0, 6, 12, 24 and 48 h. Whole cell lysates were prepared from the immortalized DPC, and the effects of DHT on the expression of Cyclin E, Cyclin D1, CDK2 and $p27^{kip1}$ were analyzed by western blots using specific antibodies. Right panel displays mean ± SE from three independent experiments. (D) The immortalized DPC were treated with 100 nM DHT for 0, 24 and 48 h. Whole cell lysates were detected by western blot analysis using antibody against phospho-ERK1/2 and ERK1/2. The lower panel displays the mean ± SE from three independent experiments. (E) The immortalized DPC were pre-treated with or without 20 μM SB203580 or U0126 for 1 h and then treated with or without DHT for 24 h. Whole cell lysates from immortalized DPC were analyzed for the expression of $p27^{kip1}$ and CDK2 by western blot. Lower panel displays mean ± SE from three independent experiments.

4.2. DHT regulates nuclear translocation of Smad2/3 but does not change the expression of TGF-β2

TGF-β signaling has an important role in the regulation of the hair cycle (Foitzik *et al.,* 2000b, Inui *et al.,* 2002). DHT-inducible TGF-β1 can inhibit epithelial cell growth (Inui *et al.,* 2002), and TGF-β2 can induce catagen transition (Soma *et al.,* 2002). We thus examined the effect of DHT on the expression of TGF-β2 in immortalized DPC. As shown in Fig. 10A, DHT did not affect the expression of TGF-β2 in immortalized DPC. Smads are crucial mediators in TGF-β signaling, and TGF-β treatment induces the translocation of Smad2/3 into nucleus (Massague *et al.,* 2000). To evaluate whether DHT induces the nuclear accumulation of Smad2/3, immortalized DPC were treated with 100 nM DHT for 0, 1, 2, 4 or 24 h. Based on western blotting (Fig. 10B) and immunofluorescence microscopy (Fig. 10C), we found that DHT increased the nuclear Smad2/3 level. These results indicate that DHT has a direct or indirect effect on TGF-β signaling in immortalized DPC.

(A)

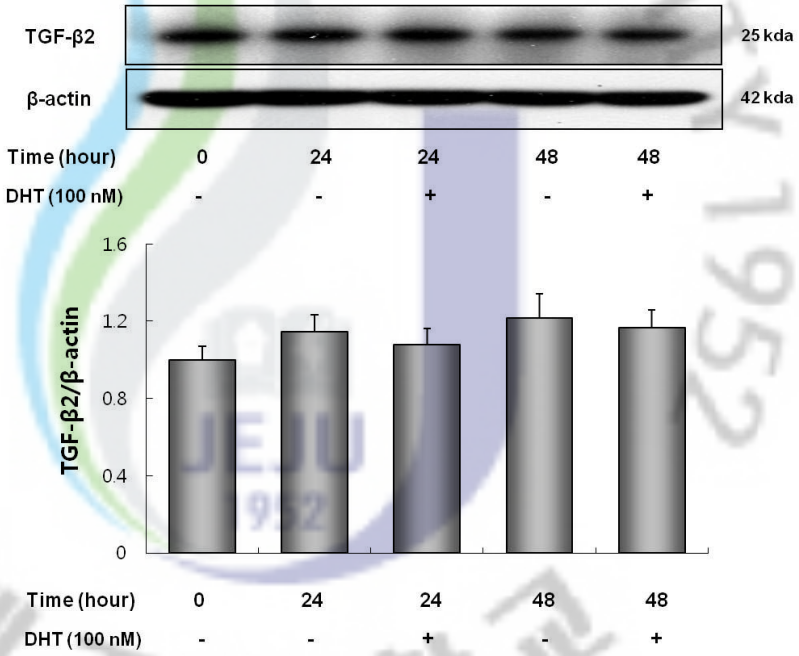

(B)

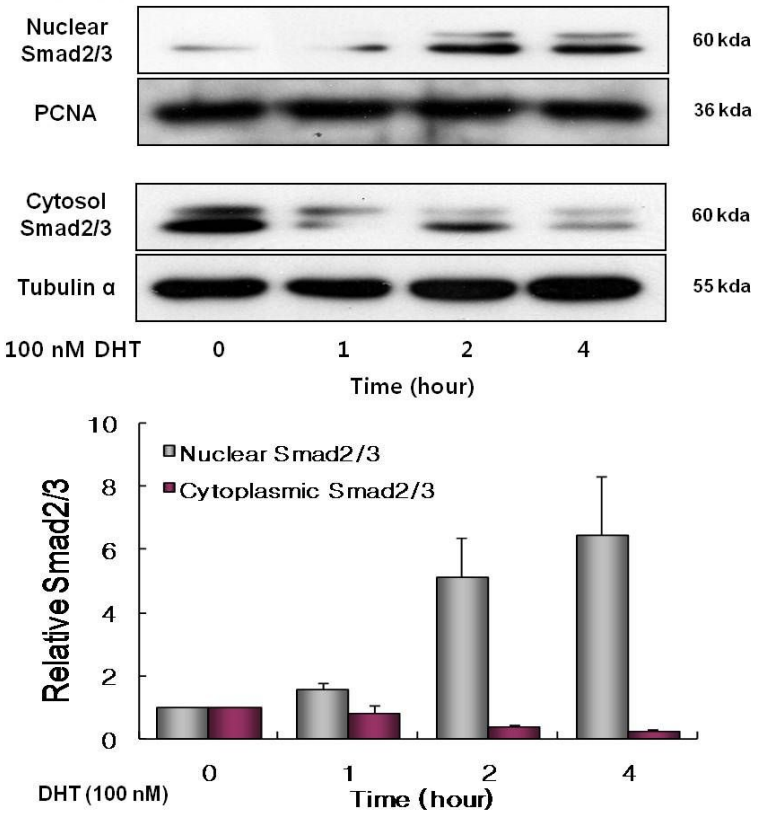

(C)

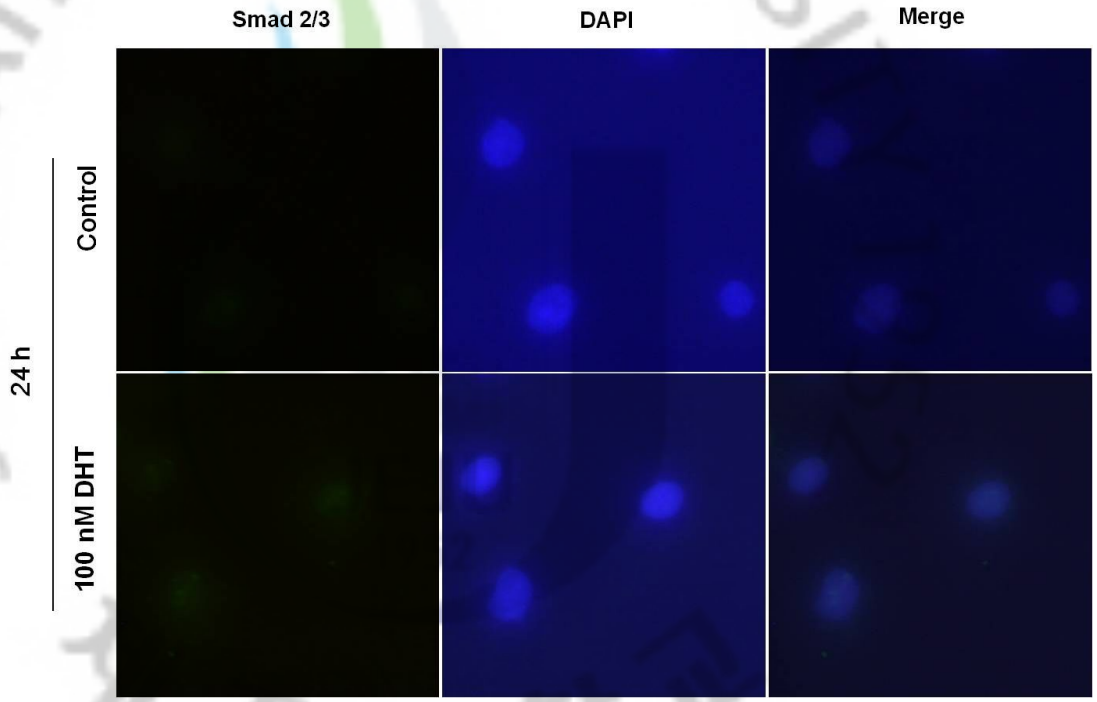

Figure 10. DHT regulates nuclear translocation of Smad2/3 but does not change the expression of TGF-β2. (A) The immortalized DPC were treated with 100 nM DHT for 0, 24 and 48 h. Whole cell lysates were detected by western blot analysis using antibody against TGF-β2. Lower panel displays the mean ± SE from three independent experiments. (B) The immortalized DPC were treated with 100 nM DHT for 0, 1, 2 and 4 h. Nuclear and cytoplasmic fractions were prepared as described in Methods. Nuclear and cytoplasmic proteins were detected by western blot analysis using antibody against Smad2/3. PCNA and Tubulin-α were used as controls for fractionation and equal loading of proteins in nuclear and cytoplasmic fraction, respectively. The lower panel displays the mean ± SE from three

independent experiments. (C) For immunostaining, cells were prepared as described in Methods. Nuclei were stained with DAPI. Cellular localization of Smad2/3 (green) and nuclei (blue) was analyzed using fluorescence microscope.

4.3. DHT enhances phosphorylation and nuclear translocation of HSP27 in immortalized DPC

Increased expression of HSP27 has been reported in balding DPC (Bahta *et al.,* 2008). DHT binding to AR leads to phosphorylation and nuclear translocation of HSP27 in prostate cancer (Zoubeidi *et al.,* 2007). To investigate the effect of DHT on HSP27 activation in DPC, western blot analyses were performed. When immortalized DPC were treated with 100nM DHT, phosphorylation of HSP27 increased at 5-30min (Fig. 11A). HSP27 is known to be phosphorylated through activation of p38 MAPK (Larsen *et al.,* 1997). We examined the effect of DHT on p38 activation by immunoblot analysis. As shown in Fig. 11B and consistent with previous reports, DHT increased the phosphorylation of p38 at 5-30 min. To examine whether nuclear translocation of HSP27 was induced by DHT, we analyzed the expression of nuclear and cytosolic HSP27. Stimulation of immortalized DPC with DHT caused nuclear translocation of HSP27 (Fig. 11C). In addition, immunofluorescence staining showed that DHT increased the nuclear localization of HSP27 for 24 h (Fig. 11D). These results suggest that DHT can cause the phosphorylation and nuclear translocation of HSP27 via p38 MAPK.

(A)

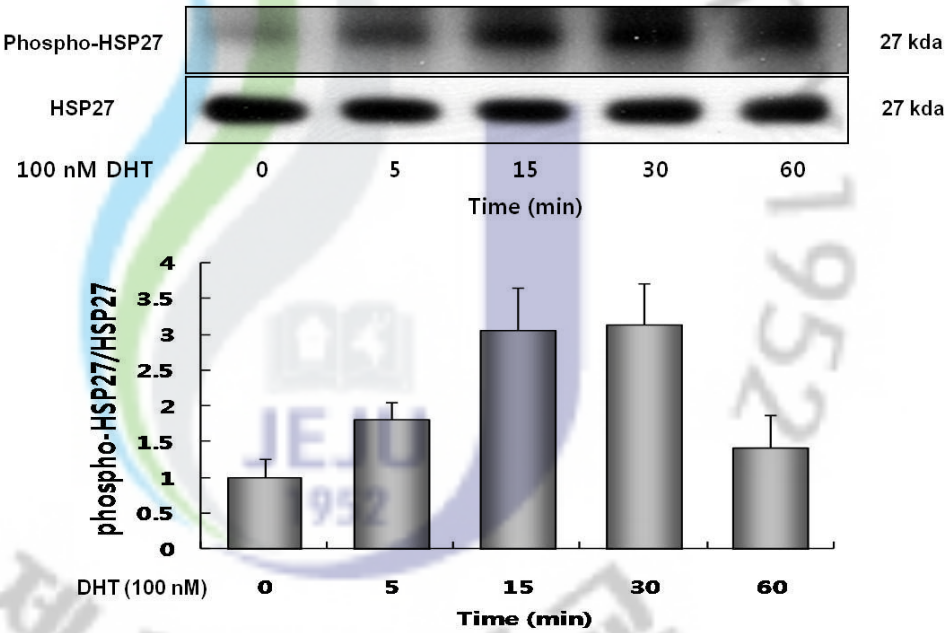

(B)

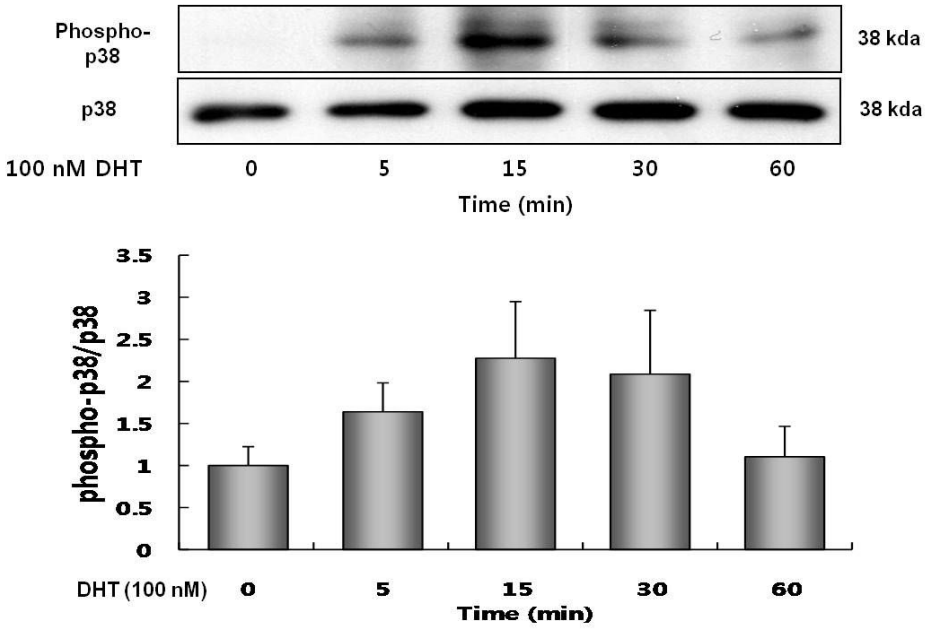

(C)

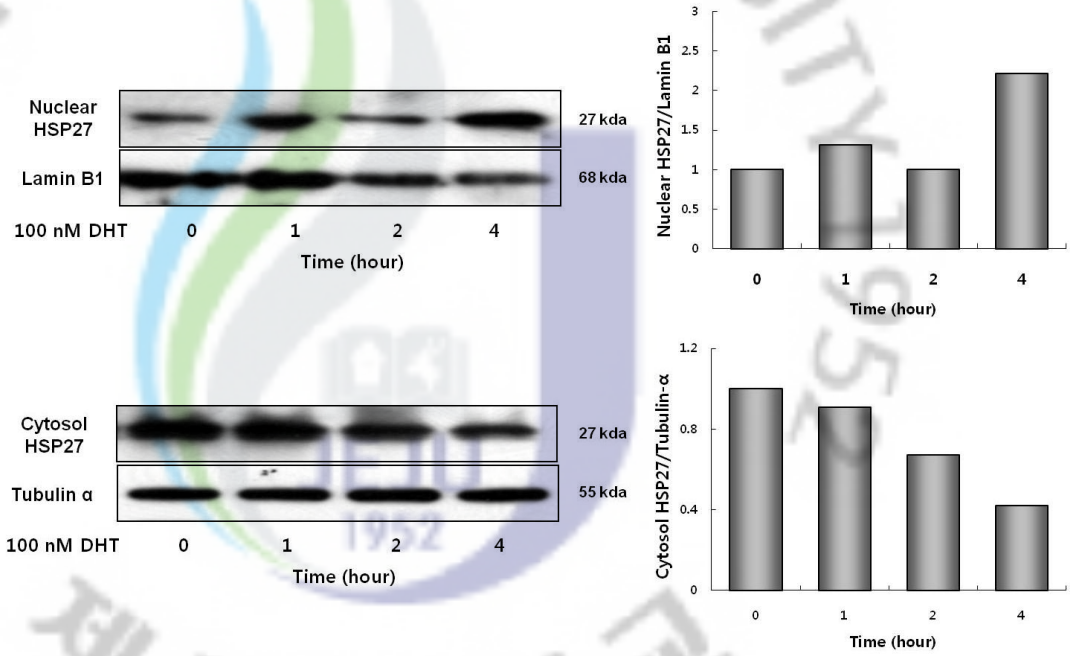

(D)

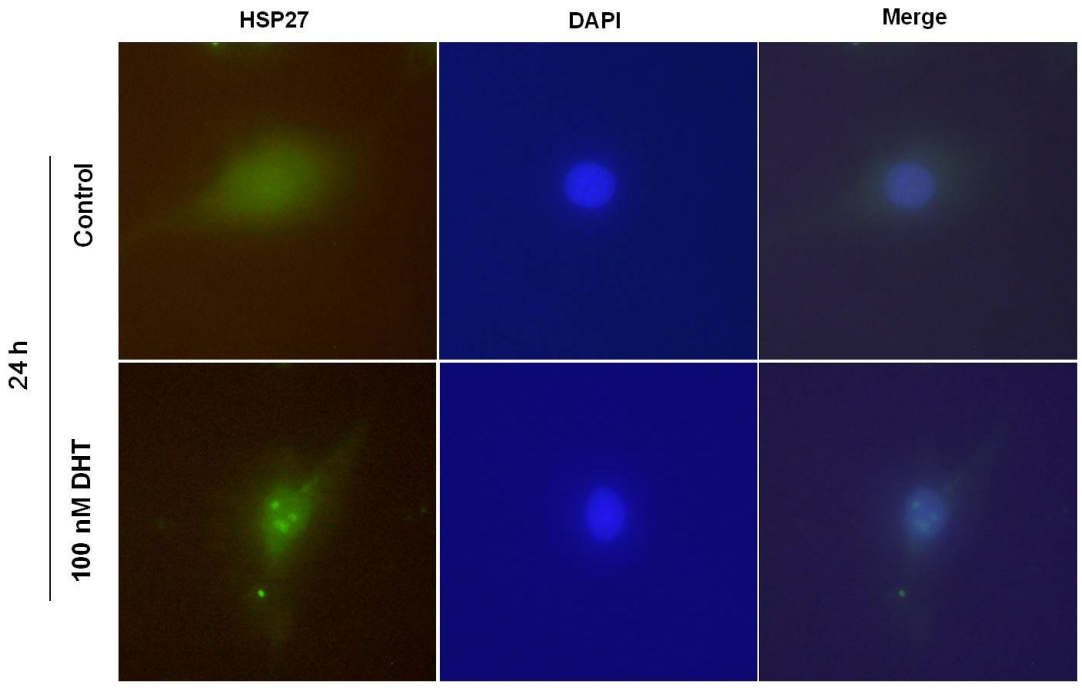

Figure 11. DHT enhances phosphorylation and nuclear translocation of HSP27 in immortalized DPC. (A and B) The immortalized DPC were treated with 100 nM DHT for 0, 5, 15, 30 and 60 min. Whole cell lysates from immortalized DPC were analyzed for the expression of phospho-HSP27, HSP27, phospho-p38 and p38 by western blot. Lower panel displays mean ± SE from three independent experiments. (C) The immortalized DPC were treated with 100 nM DHT for 0, 1, 2 and 4 h. Nuclear and cytoplasmic fractions were prepared as described in Methods. Nuclear and cytoplasmic proteins were detected by western blot analysis using antibody against HSP27. Lamin B1 and Tubulin-α were used as controls for fractionation and equal loading of proteins in nuclear and cytoplasmic fractions, respectively. (D) For immunostaining, cells were prepared as described in Methods. Nuclei were stained with DAPI. Cellular localization of HSP27 (green) and nuclei (blue) was analyzed using a fluorescence microscope.

4.4. DHT regulates the expression of β-catenin in immortalized DPC

The Wnt/β-catenin pathway plays a pivotal role in regulation of hair growth (Ouji *et al.,* 2007, Yamauchi *et al.,* 2009). Therefore, the actions of DHT on the expression of β-catenin were examined. When immortalized DPC were treated with 10, 100 or 1000 nM DHT for 24 h, down-regulation of β-catenin was confirmed by immunoblotting (Fig. 12A). To examine whether nuclear expression of β-catenin was affected by DHT, the level of nuclear β-catenin was analyzed. As expected, DHT attenuated the level of nuclear β-catenin (Fig 12B). To elucidate whether down-regulation of β-catenin by DHT was mediated through GSK3β, immortalized DPC were treated with LiCl, a GSK3β inhibitor. As shown in Fig. 12C, LiCl treatment enhanced the expression of nuclear β-catenin. Consistent with immunoblotting results, immunofluorescence results showed that DHT decreased the basal nuclear β-catenin level (Fig. 12D), whereas pretreatment of immortalized DPC with LiCl attenuated this down-regulation of β-catenin level by DHT in immortalized DPC (Fig. 12E). These results suggest that DHT decreased the level of β-catenin expression through regulation of GSK3β.

(A)

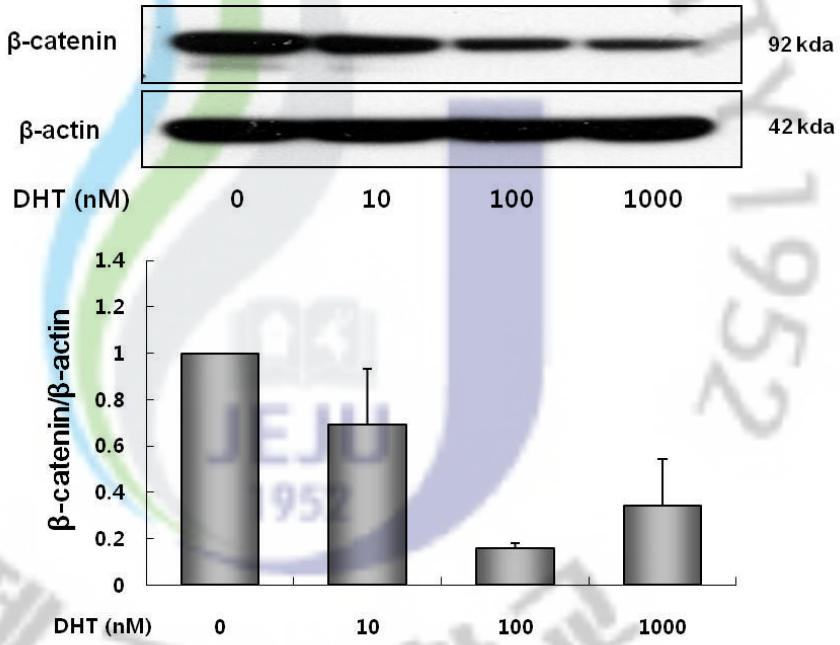

(B)

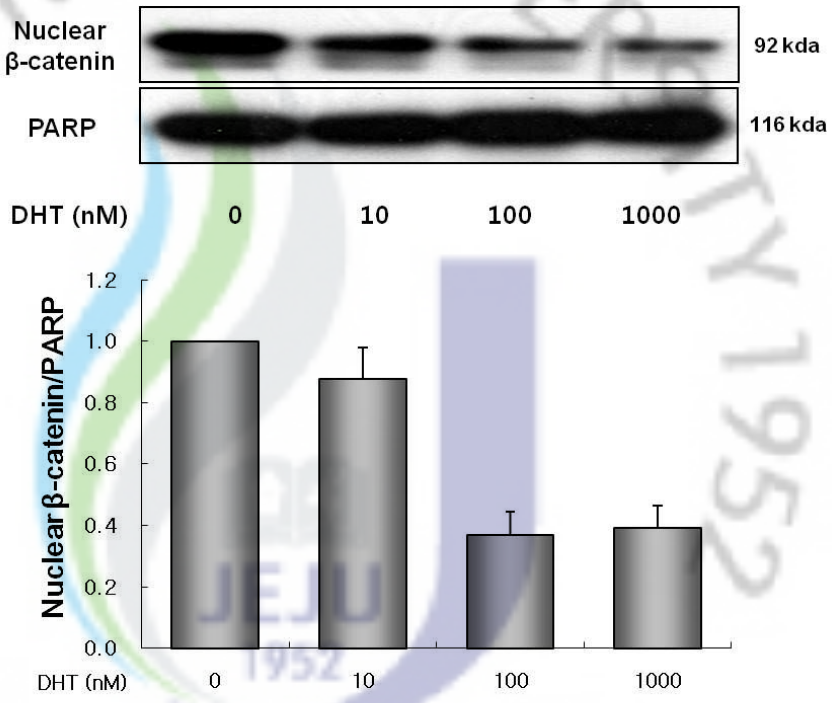

(C)

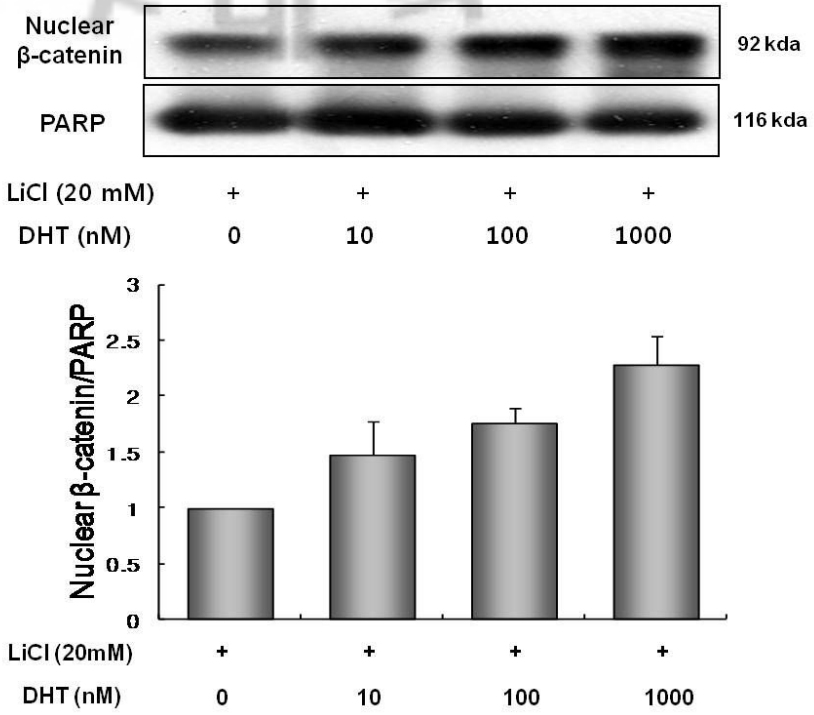

(D)

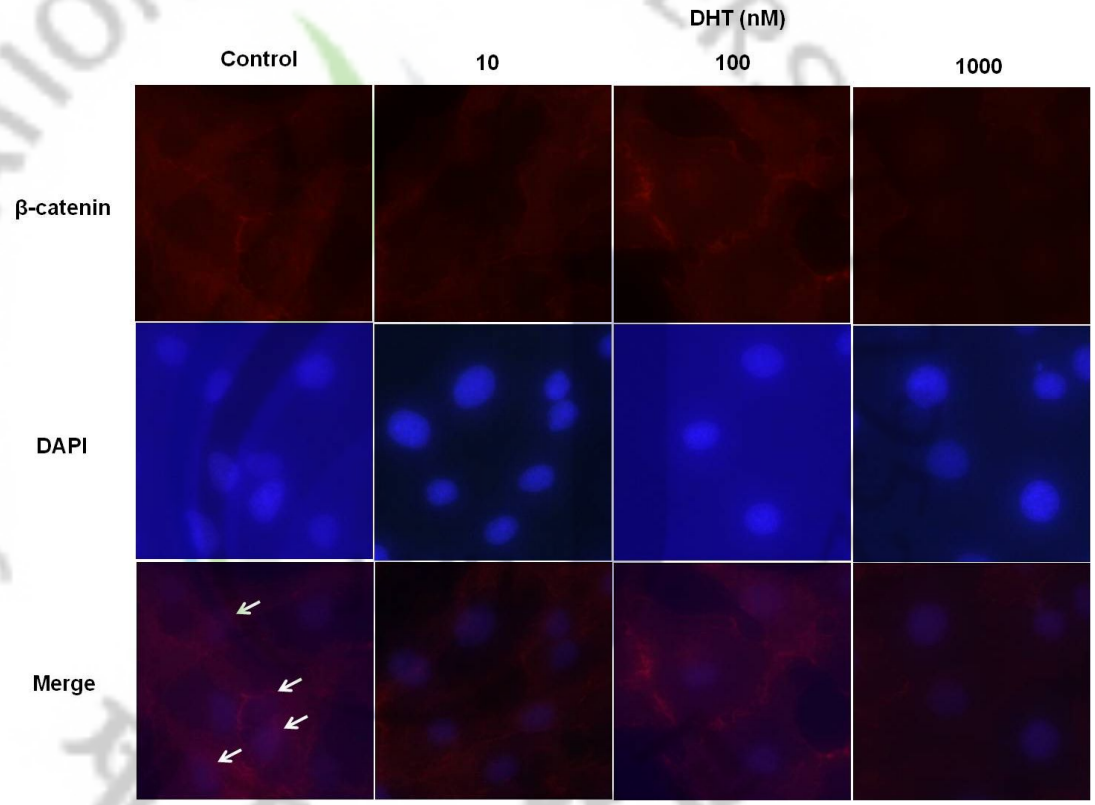

(E)

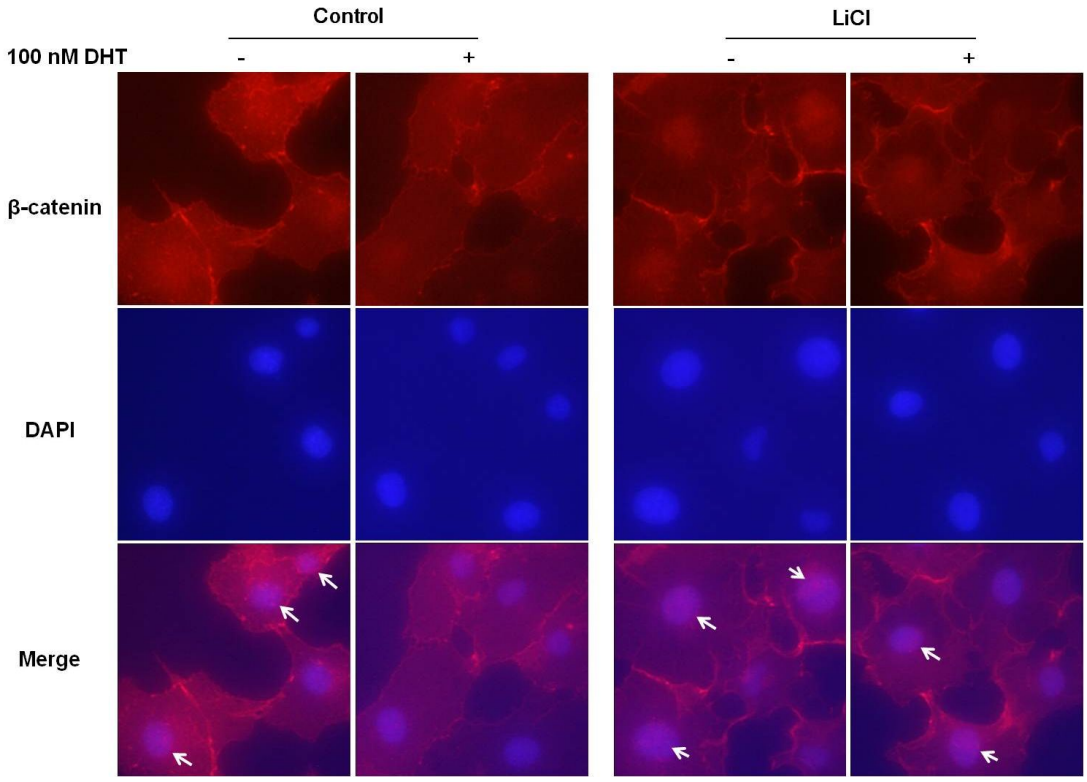

Figure 12. DHT regulates the expression of β-catenin in immortalized DPC. (A) The immortalized DPC were treated with or without DHT for 24h. Whole cell lysates from immortalized DPC were analyzed by western blot for β-catenin expression. Lower panel displays mean ± SE from three independent experiments. (B) The immortalized DPC were treated with or without DHT for 24h. Nuclear fractions were prepared as described in Methods. Nuclear proteins were detected by western blot analysis using antibody against β-catenin. PARP was used as a control for fractionation and equal loading of proteins in the nuclear fraction, respectively. Lower panel displays the mean ± SE from three independent experiments. (C) The immortalized DPC were pre-treated with 20mM LiCl for 1h and then treated with or without DHT for 24h. Nuclear proteins were detected by western blot analysis using antibody against β-catenin. PARP was used as a control for fractionation and equal loading of proteins in nuclear fraction, respectively. Lower panel displays the mean ± SE from three independent experiments. (D and E) For immunostaining, cells were prepared as described in Methods. Nuclei were stained with DAPI. Cellular localization of β-catenin (red) and nuclei (blue) was analyzed using a fluorescence microscope.

4.5. DHT decreases the expression of Cox-2 and NF-κB p65

Latanoprost, a PG analogue, increases eyelash growth in human (Johnstone *et al.,* 2002). Cox-1 is strongly expressed in DPC of anagen hair follicle whereas Cox-2 is weakly expressed (Michelet *et al.,* 1997). Nevertheless, we do not fully understood how PG is involved in hair growth. We thus investigated the effect of DHT on the expression of Cox-2, a key enzyme in PG synthesis, in immortalized DPC. When immortalized DPC were treated with 10, 100 or 1000 nM DHT for 24 h, DHT reduced the level of Cox-2 (Fig. 13A). NF-κB is known to regulate the expression of Cox-2 (Schmedtje *et al.,* 1997). We thus investigated whether DHT affects the expression of NF-κB p65 in immortalized DPC. DHT reduced the expression of nuclear NF-κB p65 (Fig. 13B). These results suggest that DHT may regulate the level of Cox-2 through reduction of nuclear NF-κB p65. MAPK play a crucial role in the transcription of Cox-2 (Subbaramaiah *et al.,* 1998). To elucidate whether expression of Cox-2 is regulated by MAPK, the effects of U0126 and SB203580, inhibitors of mitogen-activated protein kinase kinase (MEK)/ERK and p38 MAPK, respectively, were examined. As shown in Fig. 13C, U0126 decreased the Cox-2 expression in immortalized DPC. However, U0126 did not have synergistic or additive effects on the decrease of DHT-induced Cox-2 level in immortalized DPC. Although SB203580 induced Cox-2 expression, SB203580 was not associated with a decrease of Cox-2 expression by DHT in immortalized

DPC. These results suggest that the DHT-induced Cox-2 level involved NF-κB p65 but was not regulated by the MAPK pathway.

(A)

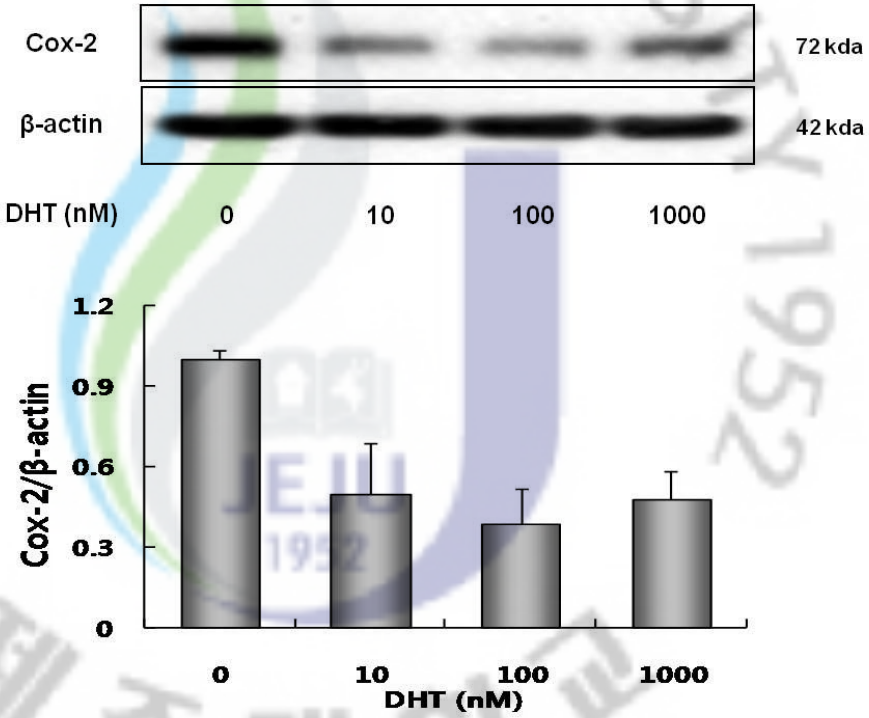

(B)

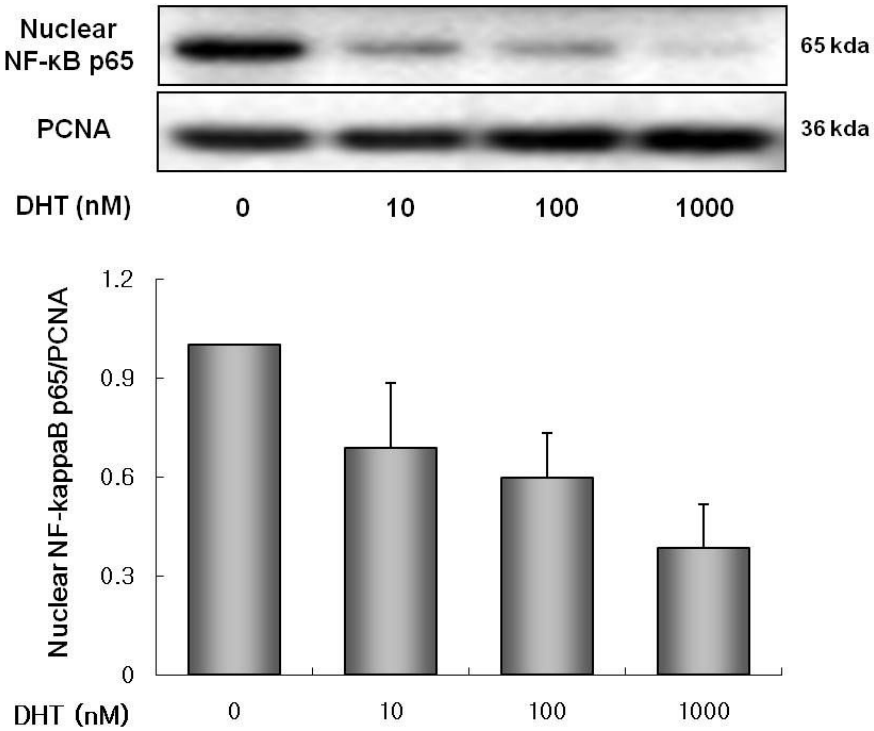

(C)

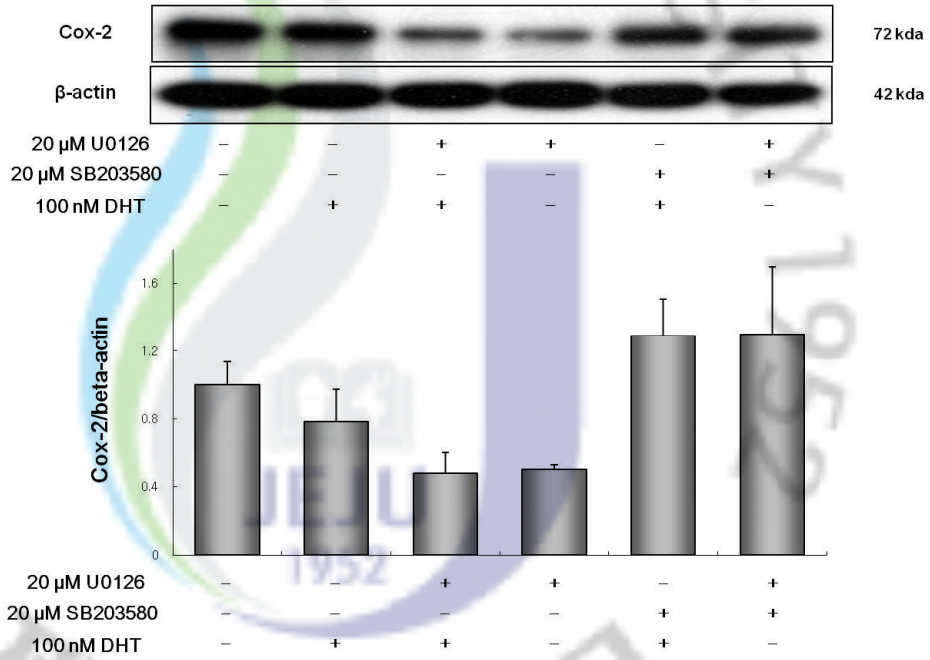

Figure 13. DHT decreased the expression of Cox-2 and NF-κB p65. The immortalized DPC were treated with or without various concentrations of DHT for 24h. (A) Whole cell lysates from immortalized DPC were analyzed by western blot for the expression of Cox-2. Lower panel displays the mean ± SE from three independent experiments. (B) Nuclear fractions were prepared as described in Methods. Nuclear proteins were detected by western blot analysis using antibody against NF-κB p65. PCNA was used as a control for fractionation and equal loading of proteins in the nuclear fraction, respectively. Lower panel displays the mean ± SE from three independent experiments. (C) The immortalized DPC were pre-treated with or without 20 μM SB203580 or U0126 for 1 h and then treated with or without DHT for 24 h. Whole cell lysates from immortalized DPC were analyzed for the expression of Cox-2

by western blot. Lower panel displays the mean ± SE from three independent experiments.

5. Discussion

Dermal papilla cells have a central role in the growth of hair follicles, which are the target organ of androgens such as testosterone and DHT (Itami *et al.,* 1991). Hair growth is related both to the cell number and the volume of DP (Elliott *et al.,* 1999, Ibrahim *et al.,* 1982). This study examined whether DHT reduced the proliferation of immortalized DPC. DHT treatment did not affect the proliferation of immortalized DPC (Fig.9A). We wondered how DHT affects hair growth, thus we further investigated the effects of DHT on cell cycle regulation in immortalized DPC. DHT treatment resulted in an increase of G1 population compared to control in a time- and dose-dependent manner (Fig. 9B). The mammalian cell cycle is a tightly regulated process, and the transition from G1 to S phase is driven by cyclins/CDKs and CDK inhibitors (Prall *et al.,* 1997). As shown in Fig.9C, the expression of cell cycle-associated proteins such as $p27^{kip1}$, cyclin E, cyclin D1 and CDK2 was also affected by DHT in a time- and dose-dependent manner. DHT decreased the expression of CDK2, cyclin E, CDK4 and cyclin D1, whereas p27kip1 expression was increased in immortalized DPC. Cell cycle arrest was also regulated by MAPK, which are crucial modulators of cell proliferation (Zhang *et al.,* 2002) and apoptosis (Keyse, 2008). It has been shown that the expression of $p27^{kip1}$ induced by U0126 is accompanied by cell cycle arrest

(Gysin *et al.,* 2005). DHT did not change the expression of ERK1/2 in immortalized DPC (Fig. 9D). The $p27^{kip1}$ expression was increased by U0126 (Fig. 9E), whereas pre-treatment of U0126 did not alter the DHT-induced $p27^{kip1}$ expression in immortalized DPC. These results indicated that DHT could modulate the expression of cell cycle genes such as $p27^{kip1}$, cyclin E, cyclin D1 and CDK2 and induce cell cycle arrest through a MEK/ERK-independent pathway.

Production of TGF-β1 in DPC is induced by androgen (Inui *et al.,* 2002), and increased TGF-β can cause the miniaturization of hair follicles (Foitzik *et al.,* 2000b). In a previous study, we also found that the extract of *Schisandra nigra* promotes hair growth through downregulation of TGF-β2 in hair follicles (Kang *et al.,* 2009). These studies suggested that TGF-β plays an important role in the regulation of hair growth. In this study, DHT did not affect the expression of TGF-β2 in immortalized DPC (Fig. 10A). TGF-β binding to its receptor leads to phosphorylation and nuclear translocation of Smad2/3 (Tsukazaki *et al.,* 1998). As shown in Fig. 10B and C, DHT increased the level of nuclear Smad2/3 in immortalized DPC. These results indicate that DHT can activate TGF-β signaling through the nuclear localization of Smad2/3.

HSP27 is expressed in hair follicles (Adly *et al.,* 2006) and DPC (Bahta *et al.,* 2008). Nevertheless, the actions of DHT on the regulation of HSP27 in DPC have not been

elucidated. Several studies revealed that phosphorylation of HSP27 are mediated by p38 pathway (Garmyn *et al.,* 2001, Schafer *et al.,* 1998). In this study, stimulation of immortalized DPC with 100 nM DHT induced p38 and HSP27 phosphorylation (Fig. 11A and B). The role of nuclear HSP27 is not fully understood, although nuclear translocation of HSP27/AR complexes has been reported in prostate cancer (Zoubeidi *et al.,* 2007). Balding DPC exhibit higher AR expression (Hibberts *et al.,* 1998) as well as higher HSP27 expression (Bahta *et al.,* 2008). These studies suggest that DHT/AR is related with activation of HSP27. In this study, DHT increased the nuclear translocation of HSP27 in immortalized DPC (Fig. 11C). It seems that DHT regulates the translocation of HSP27/AR complexes. Although the activation of HSP27 was regulated by p38 MAPK (Fig. 11), DHT-induced up-regulation of $p27^{kip1}$ was not altered by SB203580 in immortalized DPC (Fig.9). These results indicate that DHT induced the expression of the cell cycle arrest gene through a p38 MAPK-independent pathway.

Treatment of hair follicle with wnt-10b promoted elongation of the hair shaft (Ouji *et al.,* 2007, Ouji *et al.,* 2008). β-Catenin is a crucial component of the wnt/β-catenin pathway. In this study, DHT treatment reduced the expression of total β-catenin in immortalized DPC (Fig. 12A). Western blot and immunofluorescence staining showed that DHT inhibited nuclear β-catenin level (Fig. 12B and D). LiCl, an inhibitor of GSK3β, enhanced the

accumulation of nuclear β-catenin in immortalized DPC (Fig. 12C and E). Repression of GSK3β induced the translocation of β-catenin into the nuclei of the cells (Hedgepeth *et al.,* 1997). These results indicate that DHT inhibits the expression of nuclear β-catenin via the regulation of GSK3β. DHT increases the level of DKK-1, a wnt antagonist (Kwack *et al.,* 2008). In this study, DHT inhibits the expression of Cyclin D1, a wnt target gene in immortalized DPC (Fig. 9C). Moreover, AR/DHT represses the β-catenin/TCF signaling pathway (Mulholland *et al.,* 2003). These studies indicate that DHT inhibits the wnt/β-catenin pathway.

$PGF_{2\alpha}$ is known to promote hair growth (Sasaki *et al.,* 2005a). However, the regulation of PG by DHT has not been elucidated. Cox-2 is not only a mediator of the PG pathway (Arias-Negrete *et al.,* 1995), but also a target gene in the wnt/β-catenin pathway (Howe *et al.,* 1999). LiCl inhibits the degradation of β-catenin and increases the level of Cox-2 in chondrocytes (Kim *et al.,* 2002). Nevertheless, the effects of DHT on the relationship between β-catenin and Cox-2 have not been studied in immortalized DPC. In this study, DHT inhibited the expression of Cox-2 (Fig. 13A), but U0126, a specific inhibitor of MEK, did not affect the DHT-induced down-regulation of Cox-2 in immortalized DPC (Fig. 13C). DHT also repressed the nuclear localization of NF-κB p65 in immortalized DPC (Fig. 13B), which is necessary for transcription of Cox-2 (Schmedtje *et al.,* 1997). These results indicate that the

effects of DHT on the regulation of Cox-2 are partly mediated through regulation of wnt/β-catenin and NF-κB p65.

In this study, we investigated the mechanisms of action of DHT as a target for the treatment of AGA. DHT attenuated cell cycle progression without changing proliferation (Fig. 9A and B). DHT-induced cell cycle arrest was accompanied by down-regulation of cyclin D1 and CDK2 and up-regulation of $p27^{kip1}$ (Fig. 9B and C). DHT increased the cell cycle arrest through the activation of Smad2/3 and HSP27 and the inhibition of β-catenin and Cox-2 (Fig. 10, 11, 12 and 13). Taken together, these results demonstrate that DHT inhibits hair growth by increasing $p27^{kip1}$, Smad2/3 and HSP27 and decreasing β-catenin and Cox-2.

Ⅲ. REFERENCES

Adly MA, Assaf HA, Hussein MR. 2006. Expression of the heat shock protein-27 in the adult human scalp skin and hair follicle: hair cycle-dependent changes. *J Am Acad Dermatol* **54**: 811-817.

Arias-Negrete S, Keller K, Chadee K. 1995. Proinflammatory cytokines regulate cyclooxygenase-2 mRNA expression in human macrophages. *Biochem Biophys Res Commun* **208**: 582-589.

Babenko AP, Aguilar-Bryan L, Bryan J. 1998. A view of sur/KIR6.X, KATP channels. *Annu Rev Physiol* **60**: 667-687.

Bahta AW, Farjo N, Farjo B, Philpott MP. 2008. Premature senescence of balding dermal papilla cells in vitro is associated with p16(INK4a) expression. *J Invest Dermatol* **128**: 1088-1094.

Behrens J, von Kries JP, Kuhl M, Bruhn L, Wedlich D, Grosschedl R, Birchmeier W. 1996. Functional interaction of beta-catenin with the transcription factor LEF-1. *Nature* **382**: 638-642.

Bradford LW. 1976. Problems of ethics and behavior in the forensic sciences. *J Forensic Sci* **21**: 763-768.

Buhl AE, Waldon DJ, Baker CA, Johnson GA. 1990. Minoxidil sulfate is the active metabolite that stimulates hair follicles. *J Invest Dermatol* **95**: 553-557.

Bunz F, Hwang PM, Torrance C, Waldman T, Zhang Y, Dillehay L, Williams J, Lengauer C, Kinzler KW, Vogelstein B. 1999. Disruption of p53 in human cancer cells alters the responses to therapeutic agents. *J Clin Invest* **104**: 263-269.

Carson C,3rd, Rittmaster R. 2003. The role of dihydrotestosterone in benign prostatic hyperplasia. *Urology* **61**: 2-7.

Castellone MD, Teramoto H, Williams BO, Druey KM, Gutkind JS. 2005. Prostaglandin E2 promotes colon cancer cell growth through a Gs-axin-beta-catenin signaling axis. *Science* **310**: 1504-1510.

Chang F, Lee JT, Navolanic PM, Steelman LS, Shelton JG, Blalock WL, Franklin RA, McCubrey JA. 2003. Involvement of PI3K/Akt pathway in cell cycle progression, apoptosis, and neoplastic transformation: a target for cancer chemotherapy. *Leukemia* **17**: 590-603.

Charalambous MP, Lightfoot T, Speirs V, Horgan K, Gooderham NJ. 2009. Expression of COX-2, NF-kappaB-p65, NF-kappaB-p50 and IKKalpha in malignant and adjacent normal human colorectal tissue. *Br J Cancer* **101**: 106-115.

Clissold SP, Heel RC. 1987. Topical minoxidil. A preliminary review of its pharmacodynamic properties and therapeutic efficacy in alopecia areata and alopecia androgenetica. *Drugs* **33**: 107-122.

Cohen JL. 2010. Enhancing the growth of natural eyelashes: the mechanism of bimatoprost-induced eyelash growth. *Dermatol Surg* **36**: 1361-1371.

Colombe L, Michelet JF, Bernard BA. 2008. Prostanoid receptors in anagen human hair follicles. *Exp Dermatol* **17**: 63-72.

Colombe L, Vindrios A, Michelet JF, Bernard BA. 2007. Prostaglandin metabolism in human hair follicle. *Exp Dermatol* **16**: 762-769.

Cotsarelis G, Millar SE. 2001. Towards a molecular understanding of hair loss and its treatment. *Trends Mol Med* **7**: 293-301.

Cowley S, Paterson H, Kemp P, Marshall CJ. 1994. Activation of MAP kinase kinase is necessary and sufficient for PC12 differentiation and for transformation of NIH 3T3 cells. *Cell* **77**: 841-852.

Danilenko DM, Ring BD, Yanagihara D, Benson W, Wiemann B, Starnes CO, Pierce GF. 1995. Keratinocyte growth factor is an important endogenous mediator of hair follicle growth, development, and differentiation. Normalization of the nu/nu follicular differentiation defect and amelioration of chemotherapy-induced alopecia. *Am J Pathol* **147**: 145-154.

DasGupta R, Fuchs E. 1999. Multiple roles for activated LEF/TCF transcription complexes during hair follicle development and differentiation. *Development* **126**: 4557-4568.

Datta SR, Brunet A, Greenberg ME. 1999. Cellular survival: a play in three Akts. *Genes Dev* **13**: 2905-2927.

Derynck R, Feng XH. 1997. TGF-beta receptor signaling. *Biochim Biophys Acta* **1333**: F105-50.

Edwards J, Bartlett JM. 2005. The androgen receptor and signal-transduction pathways in hormone-refractory prostate cancer. Part 2: Androgen-receptor cofactors and bypass pathways. *BJU Int* **95**: 1327-1335.

Ekman P. 2000. The prostate as an endocrine organ: androgens and estrogens. *Prostate Suppl* **10**: 14-18.

Elliott K, Stephenson TJ, Messenger AG. 1999. Differences in hair follicle dermal papilla volume are due to extracellular matrix volume and cell number: implications for the control of hair follicle size and androgen responses. *J Invest Dermatol* **113**: 873-877.

Evan GI, Vousden KH. 2001. Proliferation, cell cycle and apoptosis in cancer. *Nature* **411**: 342-348.

Fatrai S, Elghazi L, Balcazar N, Cras-Meneur C, Krits I, Kiyokawa H, Bernal-Mizrachi E. 2006. Akt induces beta-cell proliferation by regulating cyclin D1, cyclin D2, and p21 levels and cyclin-dependent kinase-4 activity. *Diabetes* **55**: 318-325.

Filsell W, Little JC, Stones AJ, Granger SP, Bayley SA. 1994. Transfection of rat dermal papilla cells with a gene encoding a temperature-sensitive polyomavirus large T antigen generates cell lines retaining a differentiated phenotype. *J Cell Sci* **107 (Pt 7)**: 1761-1772.

Foitzik K, Lindner G, Mueller-Roever S, Maurer M, Botchkareva N, Botchkarev V, Handjiski B, Metz M, Hibino T, Soma T et al. 2000a. Control of murine hair follicle regression (catagen) by TGF-beta1 in vivo. *FASEB J* **14**: 752-760.

Foitzik K, Lindner G, Mueller-Roever S, Maurer M, Botchkareva N, Botchkarev V, Handjiski B, Metz M, Hibino T, Soma T et al. 2000b. Control of murine hair follicle regression (catagen) by TGF-beta1 in vivo. *FASEB J* **14**: 752-760.

Fried J, Perez AG, Clarkson BD. 1976. Flow cytofluorometric analysis of cell cycle distributions using propidium iodide. Properties of the method and mathematical analysis of the data. *J Cell Biol* **71**: 172-181.

Gandour-Edwards R, McClaren M, Isseroff RR. 1994. Immunolocalization of low-molecular-weight stress protein HSP 27 in normal skin and common cutaneous lesions. *Am J Dermatopathol* **16**: 504-509.

Garmyn M, Mammone T, Pupe A, Gan D, Declercq L, Maes D. 2001. Human keratinocytes respond to osmotic stress by p38 map kinase regulated induction of HSP70 and HSP27. *J Invest Dermatol* **117**: 1290-1295.

Gelmann EP. 2002. Molecular biology of the androgen receptor. *J Clin Oncol* **20**: 3001-3015.

Goni-Allo B, Puerta E, Ramos M, Lasheras B, Jordan J, Aguirre N. 2008. Minoxidil prevents 3,4-methylenedioxymethamphetamine-induced serotonin depletions: role of mitochondrial ATP-sensitive potassium channels, Akt and ERK. *J Neurochem* **104**: 914-925.

Gray LE, Ostby J, Furr J, Wolf CJ, Lambright C, Parks L, Veeramachaneni DN, Wilson V, Price M, Hotchkiss A et al. 2001. Effects of environmental antiandrogens on reproductive development in experimental animals. *Hum Reprod Update* **7**: 248-264.

Gysin S, Lee SH, Dean NM, McMahon M. 2005. Pharmacologic inhibition of RAF-->MEK-->ERK signaling elicits pancreatic cancer cell cycle arrest through induced expression of p27Kip1. *Cancer Res* **65**: 4870-4880.

Hamada K, Randall VA. 2006. Inhibitory autocrine factors produced by the mesenchyme-derived hair follicle dermal papilla may be a key to male pattern baldness. *Br J Dermatol* **154**: 609-618.

Han JH, Kwon OS, Chung JH, Cho KH, Eun HC, Kim KH. 2004. Effect of minoxidil on proliferation and apoptosis in dermal papilla cells of human hair follicle. *J Dermatol Sci* **34**: 91-98.

Hanson WR, Pelka AE, Nelson AK, Malkinson FD. 1992. Subcutaneous or topical administration of 16,16 dimethyl prostaglandin E2 protects from radiation-induced alopecia in mice. *Int J Radiat Oncol Biol Phys* **23**: 333-337.

Harmon CS, Lutz D, Ducote J. 1993. Potassium channel openers stimulate DNA synthesis in mouse epidermal keratinocyte and whole hair follicle cultures. *Skin Pharmacol* **6**: 170-178.

He TC, Sparks AB, Rago C, Hermeking H, Zawel L, da Costa LT, Morin PJ, Vogelstein B, Kinzler KW. 1998. Identification of c-MYC as a target of the APC pathway. *Science* **281**: 1509-1512.

Hedgepeth CM, Conrad LJ, Zhang J, Huang HC, Lee VM, Klein PS. 1997. Activation of the Wnt signaling pathway: a molecular mechanism for lithium action. *Dev Biol* **185**: 82-91.

Herlaar E, Brown Z. 1999. p38 MAPK signalling cascades in inflammatory disease. *Mol Med Today* **5**: 439-447.

Hibberts NA, Howell AE, Randall VA. 1998. Balding hair follicle dermal papilla cells contain higher levels of androgen receptors than those from non-balding scalp. *J Endocrinol* **156**: 59-65.

Hibino T, Nishiyama T. 2004. Role of TGF-beta2 in the human hair cycle. *J Dermatol Sci* **35**: 9-18.

Hirosumi J, Nakayama O, Fagan T, Sawada K, Chida N, Inami M, Takahashi S, Kojo H, Notsu Y, Okuhara M. 1995. FK143, a novel nonsteroidal inhibitor of steroid 5 alpha-reductase: (1) In vitro effects on human and animal prostatic enzymes. *J Steroid Biochem Mol Biol* **52**: 357-363.

Hoozemans JJ, Bruckner MK, Rozemuller AJ, Veerhuis R, Eikelenboom P, Arendt T. 2002. Cyclin D1 and cyclin E are co-localized with cyclo-oxygenase 2 (COX-2) in pyramidal neurons in Alzheimer disease temporal cortex. *J Neuropathol Exp Neurol* **61**: 678-688.

Howe LR, Subbaramaiah K, Chung WJ, Dannenberg AJ, Brown AM. 1999. Transcriptional activation of cyclooxygenase-2 in Wnt-1-transformed mouse mammary epithelial cells. *Cancer Res* **59**: 1572-1577.

Huang L, Li B, Li W, Guo H, Zou F. 2009. ATP-sensitive potassium channels control glioma cells proliferation by regulating ERK activity. *Carcinogenesis* **30**: 737-744.

Huelsken J, Vogel R, Erdmann B, Cotsarelis G, Birchmeier W. 2001. beta-Catenin controls hair follicle morphogenesis and stem cell differentiation in the skin. *Cell* **105**: 533-545.

Huot J, Lambert H, Lavoie JN, Guimond A, Houle F, Landry J. 1995. Characterization of 45-kDa/54-kDa HSP27 kinase, a stress-sensitive kinase which may activate the

phosphorylation-dependent protective function of mammalian 27-kDa heat-shock protein HSP27. *Eur J Biochem* **227**: 416-427.

Ibrahim L, Wright EA. 1982. A quantitative study of hair growth using mouse and rat vibrissal follicles. I. Dermal papilla volume determines hair volume. *J Embryol Exp Morphol* **72**: 209-224.

Igata M, Motoshima H, Tsuruzoe K, Kojima K, Matsumura T, Kondo T, Taguchi T, Nakamaru K, Yano M, Kukidome D et al. 2005. Adenosine monophosphate-activated protein kinase suppresses vascular smooth muscle cell proliferation through the inhibition of cell cycle progression. *Circ Res* **97**: 837-844.

Iino M, Ehama R, Nakazawa Y, Iwabuchi T, Ogo M, Tajima M, Arase S. 2007. Adenosine stimulates fibroblast growth factor-7 gene expression via adenosine A2b receptor signaling in dermal papilla cells. *J Invest Dermatol* **127**: 1318-1325.

Imai R, Jindo T, Miura Y, Mochida K, Takamori K, Ogawa H. 1993. Organ culture of human hair follicles in serum-free medium. *Arch Dermatol Res* **284**: 466-471.

Inui S, Fukuzato Y, Nakajima T, Yoshikawa K, Itami S. 2002. Androgen-inducible TGF-beta1 from balding dermal papilla cells inhibits epithelial cell growth: a clue to understand paradoxical effects of androgen on human hair growth. *FASEB J* **16**: 1967-1969.

Itami S, Kurata S, Sonoda T, Takayasu S. 1991. Mechanism of action of androgen in dermal papilla cells. *Ann N Y Acad Sci* **642**: 385-395.

Ito M, Yang Z, Andl T, Cui C, Kim N, Millar SE, Cotsarelis G. 2007. Wnt-dependent de novo hair follicle regeneration in adult mouse skin after wounding. *Nature* **447**: 316-320.

Ito T, Ito N, Saathoff M, Bettermann A, Takigawa M, Paus R. 2005. Interferon-gamma is a potent inducer of catagen-like changes in cultured human anagen hair follicles. *Br J Dermatol* **152**: 623-631.

Jahoda CA. 1998. Cellular and developmental aspects of androgenetic alopecia. *Exp Dermatol* **7**: 235-248.

Jansen KM, Pavlath GK. 2008. Prostaglandin F2alpha promotes muscle cell survival and growth through upregulation of the inhibitor of apoptosis protein BRUCE. *Cell Death Differ* **15**: 1619-1628.

Jia Y, Ransom RF, Shibanuma M, Liu C, Welsh MJ, Smoyer WE. 2001. Identification and characterization of hic-5/ARA55 as an hsp27 binding protein. *J Biol Chem* **276**: 39911-39918.

Johnson DG, Walker CL. 1999. Cyclins and cell cycle checkpoints. *Annu Rev Pharmacol Toxicol* **39**: 295-312.

Johnstone MA, Albert DM. 2002. Prostaglandin-induced hair growth. *Surv Ophthalmol* **47 Suppl 1**: S185-202.

Kang JI, Kim SC, Hyun JH, Kang JH, Park DB, Lee YJ, Yoo ES, Kang HK. 2009. Promotion effect of Schisandra nigra on the growth of hair. *Eur J Dermatol* **19**: 119-125.

Kaufman KD. 1996. Androgen metabolism as it affects hair growth in androgenetic alopecia. *Dermatol Clin* **14**: 697-711.

Keyse SM. 2008. Dual-specificity MAP kinase phosphatases (MKPs) and cancer. *Cancer Metastasis Rev* **27**: 253-261.

Kim SJ, Im DS, Kim SH, Ryu JH, Hwang SG, Seong JK, Chun CH, Chun JS. 2002. Beta-catenin regulates expression of cyclooxygenase-2 in articular chondrocytes. *Biochem Biophys Res Commun* **296**: 221-226.

Koblenzer PJ, Baker L. 1968. Hypertrichosis lanuginosa associated with diazoxide therapy in prepubertal children: a clinicopathologic study. *Ann N Y Acad Sci* **150**: 373-382.

Koyama M, Matsuzaki Y, Yogosawa S, Hitomi T, Kawanaka M, Sakai T. 2007. ZD1839 induces p15INK4b and causes G1 arrest by inhibiting the mitogen-activated protein kinase/extracellular signal-regulated kinase pathway. *Mol Cancer Ther* **6**: 1579-1587.

Kwack MH, Sung YK, Chung EJ, Im SU, Ahn JS, Kim MK, Kim JC. 2008. Dihydrotestosterone-inducible dickkopf 1 from balding dermal papilla cells causes apoptosis in follicular keratinocytes. *J Invest Dermatol* **128**: 262-269.

Lachgar S, Moukadiri H, Jonca F, Charveron M, Bouhaddioui N, Gall Y, Bonafe JL, Plouet J. 1996. Vascular endothelial growth factor is an autocrine growth factor for hair dermal papilla cells. *J Invest Dermatol* **106**: 17-23.

Larsen JK, Yamboliev IA, Weber LA, Gerthoffer WT. 1997. Phosphorylation of the 27-kDa heat shock protein via p38 MAP kinase and MAPKAP kinase in smooth muscle. *Am J Physiol* **273**: L930-40.

Lavoie JN, Gingras-Breton G, Tanguay RM, Landry J. 1993. Induction of Chinese hamster HSP27 gene expression in mouse cells confers resistance to heat shock. HSP27 stabilization of the microfilament organization. *J Biol Chem* **268**: 3420-3429.

Lavoie JN, L'Allemain G, Brunet A, Muller R, Pouyssegur J. 1996. Cyclin D1 expression is regulated positively by the p42/p44MAPK and negatively by the p38/HOGMAPK pathway. *J Biol Chem* **271**: 20608-20616.

Lee JL, Mukhtar H, Bickers DR, Kopelovich L, Athar M. 2003. Cyclooxygenases in the skin: pharmacological and toxicological implications. *Toxicol Appl Pharmacol* **192**: 294-306.

Lewis RS, Cahalan MD. 1988. The plasticity of ion channels: parallels between the nervous and immune systems. *Trends Neurosci* **11**: 214-218.

Libecco JF, Bergfeld WF. 2004. Finasteride in the treatment of alopecia. *Expert Opin Pharmacother* **5**: 933-940.

Logan CY, Nusse R. 2004. The Wnt signaling pathway in development and disease. *Annu Rev Cell Dev Biol* **20**: 781-810.

Masckauchan TN, Shawber CJ, Funahashi Y, Li CM, Kitajewski J. 2005. Wnt/beta-catenin signaling induces proliferation, survival and interleukin-8 in human endothelial cells. *Angiogenesis* **8**: 43-51.

Massague J, Wotton D. 2000. Transcriptional control by the TGF-beta/Smad signaling system. *EMBO J* **19**: 1745-1754.

Messenger AG, Rundegren J. 2004. Minoxidil: mechanisms of action on hair growth. *Br J Dermatol* **150**: 186-194.

Michelet JF, Commo S, Billoni N, Mahe YF, Bernard BA. 1997. Activation of cytoprotective prostaglandin synthase-1 by minoxidil as a possible explanation for its hair growth-stimulating effect. *J Invest Dermatol* **108**: 205-209.

Miller TA, Jacobson ED. 1979. Gastrointestinal cytoprotection by prostaglandins. *Gut* **20**: 75-87.

Moon RT, Brown JD, Torres M. 1997. WNTs modulate cell fate and behavior during vertebrate development. *Trends Genet* **13**: 157-162.

Mulholland DJ, Read JT, Rennie PS, Cox ME, Nelson CC. 2003. Functional localization and competition between the androgen receptor and T-cell factor for nuclear beta-catenin: a means for inhibition of the Tcf signaling axis. *Oncogene* **22**: 5602-5613.

Naito A, Sato T, Matsumoto T, Takeyama K, Yoshino T, Kato S, Ohdera M. 2008. Dihydrotestosterone inhibits murine hair growth via the androgen receptor. *Br J Dermatol* **159**: 300-305.

Nilius B, Wohlrab W. 1992. Potassium channels and regulation of proliferation of human melanoma cells. *J Physiol* **445**: 537-548.

Omer CA, Miller PJ, Diehl RE, Kral AM. 1999. Identification of Tcf4 residues involved in high-affinity beta-catenin binding. *Biochem Biophys Res Commun* **256**: 584-590.

Ouji Y, Yoshikawa M, Moriya K, Ishizaka S. 2007. Effects of Wnt-10b on hair shaft growth in hair follicle cultures. *Biochem Biophys Res Commun* **359**: 516-522.

Ouji Y, Yoshikawa M, Moriya K, Nishiofuku M, Matsuda R, Ishizaka S. 2008. Wnt-10b, uniquely among Wnts, promotes epithelial differentiation and shaft growth. *Biochem Biophys Res Commun* **367**: 299-304.

Ouji Y, Yoshikawa M, Shiroi A, Ishizaka S. 2006. Promotion of hair follicle development and trichogenesis by Wnt-10b in cultured embryonic skin and in reconstituted skin. *Biochem Biophys Res Commun* **345**: 581-587.

Paus R, Cotsarelis G. 1999. The biology of hair follicles. *N Engl J Med* **341**: 491-497.

Paus R, Foitzik K, Welker P, Bulfone-Paus S, Eichmuller S. 1997. Transforming growth factor-beta receptor type I and type II expression during murine hair follicle development and cycling. *J Invest Dermatol* **109**: 518-526.

Pene F, Claessens YE, Muller O, Viguie F, Mayeux P, Dreyfus F, Lacombe C, Bouscary D. 2002. Role of the phosphatidylinositol 3-kinase/Akt and mTOR/P70S6-kinase pathways in the proliferation and apoptosis in multiple myeloma. *Oncogene* **21**: 6587-6597.

Philpott MP, Kealey T. 2000. Cyclical changes in rat vibrissa follicles maintained In vitro. *J Invest Dermatol* **115**: 1152-1155.

Prall OW, Sarcevic B, Musgrove EA, Watts CK, Sutherland RL. 1997. Estrogen-induced activation of Cdk4 and Cdk2 during G1-S phase progression is accompanied by increased cyclin D1 expression and decreased cyclin-dependent kinase inhibitor association with cyclin E-Cdk2. *J Biol Chem* **272**: 10882-10894.

Radzio-Andzelm E, Lew J, Taylor S. 1995. Bound to activate: conformational consequences of cyclin binding to CDK2. *Structure* **3**: 1135-1141.

Rane MJ, Coxon PY, Powell DW, Webster R, Klein JB, Pierce W, Ping P, McLeish KR. 2001. p38 Kinase-dependent MAPKAPK-2 activation functions as 3-phosphoinositide-dependent kinase-2 for Akt in human neutrophils. *J Biol Chem* **276**: 3517-3523.

Rane MJ, Pan Y, Singh S, Powell DW, Wu R, Cummins T, Chen Q, McLeish KR, Klein JB. 2003. Heat shock protein 27 controls apoptosis by regulating Akt activation. *J Biol Chem* **278**: 27828-27835.

Rulifson IC, Karnik SK, Heiser PW, ten Berge D, Chen H, Gu X, Taketo MM, Nusse R, Hebrok M, Kim SK. 2007. Wnt signaling regulates pancreatic beta cell proliferation. *Proc Natl Acad Sci U S A* **104**: 6247-6252.

Sanders DA, Fiddes I, Thompson DM, Philpott MP, Westgate GE, Kealey T. 1996. In the absence of streptomycin, minoxidil potentiates the mitogenic effects of fetal calf serum, insulin-like growth factor 1, and platelet-derived growth factor on NIH 3T3 fibroblasts in a K+ channel-dependent fashion. *J Invest Dermatol* **107**: 229-234.

Sasaki S, Hozumi Y, Kondo S. 2005a. Influence of prostaglandin F2alpha and its analogues on hair regrowth and follicular melanogenesis in a murine model. *Exp Dermatol* **14**: 323-328.

Sasaki S, Hozumi Y, Kondo S. 2005b. Influence of prostaglandin F2alpha and its analogues on hair regrowth and follicular melanogenesis in a murine model. *Exp Dermatol* **14**: 323-328.

Schafer C, Ross SE, Bragado MJ, Groblewski GE, Ernst SA, Williams JA. 1998. A role for the p38 mitogen-activated protein kinase/Hsp 27 pathway in cholecystokinin-induced changes in the actin cytoskeleton in rat pancreatic acini. *J Biol Chem* **273**: 24173-24180.

Schmedtje JF,Jr, Ji YS, Liu WL, DuBois RN, Runge MS. 1997. Hypoxia induces cyclooxygenase-2 via the NF-kappaB p65 transcription factor in human vascular endothelial cells. *J Biol Chem* **272**: 601-608.

Scudiero DA, Shoemaker RH, Paull KD, Monks A, Tierney S, Nofziger TH, Currens MJ, Seniff D, Boyd MR. 1988. Evaluation of a soluble tetrazolium/formazan assay for cell growth and drug sensitivity in culture using human and other tumor cell lines. *Cancer Res* **48**: 4827-4833.

Seibert K, Zhang Y, Leahy K, Hauser S, Masferrer J, Perkins W, Lee L, Isakson P. 1994. Pharmacological and biochemical demonstration of the role of cyclooxygenase 2 in inflammation and pain. *Proc Natl Acad Sci U S A* **91**: 12013-12017.

Sha WC. 1998. Regulation of immune responses by NF-kappa B/Rel transcription factor. *J Exp Med* **187**: 143-146.

Sheng H, Shao J, Morrow JD, Beauchamp RD, DuBois RN. 1998. Modulation of apoptosis and Bcl-2 expression by prostaglandin E2 in human colon cancer cells. *Cancer Res* **58**: 362-366.

Sherr CJ. 1996. Cancer cell cycles. *Science* **274**: 1672-1677.

Sherr CJ, Roberts JM. 1999. CDK inhibitors: positive and negative regulators of G1-phase progression. *Genes Dev* **13**: 1501-1512.

Shieh CC, Coghlan M, Sullivan JP, Gopalakrishnan M. 2000. Potassium channels: molecular defects, diseases, and therapeutic opportunities. *Pharmacol Rev* **52**: 557-594.

Shorter K, Farjo NP, Picksley SM, Randall VA. 2008. Human hair follicles contain two forms of ATP-sensitive potassium channels, only one of which is sensitive to minoxidil. *FASEB J* **22**: 1725-1736.

Sinclair R. 1998. Male pattern androgenetic alopecia. *BMJ* **317**: 865-869.

Soma T, Ogo M, Suzuki J, Takahashi T, Hibino T. 1998. Analysis of apoptotic cell death in human hair follicles in vivo and in vitro. *J Invest Dermatol* **111**: 948-954.

Soma T, Tsuji Y, Hibino T. 2002. Involvement of transforming growth factor-beta2 in catagen induction during the human hair cycle. *J Invest Dermatol* **118**: 993-997.

Steers WD. 2001. 5alpha-Reductase Activity in the Prostate. *Urology* **58**: 17-24; discussion 24.

Stenn KS, Paus R. 2001. Controls of hair follicle cycling. *Physiol Rev* **81**: 449-494.

Subbaramaiah K, Chung WJ, Dannenberg AJ. 1998. Ceramide regulates the transcription of cyclooxygenase-2. Evidence for involvement of extracellular signal-regulated kinase/c-Jun N-terminal kinase and p38 mitogen-activated protein kinase pathways. *J Biol Chem* **273**: 32943-32949.

Suda T, Arai F. 2008. Wnt signaling in the niche. *Cell* **132**: 729-730.

Takayama S, Reed JC, Homma S. 2003. Heat-shock proteins as regulators of apoptosis. *Oncogene* **22**: 9041-9047.

Tauchi M, Fuchs TA, Kellenberger AJ, Woodward DF, Paus R, Lutjen-Drecoll E. 2010. Characterization of an in vivo model for the study of eyelash biology and trichomegaly: mouse eyelash morphology, development, growth cycle, and anagen prolongation by bimatoprost. *Br J Dermatol* **162**: 1186-1197.

Tetsu O, McCormick F. 1999. Beta-catenin regulates expression of cyclin D1 in colon carcinoma cells. *Nature* **398**: 422-426.

Tosti A, Pazzaglia M, Voudouris S, Tosti G. 2004. Hypertrichosis of the eyelashes caused by bimatoprost. *J Am Acad Dermatol* **51**: S149-50.

Trauner D, Kramer RH. 2004. Metabolic modulation of potassium channels. *Sci STKE* **2004**: pe22.

Tseng WW, Deganutti A, Chen MN, Saxton RE, Liu CD. 2002. Selective cyclooxygenase-2 inhibitor rofecoxib (Vioxx) induces expression of cell cycle arrest genes and slows tumor growth in human pancreatic cancer. *J Gastrointest Surg* **6**: 838-43; discussion 844.

Tsukazaki T, Chiang TA, Davison AF, Attisano L, Wrana JL. 1998. SARA, a FYVE domain protein that recruits Smad2 to the TGFbeta receptor. *Cell* **95**: 779-791.

Vander Heiden MG, Thompson CB. 1999. Bcl-2 proteins: regulators of apoptosis or of mitochondrial homeostasis?. *Nat Cell Biol* **1**: E209-16.

Villalonga N, Ferreres JC, Argiles JM, Condom E, Felipe A. 2007. Potassium channels are a new target field in anticancer drug design. *Recent Pat Anticancer Drug Discov* **2**: 212-223.

Vlad A, Rohrs S, Klein-Hitpass L, Muller O. 2008. The first five years of the Wnt targetome. *Cell Signal* **20**: 795-802.

Wang Y, Ahmad N, Kudo M, Ashraf M. 2004. Contribution of Akt and endothelial nitric oxide synthase to diazoxide-induced late preconditioning. *Am J Physiol Heart Circ Physiol* **287**: H1125-31.

Watts CK, Sweeney KJ, Warlters A, Musgrove EA, Sutherland RL. 1994. Antiestrogen regulation of cell cycle progression and cyclin D1 gene expression in MCF-7 human breast cancer cells. *Breast Cancer Res Treat* **31**: 95-105.

Whelchel A, Evans J, Posada J. 1997. Inhibition of ERK activation attenuates endothelin-stimulated airway smooth muscle cell proliferation. *Am J Respir Cell Mol Biol* **16**: 589-596.

Whiting DA. 1998. Male pattern hair loss: current understanding. *Int J Dermatol* **37**: 561-566.

Wilcken NR, Prall OW, Musgrove EA, Sutherland RL. 1997. Inducible overexpression of cyclin D1 in breast cancer cells reverses the growth-inhibitory effects of antiestrogens. *Clin Cancer Res* **3**: 849-854.

Woo KJ, Jeong YJ, Park JW, Kwon TK. 2004. Chrysin-induced apoptosis is mediated through caspase activation and Akt inactivation in U937 leukemia cells. *Biochem Biophys Res Commun* **325**: 1215-1222.

Woodward DF, Krauss AH, Chen J, Lai RK, Spada CS, Burk RM, Andrews SW, Shi L, Liang Y, Kedzie KM et al. 2001. The pharmacology of bimatoprost (Lumigan). *Surv Ophthalmol* **45 Suppl 4**: S337-45.

Woodward DF, Liang Y, Krauss AH. 2008. Prostamides (prostaglandin-ethanolamides) and their pharmacology. *Br J Pharmacol* **153**: 410-419.

Yamaguchi H, Wang HG. 2001. The protein kinase PKB/Akt regulates cell survival and apoptosis by inhibiting Bax conformational change. *Oncogene* **20**: 7779-7786.

Yamauchi K, Kurosaka A. 2009. Inhibition of glycogen synthase kinase-3 enhances the expression of alkaline phosphatase and insulin-like growth factor-1 in human primary dermal papilla cell culture and maintains mouse hair bulbs in organ culture. *Arch Dermatol Res* **301**: 357-365.

Yang J, Liu X, Bhalla K, Kim CN, Ibrado AM, Cai J, Peng TI, Jones DP, Wang X. 1997. Prevention of apoptosis by Bcl-2: release of cytochrome c from mitochondria blocked. *Science* **275**: 1129-1132.

Zhang L, Yu J, Park BH, Kinzler KW, Vogelstein B. 2000. Role of BAX in the apoptotic response to anticancer agents. *Science* **290**: 989-992.

Zhang W, Liu HT. 2002. MAPK signal pathways in the regulation of cell proliferation in mammalian cells. *Cell Res* **12**: 9-18.

Zhou H, Summers SA, Birnbaum MJ, Pittman RN. 1998. Inhibition of Akt kinase by cell-permeable ceramide and its implications for ceramide-induced apoptosis. *J Biol Chem* **273**: 16568-16575.

Zoubeidi A, Zardan A, Beraldi E, Fazli L, Sowery R, Rennie P, Nelson C, Gleave M. 2007. Cooperative interactions between androgen receptor (AR) and heat-shock protein 27 facilitate AR transcriptional activity. *Cancer Res* **67**: 10455-10465.

Ⅳ. ABSTRACT IN KOREAN

1. Bimatoprost의 모발성장 효과 및 기전

Prostaglandin 유도체들은 항염, 발암, 및 모발 성장을 포함하는 다양한 생물학적 활성을 갖고 있다. 하지만 prostaglandin 유도체들이 모발 성장을 조절하는 정확한 기전은 완전히 밝혀지지 않았다. 본 연구에서는 prostaglandin 유도체들의 모발 성장 효과 및 기전을 조사하였다. Rat vibrissa 모낭에서 유래한 immortalized dermal papilla cells (DPC)에 latanoprost, bimatoprost, unoprostone isopropyl ester, 및 travoprost 등의 prostaglandin 유도체들을 처리하였을 때, 그중에서 bimatoprost는 immortalized DPC 증식 효능을 나타내었다. 모낭에서의 hair fiber 길이 성장 효능이 있는지 조사하기 위하여 rat vibrissa 모낭에 bimatoprost를 처리하였을 때, rat vibrissa 모낭의 hair fiber 길이가 유의성 있게 증가하였다. Bimatoprost의 immortalized DPC 증식 효과의 기전을 규명하기 위하여 세포 주기를 분석하였다. Bimatoprost 처리에 의하여 sub-G1 peaks가 감소하였고, cyclin E 와 CDK2 levels이 증가되었다. Bimatoprost에 의해 유도된 cell cycle progression의 기전을 설명하기 위해서, 모발 성장에서 중요한 역할을 하는 β-catenin의 발현을 조사하였다. Bimatoprost는 nuclear β-catenin level 뿐만 아니라 wnt/β-catenin 경로의 표적 유전자로 알려져 있는 Cox-2의 level을 증가시킴을 확인하였다. 모발 성장제인 minoxidil은 ATP-의존성 K^+ 채널 개방에 의해 NIH3T3 섬유아세포의 증식을 유도할 수 있음이 알려져 있다. Prostaglandin 유도체들이 ATP-의존성 K^+ 채널 개방 작용이 있는지 NIH3T3 섬유아세포에서 증식 효과를 조사하였다. Bimatoprost 의 처리에 의하여 NIH3T3 섬유아세포의 증식이 증가되었다. Bimatoprost는 minoxidil과 마찬가지로 NIH3T3 섬유아세포의 cell cycle progression을 유도하였고, $p27^{kip1}$의 발현을

감소시켰다. 또한 bimatoprost 처리에 따라 pro-apoptotic 인자인 Bax level은 감소하였고 anti-apoptotic 인자인 Bcl-2 level은 증가되었다. 이러한 결과들은 bimatoprost가 anti-apoptotic 효과를 나타내어 세포 증식을 유도함을 보여준다. Bimatoprost는 NIH3T3 섬유아세포에서도 β-catenin과 Cox-2를 증가시킴을 관찰하였다. Bimatoprost의 세포 증식 효과가 ATP-의존성 K^+ 채널 차단제인 glibenclamide에 의해서 차단되는지 조사하였다. Glibenclamide는 NIH3T3 섬유아세포에서 bimatoprost에 의해 유도된 세포 증식과 cell cycle progression을 억제하였다. Bimatoprost와 minoxidil은 세포의 증식에 관련된 Akt의 인산화를 유도하는 반면, glibenclamide는 bimatoprost에 의해 유도된 Akt의 인산화를 감소시킴을 확인하였다. Glibenclamide 전처리는 bimatoprost에 의해 유도된 Bcl-2, β-catenin과 Cox-2의 증가를 감소시킴을 확인하였다. 종합해보면, 이러한 결과들은 bimatoprost가 immortalized DPC에서 β-catenin과 Cox-2의 증가를 통한 cell cycle progression 촉진에 의해 모발 성장을 증가시킴을 보여준다. 또한, bimatoprost는 NIH3T3 섬유아세포에서 β-catenin 증가와 ATP-의존성 K^+ 채널 활성화를 통한 anti-apoptotic 경로의 활성화에 의해 세포 증식을 증가시킴을 확인하였다. 본 연구 결과들은 bimatoprost를 탈모 치료제로 이용할 수 있는 근거를 제시하였다.

2. Immortalized dermal papiila cells에서 dihydrotestosterone의 효과 및 기전

탈모의 대부분을 차지하는 androgenetic alopecia (AGA)는 모낭의 dermal papilla cells (DPC)에서의 dihydrotestosterone (DHT)의 작용에 의해 일어나는 것으로 알려져 있다. 하지만, DPC에서 DHT의 작용 기전은 완전히 이해되지 않고 있다. 그래서 본 연구에서는 모발 주기와 모낭 성장의 조절에 중요한 세포인 DPC에서 DHT의 효과를 immortalized DPC을 이용하여 조사하였다. DHT는 immortalized DPC의 증식에 영향을 주지 않음을 확인하였다. 그러나 DHT가 immortalized

DPC의 cell cycle arrest를 증가시킴을 유세포 분석기를 이용하여 확인하였고, $p27^{kip1}$ level 증가, cyclin E, cyclin D1 및 CDK2 levels 감소시킴을 확인하였다. MEK/ERK 1/2의 저해재인 U0126 처리는 $p27^{kip1}$ 발현을 증가시켰으나, U0126은 DHT에 의한 $p27^{kip1}$ 증가에는 영향을 주지 않음을 확인하였다. 모낭의 성장기에서 퇴행기로의 이행에 transforming growth factor-β (TGF-β) 경로가 관련되어 있음이 알려져 있다. 그러나 DHT는 TGF-β2 발현에 영향을 주지 않음을 관찰하였다. 하지만 DHT의 처리에 의해 TGF-β 경로의 매개체인 Smad2/3의 인산화와 nuclear translocation을 유도함을 확인하였다. Androgen은 androgen receptor (AR)에 결합한 후에 heat shock protein 27 (HSP27)과 함께 nuclear translocation하여 표적 유전자의 전사를 활성화하는 것으로 알려져 있다. 본 연구에서 DHT는 immortalized DPC에서 p38 MAPK 경로를 통하여 HSP27 인산화와 nuclear tranlocation을 유도함을 확인하였다. DHT의 처리에 의하여 모발 성장과 증식에서 중요한 조절자인 total과 nuclear β-catenin의 발현을 감소함을 확인하였다. DHT에 의해 유도된 β-catenin의 감소는 glycogen synthase kinase-3β (GSK-3β) 저해제인 LiCl에 의해 감소됨을 확인하였다. DHT는 wnt 표적 유전자인 Cox-2의 발현을 감소시켰고, Nuclear factor-κB p65 (NF-κB p65)를 감소시킴을 확인하였다. 또한 MEK/ERK 1/2의 저해재인 U0126은 Cox-2의 발현을 감소시키는 반면, p38 MAPK 저해제인 SB203580은 Cox-2의 발현을 증가시킴을 확인하였다. 하지만, U0126과 SB203580은 DHT에 의한 Cox-2 level 감소와 관련되지 않음을 확인하였다. 이러한 결과들로 미루어보아, DHT에 의해 유도된 immortalized DPC의 cell cycle arrest는 TGF-β/Smad의 활성화, HSP27의 활성화 및 β-catenin의 억제를 통해서 유도될 수 있을 것이라 사료된다.

Acknowlegement

시작할 때의 마음가짐으로 꾸준히 나아갔더라면 지금보다 더 나은 결실을 맺을 수 있지 않았을까 하는 아쉬움을 남긴채, 이제는 4년 6개월 동안의 기간을 뒤로하고 논문을 마무리 하려합니다. 제가 이 과정까지 올 수 있도록 도와주신 모든 분들께 이 지면을 통해 감사의 마음을 전하려 합니다.

누구보다도 여러 모로 부족하기만한 저를 끊임없이 가르치시고 힘을 내도록 다독여 주신 지도교수님인 강희경 교수님께 감사의 말씀을 전합니다. 강희경 교수님, 교수님께서 제게 보여주셨던 열정과 노력들을 잊지 않고 교수님의 제자로써 앞으로 좀 더 나아져가는 모습을 보여드리도록 노력하겠습니다. 항상 건강하시길 바랍니다. 그리고 바쁘신 와중에 저의 미흡한 논문을 성의껏 심사해 주신 유은숙 교수님, 박덕배 교수님, 이창훈 교수님, 현진원 교수님 정말 감사합니다. 특히, 멀리서 심사 때문에 오시느라 고생하신 이창훈 교수님 다시 한번 감사의 말을 드립니다. 그리고 대학원 과정동안 관심과 조언으로 많은 가르침을 주신 이영기 교수님, 조문제 교수님, 고영상 교수님, 강현욱 교수님, 정영배 교수님, 은수용 교수님, 김수영 교수님, 정성철 교수님께도 감사드립니다.

길다면 긴 6 년여 동안 한 장소에서 같이 열심히 실험하며 지냈고 지금은 각자의 길을 가고 있는 김상철박사, 윤원종박사, 이혜자박사, 경진, 내 대화상대 상철이, 민경이, 은진이, 선순이, 혜진이, 그리고 막내 은지, 재희, 엘비라 샘까지 모두에게 감사하다는 말을 하고 싶습니다. 특히, 실험실에서 많은 시간을 함께한 상철이형! 그리고 항상 내가 지쳐할 때 술 한잔 나눴던 원종이형!! 멀리 있지만 항상 신경써주는 혜자누나!! 약리학 교실 선배들이 있었기에 지금의 제가 있다고 생각합니다. 선배들 도와주느라 예전에 고생했거나, 지금도 수고하고 있는

약리학 교실 후배들 모두에게도 감사의 마음을 전합니다. 그리고 함께 졸업준비의 기간을 보냈던 경진이에게 다시 한번 축하한다는 말을 전합니다.

그리고 의대에서 항상 웃는 얼굴로 반갑게 맞이해준 영미누나, 희경누나, 지금은 다른 장소에서 지내고 있는 재우형&지은누나, 경아, 정은이, 진영이, 곧 결혼하는 지강이형~축하해요. 그리고 내가 필요로 할때마다 뭐든지 흔쾌히 빌려준 옆방 연희, 금희씨, 그리고 이제야 조금 알아가는 기천이, 문석이, 창희에게도 고맙다는 말을 전합니다.

귀하게 키운 딸을 부족한 저에게 주시고 옆에서 항상 따듯하게 대해 주시는 장인어른과 장모님, 처형과 형님 그리고 조카들 (형수 와 수희), 두 처남에게도 이 지면을 빌어 사랑한다는 말과 함께 감사의 마음을 전합니다. 그리고 항상 넘치는 사랑을 제게 주시는 아버지, 어머니, 그 밖에 일일이 거론하지 못한 친척들, 나이만 많은 오빠를 잘 챙겨주는 여동생 현미와 매제 하림이 그리고 조카 시우에게도 사랑과 감사의 마음을 전합니다. 마지막으로, 힘들면서도 내가 기운낼 수 있도록 도와준 나의 사랑하는 아내 이정이와 뱃속의 아이 (햇살이)에게 이 논문을 바칩니다.